Beitr. Paläont., **31**:345–389, Wien 2009

The Late Miocene Mammal Faunas of the Mytilinii Basin, Samos Island, Greece: New Collection

14. Bovidae

by

Dimitris S. Kostopoulos*)

Kostopoulos, D.S., 2009. The Late Miocene Mammal Faunas of the Mytilinii Basin, Samos Island, Greece: New Collection. 14. Bovidae. — Beitr. Paläont., **31**:345–389, Wien.

Abstract

New bovid material collected from five fossil sites of Mytilinii basin, Samos, Greece, allows recognizing thirteen species of the genera *Miotragocerus*, *Tragoportax*, *Gazella*, *Sporadotragus*, *Palaeoryx*, *Urmiatherium* and the newly defined *Skoufotragus*, which includes *Pachytragus laticeps* Andrée, part of *Pachytragus crassicornis* Andrée and the new species *Skoufotragus zemalisorum*. Combination of data from old and new collections leads to an extensive systematic revision of the entire Samos bovid assemblage, validating 27 species. *Tragoportax curvicornis* Andrée, 1926 is considered to be synonymous with *Tragoportax punjabicus* (Pilgrim, 1910); the systematic status of the Samos *Gazella* has been restored, recognizing four species; *Pachytragus crassicornis* Schlosser, 1904, *Pseudotragus capricornis* Schlosser, 1904 and *Pseudotragus longicornis* Andrée, 1926 are grouped into *Protoryx capricornis* (Schlosser, 1904); *Palaeoryx pallasi* and *Palaeoryx majori* Schlosser, 1904 are fully acknowledged; *Tragoreas oryxoides* Schlosser, 1904 is regarded as a valid taxon close to some Chinese forms. Analysing the time distribution of the Samos bovids, four successive chronological assemblages have been recognized, ranging from late Early to early Late Turolian.

Keywords: Turolian, Samos, Greece, Bovidae, Systematics, Biochronology.

Zusammenfassung

Das neue Bovidenmaterial aus fünf Fundstellen des Mytilinii Beckens (Samos, Griechenland) kann insgesamt dreizehn Gattungen zugeordnet werden: *Miotragocerus*, *Tragoportax*, *Gazella*, *Sporadotragus*, *Palaeoryx*, *Urmiatherium* und der neu aufgestellten Gattung *Skoufotragus*, welche *Pachytragus laticeps* Andrée, teilweise *Pachytragus crassicornis* Andrée und die neue Art *Skoufotragus zemalisorum* inkludiert. Die gemeinsame Bearbeitung der Funde aus der alten und neuen Grabung führt zu einer intensiven systematischen Revision der gesamten Bovidenvergesellschaftung von Samos, die jetzt 27 Arten umfasst. *Tragoportax curvicornis* Andrée 1926 wird mit *Tragopartax punjabicus* (Pilgrim, 1910) synonymisiert. Die systematische Stellung der Samos *Gazella* führt zu der Einteilung in vier Arten: *Pachytragus crassicornis* Schlosser, 1905, *Pseudotragus capricornis* Schlosser, 1904 und *Pseudotragus longicornis* Andrée, 1926 werden zu *Protoryx capricornis* (Schlosser, 1904); *Palaeoryx pallasi* und *Palaeoryx majori* Schlosser, 1904 sind getrennt zu betrachten. *Tragoreas oryxoides* Schlosser, 1904, ist eine gültige Art, die den chinesischen Formen nahe steht. Die zeitliche Verbreitung der Samos Boviden spricht für ein Abfolge von vier Vergesellschaftungen, die vom späten Frühturolium bis zum frühen Spätturolium reicht.

Schlüsselworte: Turolium, Samos, Griechenland, Bovidae, Systematik, Biochronologie.

1. Introduction

In the study of fossil assemblages, the most difficult situations by far arise with old and exhaustively studied sites documented by a long-standing reference record; it is still worse when the fossil site in question is considered to be "classical". Fossil mammals from the famous late Miocene site(s) of Samos Island (Greece) certainly fall within this case. Bovids from Samos were already known from Forsyth-Major's time (1888, 1891a, 1891b, 1894), but more thorough and detailed works were published later by Schlosser (1904), Andrée (1926), Sickenberg (1932, 1936), Gentry (1971) and Solounias (1981). All these authors deal with the late 19th and early 20th centuries'

*) Dr. Dimitris S. Kostopoulos, Aristotle University of Thessaloniki. Department of Geology, Laboratory of Geology and Palaeontology, GR-54124 Thessaloniki, Greece, e-mail: dkostop@geo.auth.gr

bovid-collections from Samos, dispersed today in several museums and institutions across the world. Reporting more than 40 species, the catalogue of the Samos Bovidae is certainly impressive, but not very credible. Solounias (1981) and Bernor et al. (1996) shortened this list to about 20 species, several of them originally known from Samos and others exclusively known from this very particular piece of land. What also seems outstanding is the high number of rare bovid taxa reported from Samos; six species are known by their holotype/lectotype only, whereas five more species are recorded by less than five specimens each. Whether this high diversity is the result of an environmental mosaic or simply fictitious, due to the amalgamation of chronologically succeeding faunal assemblages has to be checked yet.

The new bovid material described in the present work originates from five fossil sites: Mytilinii 4 (MLN), Mytilinii-3 (MYT), Mytilinii 1A (MTLA), Mytilinii 1B (MTLB) and Mytilinii 1C (MTLC) located in the Mytilinii Neogene basin (Weidmann et al., 1984, Koufos et al., 1997; Kostopoulos et al., 2003). The chrono-stratigraphic arrangement of these sites and their correlation with old fossil-quarries from the same basin is given by Kostopoulos et al. (2003) and elsewhere in the present volume (Kostopoulos et al., this volume). Some additional specimens collected by professor Melentis in the early 60ies and 80ies (Melentis, 1969; Koufos & Melentis, 1982) from Adrianos ravine and labelled PMMS (Palaeontological Museum of Mytilinii, Samos) are also incorporated in this study. Since several bovid species are equally present in successive fossil horizons, the description is given by taxonomical order. The comparison of the new material necessitates cross-reference with the old material, housed at the American Museum of Natural History (AMNH, B. Brown's collection; sites: Quarry x-Qx, Quarry 1-Q1, Quarry 2-Q2, Quarry 4-Q4, Quarry 5-Q5 and Quarry 6-Q6), the Natural History Museum in London (NHML, Forsyth-Major's collection), the Paleontological Institute of Münster (PIM), the Museum of Natural History, Vienna (NHMW), the Department of Geology of the Lausanne University (MGL, Forsyth-Major collection: 'Stefano', 'Potamies' and 'Adriano' samples), the Senckenbergisches Naturhistorisches Museum, Frankfurt (SMF), and the Staatliches Museum für Naturkunde, Stuttgart (SMNS). Special attention is paid to unresolved taxonomic problems, as well as to biochronological inferences extracted from the study of the bovid association of Samos.

Abbreviations:
TD: transverse diameter; APD: anteroposterior diameter; L: length; W: width; H: height; PM(pm) : P2-M3(p2-m3); P(p): P2-P4(p2-p4); M(m): M1-M3(m1-m3); hc: horn-core; ptbc: posterior tuberosities of the basioccipital; atbc: anterior tuberosities of the basioccipital. All measurements are given in millimeters (mm).

2. Systematic Palaeontology

Boselaphini Knottnerus-Meyer, 1907

Genus *Miotragocerus* Stromer, 1928

***Miotragocerus valenciennesi* (Gaudry, 1861)**

Synonyms: see discussion in Kostopoulos (2005:763)
Lectotype: frontlet MNHNP PIK2367 illustrated by Gaudry (1861:Pl. VIII, figs. 4-5; 1862-67:288, pl. XLVI-II, figs. 2-3); note that both illustrations show a 'negative' (left as right) view of the same specimen.
Diagnosis: as in Spassov & Geraads (2004:353)
Type Locality: Pikermi, Greece
Occurences: Samos, Halmyropotamos, Maragheh, Ak-

	MTLB161	MTLC33	MTLA324	MTLA492	MTLA190		MTLC25	MTLA299	MTLA284	MTLA184
LPM	97.0		93.0	86.3	87.0	Lpm	104.7	91.8	93.0	
LP	44.1	44.5	43.3	38.3		Lp	44.8	40.8		
LM	54.7		51.0	47.5	47.5	Lm	58.9	51.3		
LP2	16.0	15.2	15.3	12.5	13.2	Lp2	12.0	11.8		
WP2		11.8		11.6		Wp2	6.4	6.2		
LP3	14.3		14.8		13.2	Lp3	16.1	14.0		
WP3	12.5		13.2		12.5	Wp3	8.6	8.0		
LP4	12.5	11.8	13.0	10.5	10.0	Lp4	16.2	15.0		
WP4	15.0	14.3	15.0	10.4	10.3	Wp4	9.0	9.0		
LM1	17.5			15.3	15.4	Lm1	14.3	13.5		
WM1	16.7				16.5	Wm1	12.4	11.0		
LM2	19.7			17.7	16.8	Lm2	17.7	16.2	16.0	
WM2	19.3			18.0	16.6	Wm2	12.5	11.5	12.0	
LM3	19.6		19.0	17.4	17.2	Lm3	24.5	21.7	21.5	21.1
WM3	19.0		18.5	16.8	15.0	Wm3	11.8	11.6	11.4	10.0

Table 1: Upper and lower dental measurements of *Miotragocerus valenciennesi* from MTLA-B-C, Samos.

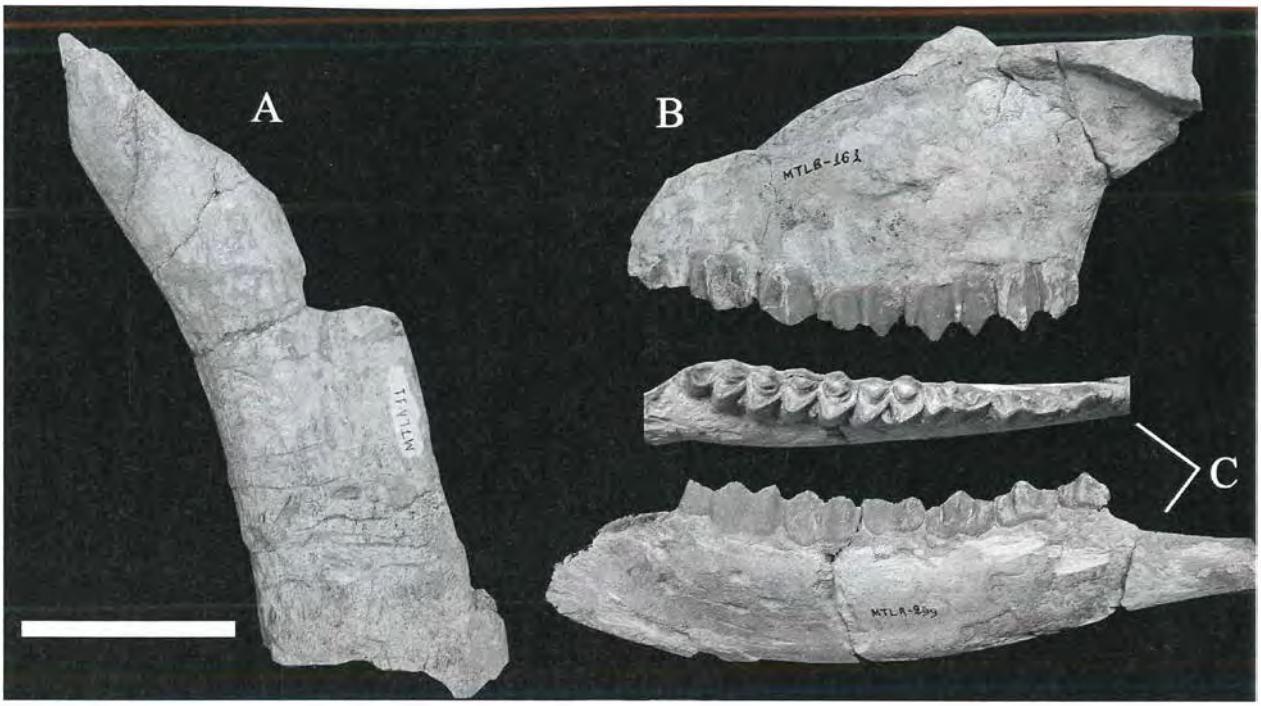

Figure 1: *Miotragocerus valenciennesi* from Samos. A. right horn-core, MTLA11 in lateral view; B. left maxilla, MTLB161 in buccal view; C. right mandible, MTLA299 in lingual and occlusal (reversed) view. Scale bar equals 5 cm.

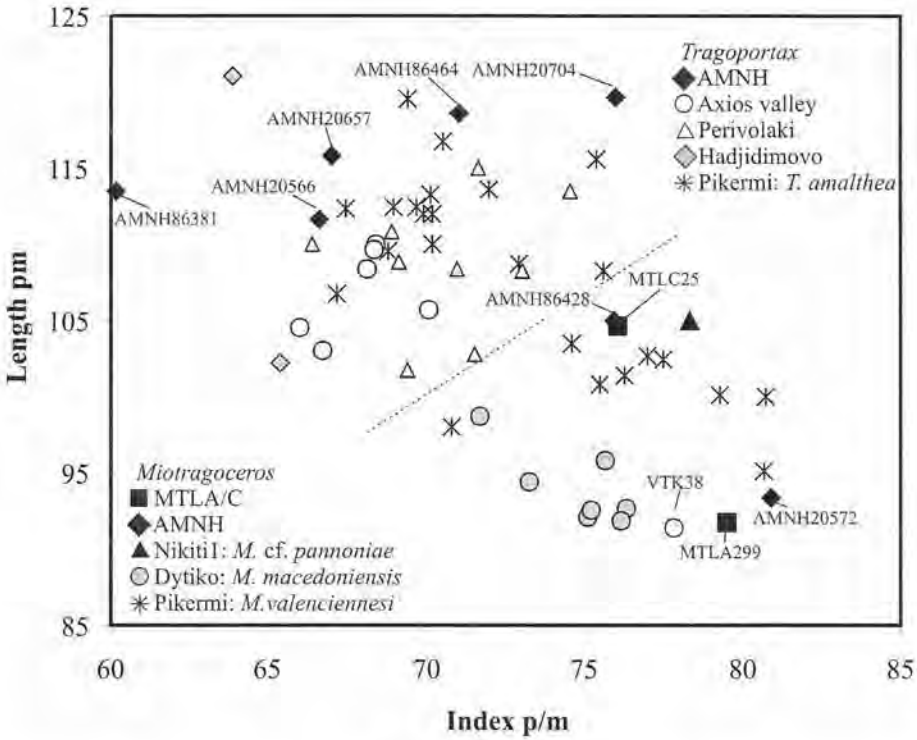

Figure 2: Scatter diagram comparing the lower premolar/molar ratio in relation to p2-m3 length of *Miotragocerus* and *Tragoportax* from several Balkan sites.

kaşdağı, Mont Luberon, Pierra, Hadjidimovo, etc.
Time Range: Turolian
Localities: Mytilinii 1A (MTLA), Mytilinii 1B (MTLB), Mytilinii 1C (MTLC); Samos Island, Greece.
Material: Frontlet, MTAL11; P2-M3sin, MTLA190, MTLB161; P2-M3dex, MTLA324, MTLA492; P2-P4dex, MTLC33; p2-m3sin, MTLA299, MTLC25; p2-m3dex, MTLA284; m3dex, MTLA184

Description & Comparison:
The badly preserved frontlet MTLA11 (Fig. 1A) does not permit significant morphological observations. The basal cross-section is elongated (APD = 60 mm; TD = 27.7 mm) with a flat medial face and a convex lateral one. The length of the horn-cores does not exceed 200 mm. The posterior face is weakly flattened. A blunt anterior keel shows one main and several secondary demarcations, suggesting that

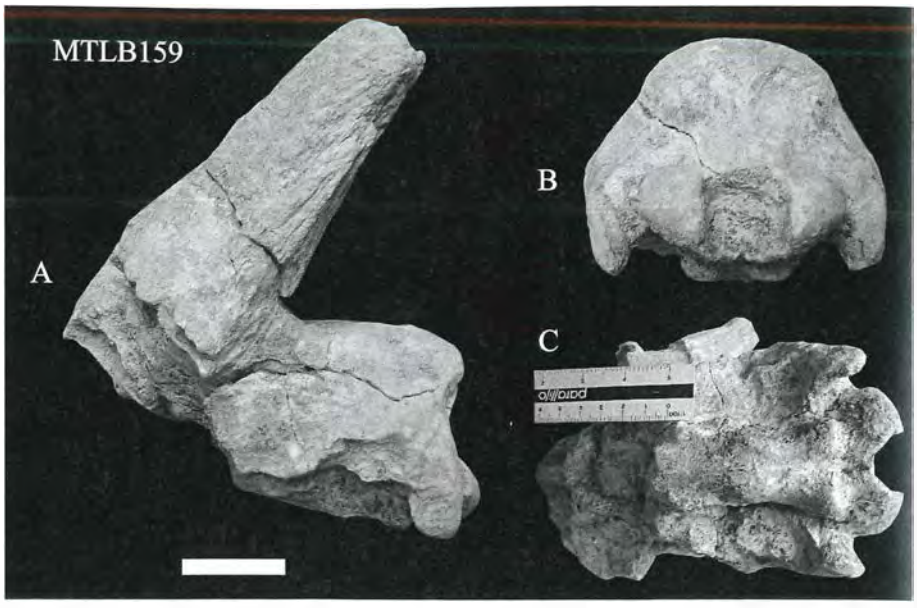

Figure 3: *Tragoportax rugosifrons*, cranium MTLB159 from Samos, in lateral (A), occipital (B) and basioccipital (C) view. Scale bar equals 5 cm.

it could belong to a subadult individual. The premolars are elongated and large compared to the molars (Table 1). The premolar/molar ratio is 80-85% (n = 3) for the upper tooth row and 76-79.5% (n = 3) for the lower one. The P2 is large, with a strong and centrally placed paracone and a bilobed lingual wall. The P3 has a strong parastyle and metastyle and a less buccally protruding paracone in a central position. On the lingual wall, the hypocone is more developed than the protocone, from which it is distinguished by a variably developed furrow. The P4 has weaker styles and a weaker paracone than P3, as well as a rounded lingual wall. The upper molars are low, with a thin basal pillar, an angular protocone, a well-developed parastyle and a thin mesostyle (Fig. 1B). A central islet is present on most molars.

The p2 is long and simple, with a strong medio-lingual cuspid. The p3 is long, with a primitive structure: the paraconid is weakly separated from the parastylid and pointing anteriorly; the metaconid is thin, elongated and points backwards; the hypoconid is separated from the protoconid through a wide groove (Fig. 1C). The p4 is similar to the p3, but the metaconid is sub-triangular and the entoconid fuses quickly with the entostylid (Fig. 1C). The molars bear a basal pillar that decreases from m1 to m3. The styles are weakly developed, whereas the lingual face of the paraconid and, but less so, the entoconid, are strongly convex (Fig. 1C). The hypoconid and the protoconid are angular labially. The third lobe of m3 is marked posteriorly by an accessory crest.

South-East European *Miotragocerus* of Turolian age have recently been discussed by Spassov & Geraads (2004) and Kostopoulos (2005), with compatible, albeit not identical, nomenclatural conclusions. MTLA11 is morphometrically similar to *M. valenciennesi* (Gaudry, 1861) from Pikermi. It differs from *M. monacensis* Stromer, 1928, from Central Europe, by having more uprightly inserted and more complicated horn-cores, and from *M.* cf. *pannoniae* (Kretzoi, 1941) from Nikiti1, Greece (Kostopoulos & Koufos, 1996) in the larger size. Dental proportions from Samos (Fig. 2) appear larger than those of *M. macedoniensis* from Axios valley, Greece (Bouvrain, 1988), and fall well within the range of the Pikermi species.

Measurements	MTLB159
L anterior hc-occipital	172.3
L back hc-occipital	96.5
L back of rugose area- occipital	64.7
W skull at the lateral edges of hc	122.5
W braincase	90.0
W bimastoids	107.5
W bicondyles	63.4
W at ptbc	40.0
W at atbc	29.0
H occiput	49.5
TD hc base	38.5
APD hc base	72.3

Table 2: Cranial measurements of *Tragoportax rugosifrons* from MTLB, Samos.

***Miotragocerus* sp.**

Locality: Mytilinii 4 (MLN); Samos Island, Greece
Material: M1-M3 sin, MLN61

Description & Comparison:
Another molar row (LM = 50 mm) from MLN is also boselaphine in appearance but significantly smaller than that of *Tragoportax* and closer to *Miotragocerus* from MTLA/B. Lacking adequate material, it is referred to as *Miotragocerus* sp.

Genus *Tragoportax* Pilgrim, 1937

Tragoportax rugosifrons (Schlosser, 1904)

Synonyms: in Spassov & Geraads (2004:341) and following discussion.

Figure 4: *Miotragocerus valenciennesi*, cranium AMNH86556 from Q2, Samos, in lateral view. Scale bar equals 5 cm.

Lectotype: skull illustrated by Schlosser (1904: Pl. XII, fig. 6)
Diagnosis: as in Spassov & Geraads (2004:341)
Type Locality: Samos - unknown level, Greece
Occurences: Ravin de Zouaves-5, Nikiti-2, Vathylakkos, Perivolaki, Hadjidimovo
Time Range: Early - Middle Turolian

Locality: Mytilinii 1B (MTLB); Samos Island, Greece
Material: part of cranium MTLB159

Description & Comparison:
The cranial roof is flat defined dorso-laterally defined by moderately developed parietal crests (Fig. 3A). The fronto-parietal depression behind the horn-cores is not well-defined and the rugosities rather weak. The lateral sides of the braincase are swelling. The hexagonal-shaped occipital face is rather low and wide with weakly concave dorso-lateral margins (Fig. 3B); the foramen magnum is large and the condyles point postero-ventrally, whereas the strong paroccipital processes point more ventrally. The basioccipital is moderately long and rather wide with strong posterior tuberosities and weaker but bulbous anterior ones placed parallel to the sagittal plane (Fig. 3C). A shallow wide groove runs centrally along the basioccipital, with a weak crest at the mid-line. The horn-cores are placed above the posterior part of the orbits, weakly tilted backwards (Fig. 3A). They should have been quite long and rather straight, with a significant anterior keel without signs of torsion, and not much extended anteroposteriorly. Their posterior surface is flat, marked by a postero-lateral blunt keel, leading to a triangular cross-section (Fig. 3A). In anterior view, the horn-cores are moderately spaced on the frontals and fairly divergent (50°). The intercornual plateau is broken anteriorly, but it should have been important.

The morphological and metrical (Table 2) characteristics of MTLB159 are very similar to those of the lectotype of *Tragoportax rugosifrons* (Schlosser, 1904: Pl. XII, fig. 6) and to the holotype of *Tragoportax recticornis* (Andrée, 1926: Pl. XI, figs. 5, 9; SMNS13269), both originally known from Samos. MTLB159 fulfils the condition described on the emended diagnosis of the species given by Spassov & Geraads (2004). It differs from *Tragoportax amalthea* (Roth & Wagner, 1854) by the less bent and untwisted horn-cores without anterior exostoses and steps.

***Tragoportax* sp.**

Locality: Mytilinii 4 (MLN); Samos Island, Greece
Material: D2-M1dex, MLN12; P2-P4sin, MLN53; m1-m3dex, MLN28.

Description & Comparison:
An upper tooth row of a young individual, an upper premolar row and a lower molar row from MLN site represent a large boselaphine. The D2-D4 length is 49.5 mm; the P2-P4 length equals 40.5 mm and the m1-m3 length is 61.3 mm. The P2 is longer than P3 and lingually strongly bilobed. The parastyle and the paracone are strong in both the P2 and the P3. The P4 is more symmetrical than P3, with a rounded lingual wall. The M1 has a hypsodonty index (Height x 100/Width) of about 92. The lower molars have weakly wrinkled enamel. A thin basal pillar appears on the first two molars. The talonid of m3 is rather large. Although the material is extremely poor for certain taxonomic conclusions it looks larger than *Miotragocerus* and similar to *Tragoportax* from several Greek sites.

Discussion:
Solounias (1981) assigned several specimens from the

old Samos collections to *Miotragocerus*, reporting two species: *M. monacensis* Stromer, 1928 and *M. valenciennesi* (Gaudry, 1861). *M. monacensis*, originally known by a couple of specimens from the Vallesian of Germany (Gentry, pers. com., 2008) is smaller than *M. valenciennesi* with simpler, more tilted, wider apart spaced horn-cores on the frontals with a better marked and stronger developed rugose area; the dental and basicranial structures are unknown. Since none of the Samos frontlets I have seen at AMNH, PIM, NHML, NHMW, SMF, SMNS and MGL fulfils the *M. monacensis* conditions, I have already abolished the presence of this species on Samos (Kostopoulos, 2005:770), attributing the specimens to *M. valenciennesi* (Figs. 2, 4). Morphological horn-core variability within the species is due to the great changes in horn-core shape, according to succeding ontogenetic stages, and is well-known from Pikermi and Akkaşdağı (Kostopoulos, 2005).

Adopting the viewpoint of most authors dealing with late Miocene Eurasian boselaphines, I also consider *Tragoportax recticornis* (Andrée, 1926) as a junior synonym of *T. rugosifrons* (Schlosser, 1904). Apart from Samos, this species has been recorded in several Turolian sites of the Southern Balkans and probably the Black Sea (Bouvrain, 1988, 1994a; Korotkevitch, 1988; Kostopoulos & Koufos, 1999; Kostopoulos, 2006a; Spassov & Geraads, 2004).

Next to *T. rugosifrons*, Andrée (1926: Pl. XI, figs. 6, 7) recognized another species originally named "*Tragocerus*" *curvicornis* on Samos, the holotype of which is PIM 70 (Pilgrim & Hopwood, 1928; Fig. 5). The species takes part of in an endless discussion, being considered either as synonymous with *Tragoportax rugosifrons* (Bouvrain, 1988, 1994a; Gentry, 1999) or as a valid species (Solounias, 1981; Moya-Sola, 1983; Spassov & Geraads, 2004). Comparing the type specimen of *T. curvicornis* (PIM70; Fig. 5), as well as the cranium AMNH 20566 from Q5 of Samos (Solounias, 1981; Fig. 5) with *T. rugosifrons* (Schosser, 1904:Pl. XII, fig. 6 and SMNS 13269), it is clear that differences are not simply restricted to the horn-core curvature as previously thought, but they highly exceed those expected for intraspecific variability. *T. curvicornis* differs from *T. rugosifrons* by the narrower and higher braincase, the less developed rugose area, the stronger occipital relief, the longer basioccipital with weaker anterior tuberosities and stronger median crest, the more anteroposteriorly oriented auditory bulla, the more anteriorly positioned foramen ovale, the more upright insertions of the horn-cores and their convergence at the front of the base and the weaker slope of the braincase on the face. Previous authors (Solounias, 1981; Spassov & Geraads, 2004) already proposed close affinities between *T. browni* Pilgrim, 1937 and *T. curvicornis* and I fully agree with them, even though the holotype of the latter species appears somewhat larger (~20%) and with less posteriorly curved horn-cores than the holotype of *T. browni* (AMNH 19662). The Samos cranium AMNH20566 from Q5 (Fig. 5) certainly justifies such a decision, as it perfectly matches with AMNH 19662, also suggesting that observed differences within the Samos material should be credited to intraspecific variability. Furthermore, I gladly adopt Moya-Sola's (1983:122) recommendation to synonymize *T. browni* with *T. punjabicus* Pilgrim, 1910; the comparison of AMNH19662 with a cast of the *T. punjabicus* holotype (AMNH9908) indicates that they are practically undistinguishable and there is no apparent reason to keep them separate; the common stratigraphic origin of both species from Dhok Pathan, middle Siwaliks strengthens such a decision. The most prominent diagnostic feature between these two species according to Pilgrim (1937) is the bending of the face on the cranial axis, a characteristic that I, however, failed to confirm. Following nomenclature rules, it is obvious that *Tragoportax punjabicus* (Pilgrim, 1910) has priority over both *T. curvicornis* and *T. browni* (see also Moya-Sola, 1983). In my view, the generic attribution of *T. punjabicus* is open, since several of its cranial characteristics are closer to *Miotragocerus* than *Tragoportax* but this issue is beyond

Figure 5: *Tragoportax punjabicus*, crania PIM70 and AMNH20566 from Samos, in lateral view. Scale bar equals 5 cm.

the scope of this work. Early authors (SCHLOSSER, 1904; ANDRÉE, 1926) also recognized *T. amalthea* on Samos, and SOLOUNIAS (1981) stated that *T. amalthea* "is more common at Samos than in Pikermi". It is worth mentioning, however, that several races of *T. amalthea,* recorded by GAUDRY (1873) and PILGRIM & HOPWOOD (1928), represent ontogenetic stages of *M. valenciennesi*, allowing confusion between these two species [i.e., '*T. amaltheus* zweite Race' in ANDRÉE (1926: textfig. 1), and the restoration of *T. amalthea* performed by SOLOUNIAS (1994), which is based on the specimens AMNH86556 and SMF M2048, the former being an adult male of *M. valenciennesi* (Fig. 4)]. Excluding isolated tooth rows, the discrimination of which from *T. rugosifrons* is quite difficult (Fig. 2), as well as some frontlets that should rather be ascribed to *T. punjabicus*, only a few specimens labelled as being from Samos could be attributed to *T. amalthea* (NHMW A4764, SMNS13270). I have difficulties in accepting that three similar-sized and ecologically neighboring species coexisted on Samos. Since the provenance of the Samos *T. amalthea* is unknown, one possibility could be that the species was present in later levels of Samos, replacing *T. rugosifrons,* as it does on the mainland.

Samokeros minotaurus SOLOUNIAS, 1981 is a large bovid that looks like an intermediate stage between *Tragoportax amalthea* and *Alephis lyrix* GROMOLARD, 1980. Apart from Samos, *S. minotaurus* is recorded at Maragheh, Iran (MNHNP MAR1396). Its particular skull morphology allows considering it either as a terminal late Miocene Boselaphini, or as an early Bovini (i.e. discussion in SOLOUNIAS 1981:132-133), but further analysis is necessary before final conclusions.

Antilopinae GRAY, 1821

Genus *Gazella* BLAINVILLE, 1816

Gazella cf. *Gazella capricornis* (WAGNER, 1848)

(Plate 1, figs. 1, 4, 8, 10)

Synonyms: in PILGRIM & HOPWOOD (1928)

Holotype: horn-core illustrated by WAGNER (1848:Pl. IV, fig. 6)

Emended Diagnosis: A gazelle with moderately long horn-cores, moderately spaced on the frontals, gently inclined to the rear and strongly divergent in their distal part; backward curvature slight to moderate; cross-section from oval at the base to rounded toward the tips; surface covered with fine longitudinal furrows; pedicles short anteriorly; postcornual groove rather large and deep; supraorbital foramina sunken into large, triangular-shaped pits; nasals rather short and convex in lateral view; relatively long opisthocranium weakly bent on the face; relatively long premolars; p3 and p4 with well distinguished paraconid-parastylid; p4 with open posterior valley.

Type Locality: Pikermi, Greece

Occurences: Samos - upper horizons, Maragheh, Vathylakkos, Akkaşdağı.

Time Range: middle-late Turolian

Localities: Mytilinii 1A (MTLA), Mytilinii 1B (MTLB), Mytilinii 1C (MTLC); Samos Island, Greece

Material: frontlet, MTLA97, MTLA298, MTLA413, MTLB14; anterior part of cranium, MTLB16; left horn-core, MTLA194, MTLA389, MTLA222, MTLB61; right horn-core, MTLA221, MTLA413, MTLA405, MTLC36; horn-core, PMMS94; P4-M3 dex & sin, MTLA460; M2-M3, MTLA493; P2-M3, MTLA488 dex, MTLA42 sin, MTLB55 sin, MTLB199 dex, MTLC34 dex; p2-m3, MTLA489 sin, MTLB5 dex, MTLC32 sin; p4-m3 sin, MTLA 417,MTLA457, MTLA541; d2-m1, MTLA490, MTLB233.

Description & Comparison:

The greatest part of the gazelle specimens collected from the MTLA site (Tables 3, 4) belongs to a small-sized species with moderately long horn-cores, well spaced on the frontals, moderately divergent, fairly tilted backwards, slightly to moderately curved with fine longitudinal grooves and an oval basal cross-section that becomes circular towards the top (TD x 100/APD = 71.6-93.8 at the base and 82.0-100.0 at 7 cm above the base) (Table 3; Fig. 6; Pl. 1, fig. 1). The postcornual fossa is large and oval-shaped. The horn-cores are inserted above the orbits, with their anterior margin at mid-orbital level. The posterior face of the horn-cores shows a weak flattening in the largest specimens. The same horn-core pattern can be seen in some MTLB specimens (Pl. 1, fig. 4), as well as in one horn-core from MTLC, and in a partially preserved horn-core from the PMMS collection. The premolar/molar ratio ranges from 67.0 to 73.0% for the upper tooth row, and it is 58.0% in one complete lower tooth row (MTLB5; Table 4). The teeth look more hypsodont than in the other described *Gazella* species. The upper molars have strong styles, the M3 bears a strong metastyle and a thin protruding mesostyle, the P2, p2 and P3 are rather small, the paraconid of p3 and p4 is well-distinguished from the parastylid, the elongated metaconid of p3 is independent from the entoconid, the metaconid of p4 is triangular-shaped and is placed posteriorly, the labial wall of the lower molars is weakly undulated and the third lobe of m3 has a semi-circular shape (Pl. 1, figs. 8, 10). The horn-core pattern and dimensions (Table 3, Fig. 6) of the prevailing gazelle from MTLA falls well within the ranges of *G. capricornis* (WAGNER, 1848) from Pikermi, Greece (but see also KOSTOPOULOS, 2005:755) and *G.* cf. *capricornis* from Akkaşdağı, Turkey (KOSTOPOULOS, 2005). Nontheless, the tooth row proportions of the Samos sample appear slightly different from the typical Pikermi form, approaching closer to the Akkaşdağı gazelle (Table 5).

Gazella pilgrimi BOHLIN, 1935a

(Plate 1, figs. 7, 11)

Synonyms: in BOHLIN (1935a), GENTRY (1970), BOUVRAIN (1996), KOSTOPOULOS (2005) and the following discussion.

Lectotype: frontlet illustrated by SCHLOSSER (1904:Pl. XIII, fig. 1)

Emended Diagnosis: A gazelle with relatively long, sub-

parallel horn-cores, set moderately apart on the frontals, slightly curved and moderately tilted backwards; strong mediolateral compression with elliptical cross-section along the horn-core length; surface covered with deep longitudinal furrows; pedicles long anteriorly; supraorbital foramina sunken into large, triangular-shaped pits; opisthocranium moderately long, fairly bent on the face; short premolar row; p3 and p4 with weakly distinguished paraconid-parastylid; p4 with closed posterior valley; small basal pillars on m1, m2; triangular talonid on m3 marked by a posterior crest.

Type Locality: Samos-unknown level, Greece

Occurences: Ravin de Zouaves-5, Nikiti-2, Prochoma, Vathylakkos, Perivolaki, Akkaşdağı

Time Range: Early-Middle Turolian

Localities: Mytilinii 4 (MLN), Mytilinii 3 (MYT); Mytilinii 1A (MTLA), Mytilinii 1B (MTLB), Samos Island, Greece

Material: Isolated horn-cores, MYT31, MTLA64, MTLA145, MTLA438, MTLA319, MTLB208a; palate, MTLA80; p2-m3 dex & sin, MTLA213; p3-m3 sin, MTLA183, MLN29; p3-m3 dex, MLN51; m1-m3 sin, MYT83; m2-m3 dex, MTLA45.

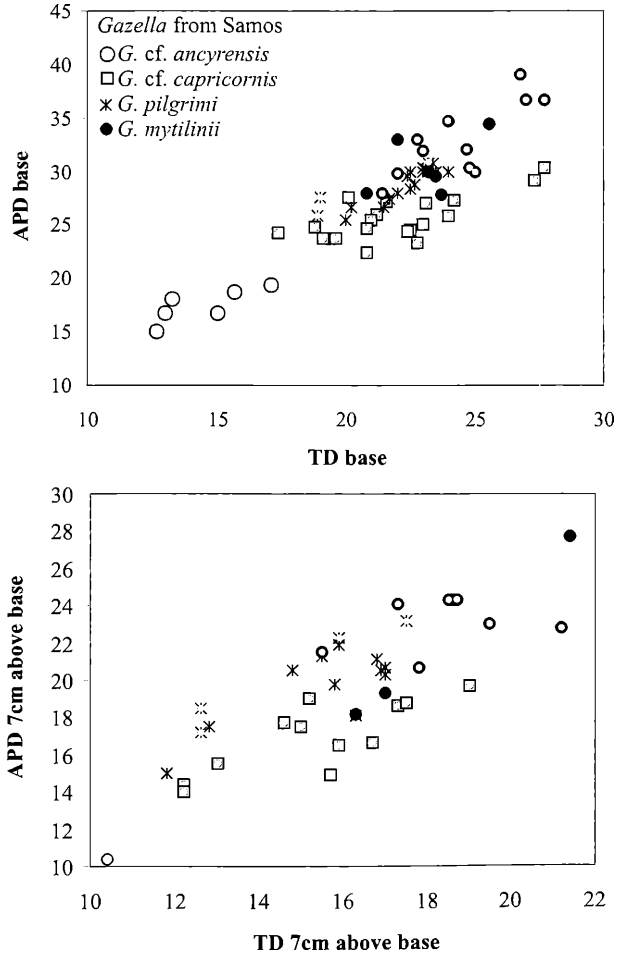

Figure 6: Scatter diagram comparing horn-core proportions of Samos *Gazella* at the base (up) and at 7 cm above the base (down). Symbols marked with an additional circle represent specimens from the new collection.

Description & Comparison:

A few isolated horn-cores from MYT, MTLA and MTLB sites (Table 3, Fig. 6) are elongated (>150 mm), strongly inclined backwards and relatively straight or feebly curved posteriorly with a strong medio-lateral compression (60.0-75.3 at the base and 68.1-75.4 at 7 cm above the base), a flat lateral face and continuous, moderately deep longitudinal grooves. The pedicles are long anteriorly. A palate of an old individual (MTLA80) and some mandibular fragments might also be attributed to the same species (Table 4). The P3 is large and trapezoidal-shaped with a strong paracone placed

	TDbase	APDbase	TD7cm	APD7cm
Gazella pilgrimi				
MYT31 ?sin	20.0	33.3	16.3	25.2
MTLB208a —	18.9	25.8	12.6	17.2
MTLA145 ?dex	23.2	30.8	17.5	23.2
MTLA438 dex	19.0	27.6	14.2	19.6
MTLA64 sin	16.7	26.3	12.6	18.5
MTLA319 —			15.9	22.3
Gazella cf. *capricornis*				
MTLA298 dex	20.8	22.4	13.0	15.5
MTLA298 sin	19.6	23.8	12.2	14.0
MTLA97 dex	21.2	26.0		
MTLA97 sin	22.5	24.5	16.7	16.7
MTLA194 sin	17.4	24.3		
MTLA413 dex	21.0	25.5	15.9	16.5
MTLA413 sin	22.8	23.4	17.3	18.6
MTLA389 sin	24.0	25.8	15.0	17.5
MTLA221 dex	18.8	24.8		
MTLA405 dex	23.1	27		
PMMS94 ?sin	19.1	23.8	12.2	14.4
MTLB61 sin	21.6	27.2	15.2	19
MTLB14 dex	20.8	24.7	14.6	17.7
MTLB14 sin	24.2	27.3		
MTLB16 dex	27.3	29.1	17.5	18.8
MTLB16 sin	27.7	30.4	19.0	19.7
Gazella mytilinii				
MTLA518 dex	25.0	30.0	18.6	24.3
MTLA518 sin	22.0	29.8	17.8	20.7
MTLB136 dex	27.7	36.7		
MTLB136 sin	27.0	36.7	21.2	22.8
MTLB225 -	22.8	33.0	17.3	24.1
MTLB58 dex	24.0	34.7	19.5	23
MTLB58 sin	26.8	39	18.5	24.3
MTLB93 dex	23.0	31.9		
MTLB92 sin	24.8	30.4		
MTLB406 dex	24.7	32.0	18.7	24.3
MTLB96 sin	21.4	28.0	15.5	21.5
MTLB62 ?dex	18.4	25.8	13.6	17.0
MTLB97 dex	20.0	25.2	14.2	17.5
MTLB91 sin	20.0	26.0		
MTLB63 dex	23.7	27.8		

Table 3: Horn-core measurements at the base and at 7 cm above the base of *Gazella* from Samos.

Specimen	LPM	LP	LM	LP2	WP2	LP3	WP3	LP4	WP4	LM1	WM1	LM2	WM2	LM3	WM3
MTLA80	53.4	23.4	31.5	8.6	5+	7.0	7.1	6.5	8.4			11.1	10.7	12.0	9.8
MTLA460			32.7					7.2	7.9	10.0	10.2	12.0	11.0	11.1	10.5
MTLA493			32.4									12.8	11.0	11.3	10.5
MTLA42	52.4	22.9	31.5	7.5	6.2	7.8	6.9	7.0	7.8	10.8	10.0	12.3	10.2		
MTLA488	54.0	22.7	33.9	7.7	6.5	7.3	6.9	7.0	8.3	11.3	10.2	13.0	11.3	11.2	10.6
MTLB16	53.4	22.3	33.0	7.3	6.6	8.6	7.3								
MTLB55	53.8	21.5	32.1	7.6	6.9	7.1	7.0	6.9	8.0	9.1	9.6	11.0	11.2	11.5	10.6
MTLB199	57.8	24.4	33.4	7.3	5.7	9.0	6.4	7.0	7.8	10.8	9.2	12.5	10.6	11.2	10.0
MTLC34	55.0	23.6	32.5	7.7	7.1	7.6		6.7	8.4	9.4	10.1	11.2	11.0	11.0	10.6
MTLB362	56.3	25.4	30.6	8.7	7.0	8.8	8.8	7.1	8.5	8.4	9.8	10.8	10.7	10.8	9.5
	Lpm	Lp	Lm	Lp2	Wp2	Lp3	Wp3	Lp4	Wp4	Lm1	Wm1	Lm2	Wm2	Lm3	Wm3
MLN29			34.5			8.0	4.0	7.2	4.7			11.4	6.3	14.0	5.4
MLN51			35.0			7.7	4.1	8.0	5.0	9.1	6.0	10.7	6.0	14.7	5.3
MTLA183			36.6			8.3	4.3	8.2	5.3			11.0	6.5	14.8	6.3
MTLA213	55.2	19.8	35.7	4.7	3.3	6.8	4.5	7.3	4.9	10.0	7.1	11.4	6.7	14.8	6.4
MTLB5	56.4	21.3	36.7	5.0	3.4	8.3	4.0	8.6	4.8	9.2	6.3	11.5	6.6	15.2	6.3
MTLA417			36.8					9.6	4.7	9.5	6.0	11.6	6.3	15.5	6.3
MTLA457								10.3	5.0					16.0	6.5
MTLA489			37.4			7.2	4.4	8.3	5.2			11.5	6.6	15.8	6.0
MTLA45												11.5	6.0	16.6	6.5
MTLA541			34.8					8.0	4.4			11.5	6.5	15.0	6.0
MYT83			38.5							10.3	5.7	11.6	6.3	17.0	6.4
MTLC32						7.4	4.1					11.1	7.2	15.2	6.0
MTLB362	57.2	21.4	36.3	6.2	3.5	6.7	4.8					11.6	6.6	14.5	6.4

Table 4: Upper and lower dental measurements of *Gazella* from MLN, MYT, MTLA-B-C, Samos.

anteriorly; the paracone and the metacone ribs of M1 and M2 are weak to absent, but the paracone rib of M3 is quite strong; the paraconid and the parastylid of p3 and p4 are weakly expressed and their metaconid points strongly to the rear, closing the posterior valley, while the anterior valley remains largely open (Pl. 1, fig. 7); the lingual wall of the lower molars is gently undulated and a thin to moderate parastylid appears (Pl. 1, fig. 7); a small basal pillar exists on m1 and also, but less so on m2; the third lobe of m3 is marked posteriorly by a fine crest. The premolars are rather short compared to the molars; the premolar/molar ratio is 74.3% in the upper (MTLA80) and 55.4% in the lower tooth row (MTLA213). Two p3-m3 specimens (Table 3) from MLN should also be ascribed to the same *Gazella* species. The molar row is about 35 mm long. The paraconid and the parastylid of p3 and p4 are weakly separated, and the metaconid is elongated and points to the rear (Pl. 1, fig. 11). A small basal pillar is present on m1 and the talonid of m3 is sub-triangular shaped, with a postero-lingual crest. The described horn-core and dental characters match those of *Gazella pilgrimi* BOHLIN, 1935a (GENTRY, 1970; BOUVRAIN, 1996; KOSTOPOULOS, 2006a), which was a replacement name for *Gazella gaudryi* SCHLOSSER, 1904 (:Pl. XIII, fig. 1) from the "braunen Tuffen" of Samos.

Gazella mytilinii PILGRIM, 1926
(Plate 1, figs. 2, 5, 6, 9)

Synonyms: in PILGRIM & HOPWOOD (1928), SOLOUNIAS (1981)

Lectotype: skull, illustrated by ANDRÉE (1926: Pl. XVI, figs. 1, 6, 7), NHMW A4777

Emended Diagnosis: A gazelle with uprightly inserted, almost parallel, moderately long and robust horn-cores, closely settled on the frontals and strongly curved backwards; a weak torsion may occur; cross-section elliptical at the base toward oval at the tips; surface covered with deep longitudinal furrows, especially strong anteriorly and posteriorly; pedicles short anteriorly; postcornual fossa rather small, rounded and deep; opisthocranium relatively long and weakly bent on the face.

Type Locality: Samos - unknown level, Greece

Time Range: middle Turolian

Localities: Mytilinii 1A (MTLA), Mytilinii 1B (MTLB); Samos Island, Greece

Material: Frontlet, MTLA518, MTLB58, MTLB169, MTLB136; left horn-core, MTLB225, MTLB91, MTLB92, MTLB96; right horn-core, MTLB93, MTLB406, MTLB63, MTLB97, MTLB62; upper and

lower dentition MTLB362. Provisionally ascribed: female cranium PMMS63.

Description & Comparison:

Most *Gazella* specimens from MTLB (Tables 3, 4) belong to a small sized species, with moderately long and robust horn-cores (Table 4; Fig. 6) that are closely settled on the frontals, weakly tilted, strongly curved backwards and running in parallel to each other (Pl. 1, figs. 2, 5, 6). The horn-cores are placed above the orbits, with their anterior margin at the mid-orbital level. The pedicles are short anteriorly (Pl. 1, figs. 2, 5). The horn-core surface bears strong and deep longitudinal grooves, especially in font and back (Pl. 1, figs. 2, 5). Their cross-section is elliptical throughout their length (68.7-87.3 at the base and 71.7-92.0 at 7 cm above the base). The postcornual fossa is rather small, round and deep. The specimens MTLB62, 63, 91 and 97 are smaller than the rest of the sample (Table 4), but they still retain the strong backward curvature and the deep furrows, suggesting that they probably represent young individuals (Davis, 1980 fide Bouvrain, 1996). A feeble torsion is present on the largest specimens (MTLB58; Pl. 1, fig. 2). The frontlet MTLA518 (Pl. 1, fig. 6) fits in perfectly with the main *Gazella* morphotype from MTLB and is regarded as conspecific.

The few badly preserved dentitions ascribed to this species belong to a single individual (Table 4; Pl. 1, fig. 9). The teeth are less hypsodont than in *G.* cf. *capricornis* and *G. pilgrimi* with comparatively large upper premolars (the premolar/molar ratio is 83), long p2, fused metaconid and entoconid on p3, narrow lower molars with a strong parastylid and entostylid, well-convex labial ribs, and a rounded third lobe on m3.

Pilgrim (1926) united *Gazella* sp. of Schlosser (1904: Pl. VIII, fig. 7; Pl. XIII, fig. 5) and *Gazella schlosseri* Andrée, 1926 under *Gazella mytilinii*. Pilgrim & Hopwood (1928) gave the first review of this species, to which they also assigned the Samos frontlet NHML M5420, an act already discussed by Solounias (1981:151) and Bouvrain (1996:124). Solounias (1981) reviewed *G. mytilinii* based mostly on the holotype cranium NHMW A4777 (Andrée, 1926:Pl. XVL, figs. 1, 6, 7; Solounias, 1981:fig. 47); he also referred the cranium SMF M1970 to this species, which I unfortunately have not seen.

Little is really known about the morphological variation of *G. mytilinii*. According to the skull specimen NHMW A4777 and the illustrations of Schlosser (1904), the horn-cores of *G. mytilinii* are uprightly inserted above the orbits, closely settled on the frontals, rather short or moderately long as those of *G. capricornis*, strongly curved backwards as most specimens of *G. deperdita* (i.e., Heintz, 1971) and parallel to each other, or weakly divergent. The basal medio-lateral compression of the horn-cores is similar to that seen in *G. pilgrimi*, but much less towards the tips, where their cross-section becomes oval-shaped (Fig. 6). The horn-core surface bears deep continuous furrows, especially marked on the anterior and posterior face. The pedicles are short anteriorly and well-distinct from the horn-cores. This set of characteristics exists on MTLA518 and in most specimens from MTLB, which consequently are assigned to *G. mytilinii*.

Solounias (1981) suggested that NHMW A4777 might represent a horned female of *G. mytilinii*. Nevertheless, a hornless skull from Samos (PMMS63; Pl. 1, fig. 3) seems to represent the female condition of this species better. PMMS63 is well-preserved, but its dentition is badly damaged. The orbit is large and rounded, with its anterior margin above the M2-M3 limit. The postero-dorsal margin of the orbit projects laterally. The lachrymal fossa is barely defined and shallow. The infraorbital foramen opens above P2-P3 limit. The palatine condition is "U"-shaped and the choane opens just behind the M3. The opisthocranium is rather short, with a bulbous fontoparietal region; its posterior part slopes strongly on the basicranial axis and forms an obtuse angle with the occiput. The occipital is rather high and faces partly laterally. The posterior tuberosities of the basioccipital are strong and the anterior ones are well-developed and closely settled togehter, separated by a deep central groove.

Discussion:

Even though abundant and widespread during the late Miocene, Old World *Gazella* remains poorly understood and insufficiently resolved from a systematic point of view. Long-lasting nomenclatural inconsistencies together with interspecific morpho-ecological overlapping and intraspecific morpho-metrical variation, usually affected by ontogenetic allometry, do not have allowed clear taxonomical allocation yet. The gazelles of Samos certainly join this case as the number of occurring species and their chronostratigraphic distribution remained unknown.

Gentry (1970) incorrectly included *Gazella* n. sp. of Andrée (1926:Pl. XVI, figs. 2, 5; PIM199) and *Gazella* sp. of Andrée (1926:169; PIM197) into *G. pilgrimi*, and the same is true for the small Samos *Gazella* at the NHML (Pilgrim & Hopwood, 1926:12). On the contrary, *G. longicornis* Andrée, 1926 (:Pl. XVI, figs. 3, 9; PIM200) is certainly synonymous with Schlosser's species, as Gentry

Table 5: Tooth row measurements and proportions of *Gazella capricornis* from Pikermi and *Gazella* cf. *capricornis* from Samos and Akkaşdağı. Data from Kostopoulos (2005).

	Gazella capricornis		
Measurement	Pikermi	Samos	Akkaşdağı
P2-M3 length	48.6-54.9 (n=9)	52.4-57.8 (n=6)	54.0-57.0 (n=6)
P2-P4/M1-M3 *100	75.4-78.4	67.0-73.0	67.7-74.6
p2-m3 length	49.4-56.4 (n=8)	56.4 (n=1)	53.7-58.8 (n=3)
p2-p4/m1-m3*100	59.7-70.8	58.0	55.2-56.4

(1970:297) already pointed out. Solounias (1981) inexplicably merged *G. pilgrimi* with *Gazella capricornis* (Wagner, 1848), originally known from Pikermi (Greece) but Bouvrain (1996) definitely fixed this misunderstanding and restored the morphological frame of *G. pilgrimi*, based on a large sample from Axios valley, Greece. Solounias (1981:fig. 48) refers the Samos cranium AMNH20580 from B. Brown's Q5 to the Chinese *G. dorcadoides* Schlosser, 1903 (re-defined by Bohlin, 1941) but this specimen also shows great similarities with skull material of *G. pilgrimi* from Axios valley (Bouvrain, 2001: fig. 4 and MNHNP Slq809, Arambourg & Piveteau, 1929:Pl. VIII, fig. 3). Although differences between the Samos and Axios valley samples do occur, they do not exceed ordinary intraspecific variability, and I assign the Q5 gazelle to *G. pilgrimi*. The frontlets AMNH20775 and AMNH20776 from B. Brown's Qx and NHMW A4776 could belong to this species, as well.

One left p2-m3 and a mandible at the NHML (M4177 and M4176, respectively) ascribed by Pilgrim & Hopwood (1928) to *G. gaudryi* Schlosser, 1904, might also belong to *G. pilgrimi*. The lower tooth row is rather small (p2-m3 = 50.3-52.5 mm), with short premolars compared to the molars (p/m ratio from 56 to 58%), a widely open anterior valley on p3 and p4 and no goat fold on the molars.

The cranium AMNH20570 from Q5, assigned by Solounias (1981:fig. 46) to his '*G. capricornis*', is indeed similar to several *G. capricornis* crania from Pikermi, from which it differs by the slightly longer and wider opisthocranium. *Gazella* n.sp. of Andrée (1926:Pl. XVI, figs. 2, 5; PIM199) is probably a young individual of *G. capricornis*, fully compatible with MTLA298. The hornless cranium AMNH97292, also from Q5, with a "V"-shaped palatine condition, the anterior border of the orbit above M3 and rather hypsodont M3 might represent a female of the same species.

I think *Gazella* sp. of Andrée (1926:169; PIM197) is *G. mytilinii*, as it shares a common morphology with the MTLB sample of this species. The skull specimen AMNH20706 from B. Brown's Q1 is probably conspecific but its smaller horn-cores might indicate an immature individual like MTLB97 and MTLB62. Although the preserved left horn-core of NHML M5420 appears somewhat larger than in *G. mytilinii*, especially at 7 cm above the base, and its longitudinal furrows are less deep and more discontinuous, the rest of its morphological features fit in pretty well with those of the species. A female cranium at AMNH (20571) from B. Brown's Q5 has a very similar structure to PMMS63, and I think both represent females of *G. mytilinii*.

The small gazelle with short, slim, fairly straight, weakly medio-laterally compressed and rather widely spaced horn-cores present in the NHML Samos collection, as well as the horn-cores MGL S950 from Forsyth-Major's 'Stefano' and NHMW1911v4, have to be attributed to a distinct species (Fig. 6). Pilgrim & Hopwood (1928) assigned the NHML sample to *G. gaudryi* Schlosser, 1904, suggesting that they represent females and young individuals of this species. Nevertheless, females of *G. pilgrimi* have been proved to be hornless (Korotkevitch, 1976; Bouvrain, 1996). The small Samos horn-cores are very similar to those of *Gazella* sp. from Kemiklitepe D and Garkin, Turkey (Köhler, 1987; Bouvrain, 1994b), as well as to several specimens from Maragheh at NHMP. Bouvrain (1996:129) suggests affinities of this group of gazelles with *Gazella gracile* Korotkevitch, 1976, from Berislav, Black Sea region, a form that was originally described as a small-sized sub-species of *G. schlosseri* Pavlow, 1913. The horn-cores of *G. schlosseri* differ from those of the small gazelle from Samos, Kemiklitepe D and Maragheh in the shorter pedicle, the more bulbous basal part, the sigmoid anterior profile and the weaker posterior curvature. Most of the morpho-metrical features of the Samos, Maragheh and Kemiklitepe D sample recall the Vallesian *Gazella ancyrensis* Tekkaya, 1973 (:Pl. I, figs. 1-2; Pl. II, fig. 1) from Middle Sinap and I suggest ascribing them to *G.* cf. *ancyrensis*.

Genus *Majoreas* Kostopoulos, 2004

?*Majoreas* sp.

Locality: Mytilinii 3 (MYT), Samos Island, Greece
Material: part of horn-core, MYT128

Description & Comparison:
A badly preserved part of a rather right torsioned horn-core, has an oval basal cross-section (minimum basal axis = 33.0 mm; maximum basal axis = 45.3 mm) and an irregular antero-medial keel restricted in its proximal part; the horn tapers abruptly upwards and the cross-section becomes sub-triangular slightly above the keel's top. The medial surface is rough, porous and bulbous at the base, whereas the lateral surface is smooth. The horn-core should have been short. Although the orientation of the horn-core (left/right) is highly speculative, its morphological features remove it from *Oioceros* Gaillard, 1902, whose horn-cores have tighter torsion, exaggerated by deep furrows. MYT128 is also different from *Samotragus* Sickenberg, 1936, whose horn-cores bear a weak antero-lateral keel, and *Samodorcas* Bouvrain & Bonis, 1985, which has very compressed horn-cores. *Protragelaphus* Dames, 1883, has more tightly torsioned horn-cores with a posterior keel, whereas *Parurmiatherium* Sickenberg, 1932, and *Criotherium* Major, 1891a, have a completely different horn-core structure. Among common late Miocene spiral-horned antelopes, *Prostrepsiceros* Major, 1891a, and *Majoreas* Kostopoulos, 2004, show the greatest similarity with MYT128. *Prostrepsiceros* is known from Samos by two species *Pr. fraasi* (Andrée, 1926) and *Pr. zitteli* (Schlosser, 1904); the former does not show keel development, whereas the latter is significantly smaller than MYT128, has a stronger antero-medial keel and a significant antero-posterior compression. *Majoreas* might fit in better with the MYT128 morphology, in having weakly spiraled and medio-laterally compressed horn-cores with a weak antero-medial keel.

Table 6: Cranial measurements of *Sporadotragus parvidens* from MTLA, PMMS, Samos.

Measurements	MTLA3	MTLA13	PMMS97
L basion-choane	99.7		
L basion-P2	155.6	158.6	
L frontonasal suture-occipital	138.5	136.8	
L frontoparietal suture-occiput	66.0	62.2	67.5
L supraorbitals-frontoparietal	72.7	63.7	71.4
L supraorbitals-occipital	131.0	120.0	127.8
L anterior hc- occipital	124.5	115.7	126.0
L anterior orbit-anterior P2	76.3	74.3	
W skull at the lateral edges of hc	99.4	101.3	100.5
W braincase	68.1	69.0	69.3
W supraorbital pits	47.6	48.5	51.0
W bicondyles	49.5	50.6	
W bimastoids	70.9	74.5	77.0
W ptbc	31.7		28.5
Watbc	24.9	26.5	
H occiput	34.5	31.4	
L hc (along anterior face)			390.0
H hc (posterior chord)			280.0
TD hc base	37.8	41.0	36.3
APD hc base	48.9	45.2	47.0
TD hc at 10 cm above the base		31.0	26.0
APD hc at 10 cm above the base		36.3	35.5

Discussion:

The Samos spiral-horned antelopes remain the least known and the most intriguing group of bovids. The current archive records six genera and eight medium-sized species: four with heteronymous spiraled horn-cores and four with homonymous ones. '*Prosinotragus*' sp. of Solounias (1981; NHMW A4778) has several features in common with *Samotragus crassicornis* Sickenberg, 1936, and they could be synonymized at generic level. The apparent high diversity of Samos spiral-horned antelopes does not, however, reflect abundance, as five species are known by their holotype/lectotype only, whereas the other three are represented by a few specimens only; the new collection has, unfortunately, nothing to add to this scrappy list of material.

What is also amazing is the weak correspondence between the spiral horned antelopes of Samos and those from continental Greece. Indeed, apart from *Protragelaphus skuzesi* Dames, 1883, the rest of the spiral-horned antelopes recorded on both sides of the Aegean Sea is quite different at species level, at least. On the Greek mainland, *Samotragus* is known only by a small and primitive late Vallesian species from Axios valley, whereas *Oioceros* is represented there by a synchronous but significantly smaller species than *O. wegneri* Andrée, 1926, from Samos. *Samodorcas* is missing from continental Greece, while the well-documented *Palaeoreas* Gaudry, 1861, is replaced on Samos by forms referred to *Majoreas* by Kostopoulos (2004). *Prostrepsiceros* is represented on Samos by *Pr. zitteli* and *Pr. fraasi,* and even though the latter species might also be present at Perivolaki (Kostopoulos, 2006b), the continental archieve mostly records *Pr. axiosi* Kostopoulos, 2004 and *Pr. rotundicornis* (Weithofer, 1888). *Pr. zitteli* has often been confused with *Pr. houtumschindleri* (Rodler & Weithofer, 1890) from Maragheh (e.g., Solounias, 1981; Bibi, 2008), but I think it is distinct, and probably closer to the early Turolian *Pr. axiosi* from Axios valley. Suggested synonymy between *Pr. fraasi* and *Pr. rotundicornis* (e.g., Gentry, 1971; Solounias, 1981) seems also unlikely to me as the horn-core pattern in the two species is quite different.

Genus *Sporadotragus* Kretzoi, 1968

Sporadotragus parvidens (Gaudry, 1861)

(Plate 2)

Synonyms: in Solounias (1981), Geraads et al. (2006)
Lectotype: incomplete skull MNHNP PIK2453, illustrated by Gaudry (1861:Pl. IX, fig. 4; 1862-67: Pl. XLVII, figs. 6, 7); note that both illustrations show a 'negative' (left as right) view of the same specimen.
Diagnosis: as in Geraads et al. (2006:474)
Type Locality: Pikermi, Greece
Occurences: Samos
Time Range: Middle Turolian

Locality: Mytilinii 1A (MTLA), Mytilinii 3 (MYT), PMMS; Samos Island, Greece
Material: Crania, MTLA3, MTLA13; part of horn-core, MYT63; opisthocranium PMMS97; palate, MTLA19, MTLA22; palate with P3-M3 dex and P2-M2 sin, MYT85; mandible, MTLA270; right mandibular ramus with p2-m3, MTLA301; p4-m3sin, MTLA434; m1-m3 dex, MTLA373; left mandibular fragment with p3-m3, MYT86.

	MTLA3	MTLA13	MTLA19	MTLA22	MYT85		MTLA301	MTLA270	MTLA373	MTLA434
PM	71.3	72.2	77.5	76.0		pm	76.0	76.0		
P	30.5	31.5	33	31.5	29.6	p	29.2	28.9		
M	41.6	43.4	48.7	46.7	43.4	m	46.5	48		48.3
LP2	10.5	10.0	10.7	9.5	9.2	Lp2	6.8	8.5		
WP2	9.0	9.5	8.6	8.3	8.5	Wp2	4.5	5.2		
LP3	10.5	10.8	11.0	10.2	10.5	Lp3	10.0	10.0		
WP3	10.2	10.5	10.7	8.7	10.1	Wp3	6.3	6.5		
LP4	9.7	9.8	10.0	9.9	10.2	Lp4	11.8	10.4		10.4
WP4	11.2	11.4	11.5	12.3	11.1	Wp4	7.5	7.0		7.2
LM1		13.5	16.0	15.0	14.4	Lm1	11.5	11.3	11.5	11.0
WM1		14.0	13.7	15.0	13.3	Wm1	9.5	9.0	9.0	9.8
LM2		15.5	18.5	18.2	16.0	Lm2	14.2	15.0	14.1	14.2
WM2	16.1	15.5	16.5	15.0	14.2	Wm2	10.0	9.5	10.4	11.2
LM3	17.8	16.5	18.2	17.2	15.0	Lm3	22.1	23.0		23.0
WM3	15.5	15.0	15.3		12.8	Wm3	10.1	9.8		10.2

Table 7: Upper and lower dental measurements of *Sporadotragus parvidens* from MTLA and MYT, Samos.

Description & Comparison:

Both cranial specimens MTLA3 and MTLA13 (Table 6; Pl. 2, figs. 1, 2) lack the anterior part of the muzzle and the distal part of the horn-cores. The opisthocranium is short compared to the face, which slopes abruptly on the braincase, but less than in most Pikermi specimens; the cranial roof forms an angle of about 100-105° with the anterior part of the frontals. In lateral aspect, the occiput forms a 120-135° angle with the cranial roof, whereas the palate forms a 25-28° angle with the basioccipital. The braincase widens anteriorly. The anterior margin of the orbit is placed above the anterior lobe of M3; the orbit is round and slightly extends laterally. The lachrymal fossa is small, rounded and rather shallow, well-localized just in front of the orbit. The frontals are strongly inflated between the horn-core bases. The interfrontal suture is constricted throughout its length. In lateral profile, the fronto-nasal region appears gently concave and the cranial roof weakly convex. A narrow ethmoidal fissure is present in MTLA3 (Pl. 2, fig. 1). The infraorbital foramen opens over the P2-P3 limit. The supraorbital foramina are small, widely spaced and open directly into the frontals. The nasals widen posteriorly and their contact with the frontals is placed just in front of the orbits. The occipital condyles do not stick out from the occiput and they point postero-ventrally. The foramen magnum is rather large and quadrangular-shaped. The occipital face is wide and low, and the occiput faces mostly posteriorly, as do the mastoids too. The external occipital crest is weakly developed. The basioccipital is long and moderately narrow, with strong crest-like posterior tuberosities and bulbous-elongated anterior ones (Pl. 2, fig. 2b). A wide, shallow groove runs along the midline of the basioccipital. The auditory bulla is probably small. The palatine condition is "U" shaped and the choane opens behind M3, whereas the lateral indentations go deeper forward, reaching M3. The horn-cores are inserted above the orbits and slightly posteriorly positioned; their anterior border is over the middle of the orbit. In anterior view, the horn-cores diverge moderately, whereas in lateral aspect, they are openly curved backwards (Pl. 2, fig. 2a). Their cross-section is oval throughout their length, with a wide front face at the base. There are no evidences of keels and the horn-core surface is ornamented by thin, asymmetrical discontinuous furrows.

The cranial specimen PMMS97 (Table 6; Pl. 2, fig. 3) lacks the face, but it preserves the complete left horn-core. The opisthocranium morphology and dimensions perfectly match those of the previously described skulls from MTLA. The horn-core is somewhat more compressed mediolaterally than in MTLA and lacks the anterior face at its base, but these differences seem to express intraspecific variability. As in MTLA, the thicker part of the horn-core base lies anteriorly. The left horn-core outlines a great arch, slightly declining inwards at its tip.

The specimen MYT63 is a distal part of a left horn-core, with a characteristically oval cross section. The speci-

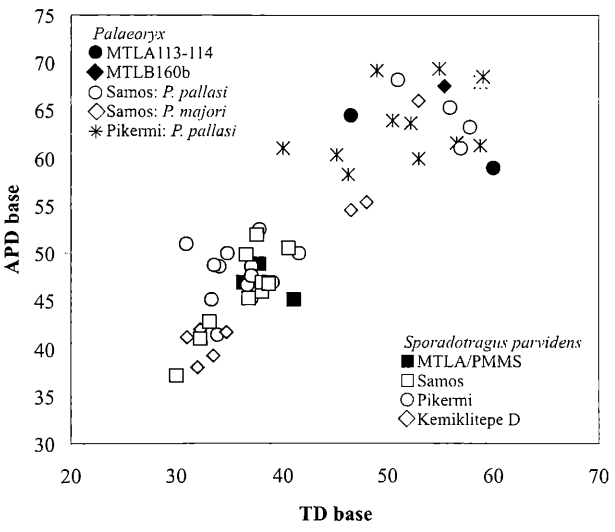

Figure 7: Scatter diagram comparing basal horn-core proportions of *Sporadotragus parvidens* and *Palaeoryx* from several sites.

men shows a strongly convex medial surface, a backward curvature and a minimal inward flexion. Its morphology and proportions in the basal preserved part (34.3 x 39.8 mm) indicate a rather medium-sized bovid, similar to *Sporadotragus parvidens* from MTLA.

The upper premolar/molar ratio ranges between 60.2 and 77.3% (n = 6) in MTLA and it is about 68% in MYT85; tooth measurements are given in Table 7. The P2 is trapezoidal-shaped, with a strong paracone rib placed anteriorly (Pl. 2, fig. 4). The P3 is less asymetrical than P2, but with a similarly developed paracone rib and a strong-sharp parastyle; lingually, there is a hint of bilobation. The P4 has a strong parastyle and metastyle and a less protruding buccally paracone rib that is placed more centrally (Pl. 2, fig. 4). The upper molars have the typical morphology of the group with a narrow, lingually protruding anterior lobe and a wide posterior one. The parastyle, the mesostyle and the paracone rib are strong, whereas the metastyle is important only on M3, however without flaring posteriorly. There are no basal pillars and M1 and M2 bear a central islet in mid-wear stage (Pl. 2, fig. 4).

The first two incisors (MTLA270; Pl. 2, fig. 6) are trapezoidal-shaped with i1 slightly wider than i2; i3 and c are oval-shaped, with the former smaller than the latter. The lower premolar row is short compared to the molars (Table 7). On p3, the paraconid and the parastylid are undistinguished, the metaconid is elongated and oblique towards the rear and the entoconid is quickly fuses with the entostylid (Pl. 2, figs. 5, 7); an incipient hypoconid appears labially. On p4 the metaconid extends anteroposteriorly and the anterior valley closes in mid-wear stage. Like on p3, the paraconid is undistinguished from the parastylid, and the entoconid and the entostylid merge rapidly (Pl. 2, figs. 5, 7). The hypoconid is well-developed on the buccal face. The lower molars have no goat folds or basal pillars (Pl. 2, figs. 5, 7). The parastylid is weak, except for m3, which is also associated by a large third lobe. The badly preserved mandibular fragment MYT86 belongs to an old individual and does not permit significant morphological observations. The molar row is 44 mm long. The anterior valley of p3 is open and the third lobe of m3 is rather large. Although the morphology is not clear enough, the teeth fit in quite well with those of the palate MYT85, suggesting that they plausibly belong to the same species.

Sporadotragus Kretzoi, 1968 and *Pseudotragus* Schlosser, 1904 take part in a long-lasting, but inconclusive discussion that considers them either as synonymous or as valid genera (e.g., Solounias, 1981; Köhler, 1987; Bohlin, 1936; Bosscha-Erdbrink, 1988; Gentry, 1999; Geraads et al., 2006). In the most recent review Geraads et al. (2006) suggested that *Pseudotragus* usage should be restricted to the lectotype of *P. capricornis* (but see the following discussion) and re-instated *Sporadotragus* for the species *S. parvidens* (Gaudry, 1861) from Pikermi = *S. schafferi* (Andrée, 1926) from Samos and the new species *S. vasili* Geraads, Spassov & Kovachev, 2006 from Bulgaria. I agree with Solounias (1981) and Geraads et al. (2006) in considering *Sporadotragus* Kretzoi, 1968 as generically distinct. The new Samos material is morpho-metrically uniform and differs from the lectotype of *Pseudotragus capricornis* Schlosser, 1904 (:Pl. X, fig. 7), as well as from other specimens referred to this species, in the weaker medio-lateral compression of the horn-cores that have a front surface and no keels, the strongly elevated frontals between the horn bases and the stronger cranio-facial angle. Skull material from MTLA, MYT and PMMS perfectly matches with other specimens of *Sporadotagus parvidens* from Samos (SMF1975, PIM133, NHMW 1911v1, AMNH20777-Qx, AMNH20689, 23035- Q1, AMNH22941-Q5). Comparison of the entire Samos *S. parvidens* sample with the Pikermi and Kemiklitepe D ones shows similar horn-core proportions (Fig. 7). Nonetheless, the Pikermi form differs from Samos *Sporadotragus* by the narrower and higher occiput that is more inclined on the cranial roof, the shorter opisthocranium with a more convex roof, the more inclined braincase on the face (95-105° for 5 Samos specimens instead of 80-93° for 5 Pikermi specimens), and the less lingually extended protocone on the molars. Although the differences between the Pikermi and the Samos population seem to be rather constant and striking enough, some Pikermi specimens (NHML M11428) weaken the observed morpho-metrical gap, making hazy a possible separation at species level hazy. Thus, I shall continue to assign the Samos *Sporadotragus* to *S. parvidens*, following Geraads et al. (2006).

Genus *Palaeoryx* Gaudry, 1861

Palaeoryx majori Schlosser, 1904

(Plate 3, fig. 1)

Synonyms: *Palaeoryx laticeps* Andrée, 1926:Pl. XIII, figs. 4, 6

Lectotype: incomplete skull, illustrated by Schlosser (1904:Pl. VII, fig. 5)

Emended Diagnosis: A large antelope with strongly laterally inserted and significantly divergent horn-cores placed behind the orbits, but upright compared to the cranial roof; horn-cores curved backwards and significantly bent inwards at their tips with weak mediolateral compression and feeble distal twisting; opisthocranium relatively short with more open occipito-parietal than fronto-parietal angle; long premolars compared to the molars.

Type Locality: Samos - unknown level, Greece

Occurences: Akkaşdağı, Halmyropotamos

Time Range: middle-late Turolian

Localities: Mytilinii 1B (MTLB), Mytilinii 1C (MTLC); Samos Island, Greece

Material: part of cranium MTLB160b; opisthocranium PMMS80; palate, MTLB157; mandible, MTLB242; p4 dex, MTLB57; right mandibular ramus with p2-m3, MTLC23

Description & Comparison:

The cranio-facial angle is about 120°. The orbits are rounded and placed beneath the horn-cores (Pl. 3, fig. 1a). The opisthocranium is short and rather narrow, but longer than in *P. pallasi* (Table 8; Pl. 3, figs. 1a, 2a). The zygomatic arches deepen towards the front. The interfrontal suture is

Measurements	MTLB160b	PMMS80	MTLA113	MTLA114	MNHNP PIK2456	NHML M10831	NHML M10832
L basion-choane			133.0			131.2	
L basion-P2			250.0			234.6	216
L frontonasal-frontoparietal	125.0		126.0	119.3	101.7	99.4	106.4
L frontonasal-occiput	176.0		187.0			151.4	161.6
L frontoparietal-occiput	64.3		75.0			65.0	68.7
W braincase	88.1	95.3	93.4	94.0		84.5	90.0
W skull behind hc	87.5		99.0	94.0	99.0		
W bi-orbital	150.0		170.9	150.0		157.0	156
W suptaorbital pits	76.6		76.0	62.5	58.5	69.5	62.4
W bimastoids	119.4	107.2	124.0			105.0	110.8
W bicondyles	76.6	72.0	73.5			72.2	66.6
W ptbc	44.5	43.1	43.5			42.6	39
W atbc	31.0	29.3	38.5			28.9	31.3
TD orbit			55.0	57.8			55.3
W palate at back of M3			55.0	51.5	62.0	55.0	55.5
H occiput	49.0	52.0	54.5			53.3	51.0
Length hc	330.0		360.0		350.0		275.0
TD hc base	55.5		60.0	46.5	59.0	55.0	45.1
APD hc base	67.5		59.0	64.5	68.5	69.4	60.3
TD hc at 10 cm above base	40.4		40.3				34.5
APD hc at 10 cm above base	48.7		44.0				42.5
L P2-M3			114.0	117.0	111.5	114	104.5
L P2-P4			49.2	50.4	49.8	49.3	45.3
L M1-M3				68.4	68.0	68.2	61.3

Table 8: Cranial measurements of *Palaeoryx* from Samos and Pikermi. *P. majori*: MTLB160b, PMMS80 Samos; *P. pallasi*: MTLA113, 114, Samos and MNHNP PIK2456, NHML M10831, 10832, Pikermi.

invisible and the frontals are not inflated between the horns. The basioccipital is elongated, sub-triangular and weakly concave in lateral aspect. The occipital face is hexagonal-shaped, forming an obtuse angle of 135° with the cranial roof (Pl. 3, fig. 1c). A thin but sharp external occipital crest is associated by deep scars on either side. The occipital condyles are widely expanded and point postero-ventrally. The paroccipital processes are moderately developed and strongly oblique with regard to the sagittal plane. The mastoid expands laterally. Both the posterior and the anterior tuberosities of the basioccipital are crest-like and vertical to the sagittal plane, with the former being stronger than the latter (Pl. 3, fig. 1d). The supraorbital foramina are simple and widely spaced. The horn-cores are inserted above the posterior part of the orbits at right angles to the cranial roof and curve strongly laterally, forming an open arch to the rear (Pl. 3, figs. 1a, b). In anterior view, they diverge significantly, but they re-curve inwards at their tips (Pl. 3, fig. 1b); they appear feebly twisted in their distal part. Their basal cross-section is oval (Table 8) with a weakly convex medial face and an extremely convex lateral one.

It is quite possible that the palate MTLB157 and the mandible MTLB242 belong to the same individual with MTLB160b (Tables 9, 10; Fig. 8). The upper premolars are large compared to the molars (P/M index 74-78). On P2, the parastyle does not reach the buccal face (Fig. 8). The paracone is placed anteriorly and is strong with a weakly concave posterior flange. On P3, there is a hint of lingual bilobation and the occlusal face is trapezoidal-shaped. The parastyle is strong and vertical to the anteroposterior axis of the tooth, while the paracone is similar to P2 (Fig. 8). The P4 is wide and narrow, with a barely observable lingual groove. The parastyle, the paracone and the metastyle are weakly developed. The molars have a rudimentary basal tubercle, but no pillar, the protocone is rather angular and the mesostyle is strong and rather thick, but less so, than the parastyle (Fig. 8). There are no central islets.

The incisor arcade is semi-rounded and the occlusal surface of i1 and i2 is sub-horizontal (Fig. 8). The i1 and i2 are equally wide, as are i3 and c. The premolar row represents 64.6-70.7% of the tooth row. The p2 is simple, without a paraconid and with an incipient entoconid (Fig. 8). On p3, the paraconid is separated from the parastylid in the upper part of the crown; the metaconid is elongated and inclines posteriorly, leaving the anterior valley open; the entoconid is vertical to the tooth axis and the hypoconid is weakly developed and narrow (Fig. 8). On p4, the metaconid has a central position, it is sub-rounded and does not fuse either with the paraconid or with the entoconid until reaching a very advanced wear stage (Fig. 8). The paraconid is weakly separated from the parastylid, whereas the entoconid and the entostylid quickly fuse together. The hypoconid is well-developed but narrow. All molars bear a rather strong but short basal pillar. The parastylid is moderately developed. The mandibular ramus MTLC23 is dimensionally close to MTLB242 (Table 10) and has a similar morphology, but

its p4 shows a continuous lingual wall and a less developed hypoconid. MTLB160B is morpho-metrically identical to a set of other Samos crania including the lectotype of *P. majori* (Schlosser, 1904:Pl. VII, fig. 5), PIM 121 (holotype of *Palaeoryx laticeps* Andrée, 1926) and NHMW A4779. Adopting Gentry's (1971) taxonomy, most of the later authors considered *Palaeoryx majori* Schlosser, 1904 as a junior synonym of *P. pallasi* (Wagner, 1857). Based on Samos and Turkish material I have recently reinstated, however, *P. majori*, and I gave differential features between these two species (Kostopoulos, 2005:780–781, fig. 24, tab. 14); Table 11 updates and summarizes these results. As I have already pointed out (Kostopoulos, 2005), the dentition of *P. majori* was not known for certain since Schlosser (1904) assigned some isolated dentitions to the species that, however, could belong to *P. pallasi* as well. Based on Akkaşdağı material, I supposed that *P. majori* had a shorter molar row than *P. pallasi*. The new material from Samos offers some more data: *P. majori* is characterized by a slightly smaller dentition than *P. pallasi* and an equally long premolar row, but the molars appear to be significantly shorter in the former species.

Palaeoryx pallasi (Wagner, 1857)

(Plate 3, figs. 2, 4)

Synonyms: *Palaeoryx woodwardi* Pilgrim & Hopwood, 1928

Lectotype: the skull and horn-cores illustrated by Wagner (1857:Pl. VII, fig. 21)

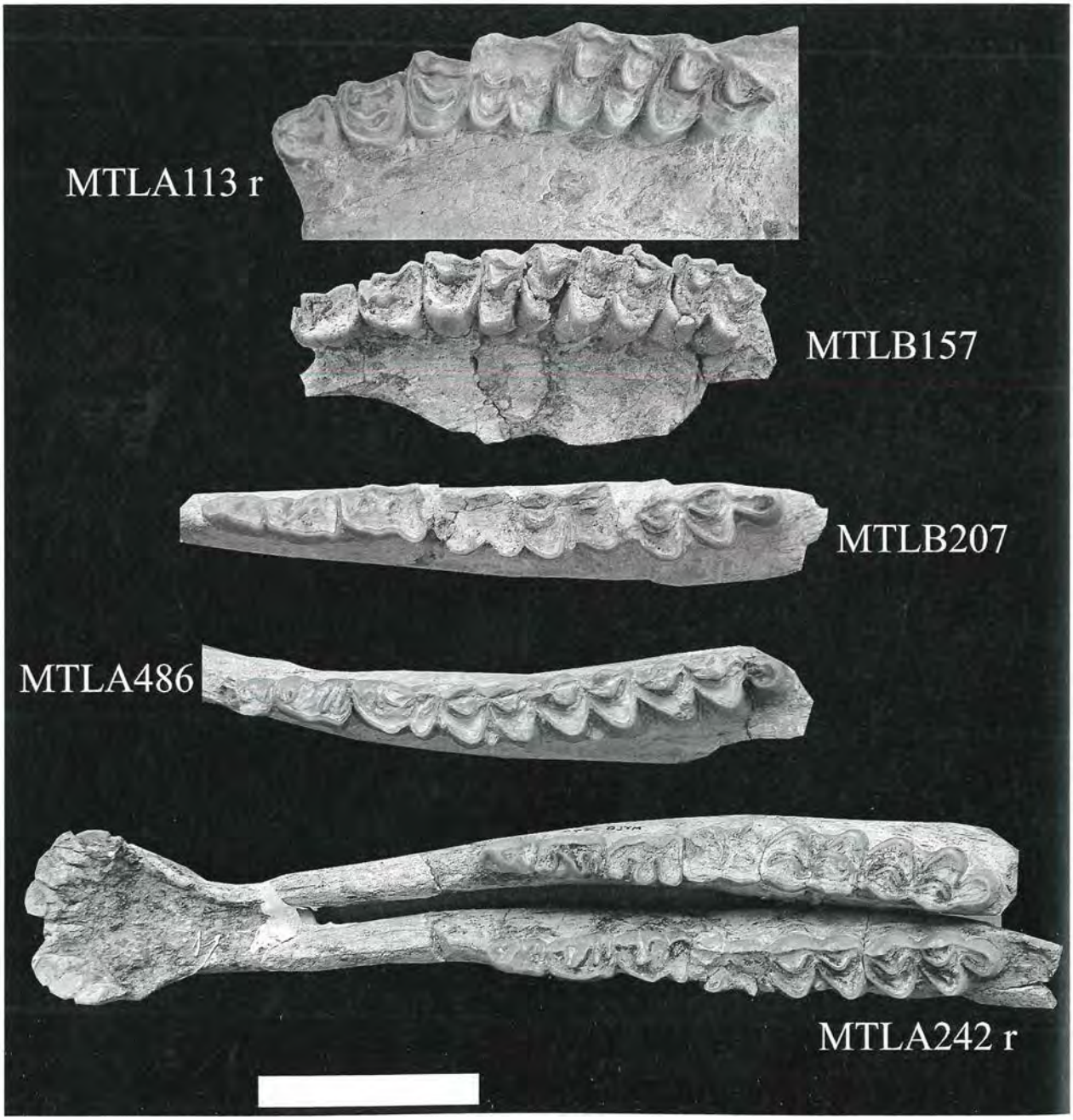

Figure 8: *Palaeoryx pallasi* (MTLA113-reversed, MTLB207, MTLA486) and *Palaeoryx majori* (MTLB157, MTLB242-reversed) tooth rows from Samos, in occlusal view. Scale bar equals 5 cm.

Emended Diagnosis: A large antelope with laterally inserted, moderately divergent, strongly tilted backwards and long, almost straight horn-cores, placed well behind the orbits and weakly recurving inwards at their tips; opisthocranium relatively short with more open fronto-parietal than occipito-parietal angle; short premolars compared to the molars.
Type Locality: Pikermi, Greece
Occurences: Samos, Maragheh, Halmyropotamos, Nova Emetovka, Taraklija, Kayadibi, ?Perivolaki, ?Sivas
Time Range: Middle Turolian

Localities: Mytilinii 1A (MTLA, Mytilinii 1B (MTLB); Samos Island, Greece
Material: cranium, MTLA113; part of cranium, MTLA 114; part of braincase MTLA347; left mandibular ramus with p3-m3, MTLA486; p2-p3 dex, MTLA214; p3 sin, MTLA192; left mandibular ramus with p2-m3, MTLB207.

Description & Comparison:
The braincase is bulbous and short compared to the face, which bends at a 135° angle on the cranial roof (Table 8; Pl. 3, figs. 2a, 4). The frontals do not rise between the horns. The interfrontal suture is visible along its length and weakly constricted. The supraorbital foramina are small, simple and widely spaced. The nuchal crest is very strong and the occiput forms an angle of 120° with the cranial roof. The occipital condyles incline downwards and the occipital faces postero-ventrally. A groove runs along the midline of the basioccipital, which is short, quadrangular-shaped and concave in lateral profile (Pl. 3, fig. 2b). The occipital face has a semi-circular shape and the external occipital crest is weak and bordered by two small and shallow ligament scars. The zygomatic arch runs parallel to the parietal sides. The fronto-nasal suture forms an 'M' (Pl. 3, fig. 2d) and the nasals are long and narrow, but expand laterally at the level of the thin ethmoidal fissure. The lachrymal fossa is deep in its distal part, large and extends anteriorly (Pl. 3, fig. 2a). The orbit is elongated, with its anterior margin above the posterior lobe of M3, or slightly posteriorly. The infraorbital foramen opens above P3. The choane opens behind M3 and the lateral indentation goes far forwards (Pl. 3, fig. 2c). The horn-cores are placed behind the orbits and point backwards (Pl. 3, figs. 2a, d). They are moderately divergent and feebly curved. Their cross-section is oval to round at the base, but the medio-lateral compression increases upwards. Basal horn-core dimensions of *P. pallasi* do not differ from those of *P. majori* (Fig. 7), making a discrimination based on this characteristic impossible.
The premolar/molar ratio varies from 69.5-73.6% for the upper tooth row and around 63.5% for the lower one, both values indicating shorter premolars than in *P. majori* (Tables 9, 10; Fig. 8). Furthermore, the dentition of *P. pallasi* differs from that of *P. majori* in the labially extended parastyle of P2, the backwardly curved parastyle of P3 partly covering the paracone, the more individualized paracone of P3 with a concave posterior flange, the less developed hypoconid on P3 and P4, the stronger asymmetry between the lingual and labial cusps on the upper molars, the constant presence of central islets in all molars and the thinner mesostyle (Fig. 8). The p2 of *P. pallasi* is larger than that of *P. majori*, the entoconid of p3 is longer and oblique, the hypoconid of p4 is wider and its metaconid is anteroposteriorly expanded, the m1 and m2 can bear a weak goat fold and the third lobe of m3 is longer, especially towards the crown's base (Fig. 8). Although

	MTLB-157dex	MTLB-157sin	MTLA-113sin	MTLA-114sin
LPM	108.0	110.0	114.0	117.0
LP	48.6	48.0	49.2	50.4
LM	62.3	64.8		68.4
LP2	16.8	17.0	15.8	16.2
WP2	14.0	13.5	15.1	13.6
LP3		16.2		16.6
WP3		16.4		16.8
LP4	14.0	14.1	14.6	16.2
WP4	17.7	17.6	18.5	
LM1	18.7			21.0
WM1	19.3	20.0		23.0
LM2	22.0	21.0	22.4	25.0
WM2	21.8		24.1	27.0
LM3	22.6	22.4		24.8
WM3	21.1	21.3	25.4	27.1

Table 9: Upper dental measurements of *Palaeoryx* from MTLA, MTLB, Samos. *P. majori*: MTLB157; *P. pallasi*: MTLA113, 114.

	MTLB-242sin	MTLC23 dex	MTLA-486sin	MTLA-214dex	MTLA-192sin	MTLB-207sin
Lpm	116.2	116.3	130.0			132.2
Lp	47.0	45.7				50.6
Lm	68.5	70.7	75.2			79.6
Lp2	13.8	13.4		14.2		14.7
Wp2	8.8	8.2		8.7		9.0
Lp3	15.5	15.6	16.5	16.7	16.5	16.3
Wp3	10.7	9.9	11.6	11.4	10.3	11.8
Lp4	18	17	19.0			19.2
Wp4	12.2	10.2	12.4			13.3
Lm1	17.8	17.7	21.0			18.8
Wm1	15.0	13.5	14.5			15.5
Lm2	21.2	21.8	22.7			22.0
Wm2	16.3	17.0	15.6			16.0
Lm3	28.5	31.2	31.5			33.0
Wm3	15.2	15.5	15.0			15.5

Table 10: Lower dental measurements of *Palaeoryx* from MTLA-B-C, Samos. *P. majori*: MTLB242, MTLC23; *P. pallasi*: MTLA486, 214, 192, MTLB207.

Skull characters	*Palaeoryx pallasi* MTLA113	*Palaeoryx majori* MTLB160b
Opisthocranium	short	longer
Orbit	elliptical, in front of the horn-cores	rounded, beneath the horn-cores
Basioccipital	relatively short; strongly concave in lateral profile	Longer; slightly concave in lateral profile
Occipital	slightly concave in lateral profile and more or less vertical to the cranial roof	flat and forming an obtuse angle with the cranial roof
Occipital condyles	large directed downwards	larger directed posteriorly
Mastoid	restricted posteriorly	expanded laterally
Paroccipital process	strong, slightly oblique to the sagittal plane	thinner, strongly oblique to the sagittal plane
Cranial roof-face angle	obtuse (120-140°)	less open (100-120°)
Horn-core insertions	on the postero-dorsal part of the orbits, slightly laterally, and directed posteriorly	above the orbits, strongly laterally and more upright in the basal part
Horn-core structure	long, rather straight, tilted backwards, moderately divergent and slightly re-curved inwards at the top	moderately long, strongly curved backwards, re-curved inwards at the top and weakly twisted

Table 11: Morphological comparison between *Palaeoryx pallasi* and *Palaeoryx majori* from Samos. (modified from KOSTOPOULOS, 2005).

slightly larger and with more divergent horn-cores, *P. pallasi* from Samos is morphologically very similar to the type sample from Pikermi (MNHNP PIK2456, NHML M10831, M10832) (Table 8; Fig. 7).

?*Palaeoryx* sp.

(Plate 3, fig. 3)

Localities: Mytilinii 4 (MLN), Mytilinii 3 (MYT); Samos Island, Greece

Material: proximal part of radius, MNL82 (L > 190 mm, TDprox = 53.7 mm); metacarpal MLN6 (L = 230.5, DTprox = 42.2, DTdia = 25.9, DTdist = 44.3); proximal metacarpal MLN7 (DTprox = 42); distal tibia, MLN49 (TDdist = 50 mm); part of calcaneum, MLN89 (APD sustentaculum tali = 30 mm); proximal part of metatarsal, MLN83 (L > 210 mm, TDdia = 20.3 mm, TDdist = 41.2 mm); distal part of humerus MYT108 (TDdist = 69.5 mm).

Description & Comparison:

A set of large postcranials from MLN and a distal part of a humerus from MYT do not fit boselaphine morphology; the metapodials are more robust than those of *Tragoportax* and *Miotragocerus* from Macedonia, Greece, and rather slender for *Samokeros* SOLOUNIAS, 1981. Protoryxoid bovids from Pikermi and Samos are also different in having even more slender metapodials. The fully preserved metacarpal MLN6 (Pl. 3, fig. 3) is rather of type A1/B of KÖHLER (1993), suggesting mixed, moderately humid habitats. According to their size they could belong to *Palaeoryx*.

Discussion:

As commented by SOLOUNIAS (1981:196-197), the cranial and horn-core pattern of *Sporadotragus* seems closer to *Palaeoryx* than to other late Miocene genera and phylogenetic relations between these two taxa are possible, with *P. majori* being nearer to their common origin than *P. pallasi*. *Palaeoryx sinensis* BOHLIN, 1935b from China looks like a large version of *P. majori*, indicating close relationships. *Sporadotragus vasili* from Kalimatsi, Bulgaria (GERAADS et al., 2006) certainly postdates the first record of *S. parvidens* on Samos and I think that the combination of a primitive cranial pattern (weak cranio-facial flexion, unraised frontals) with an advanced horn-core morphology (clear antero-medial keel, deeply grooved horn-cores, increasing medio-lateral compression toward the apexes) removes the Bulgarian species from *Sporadotragus* s.s. and puts it closer to some other Samos forms like *Pseudotragus longicornis* ANDRÉE, 1926, which will be discussed later.

Both *Sporadotragus* and *Palaeoryx* are caprine-like in appearance and *Sporadotragus* seems indeed closer to sheep than to goat, as GENTRY (1971) already pointed out. The strongly arched horn-cores of *S. parvidens* may already be in the direction of a sheep characteristic, in which a backward component to the curvature is retained (GENTRY, 2001). GENTRY (1971:281) deduced affiliations between *Palaeoryx* and the Pliocene *Megalovis* SCHAUB, 1923, but *Gallogoral* GUÉRIN, 1965 could be also related to it.

Genus *Protoryx* MAJOR, 1891a

Type species: *Protoryx carolinae* MAJOR, 1891a

Diagnosis: as in GENTRY (1971:241)

Protoryx capricornis (SCHLOSSER, 1904)

Synonyms:

1904 *Pseudotragus capricornis* SCHLOSSER:51, Pl. X, fig. 7

1904 *Pachytragus crassicornis* SCHLOSSER:56, Pl. XI, fig. 11

1926 *Pseudotragus longicornis* ANDRÉE:147, Pl. X, figs. 2-3, NHMW v37.

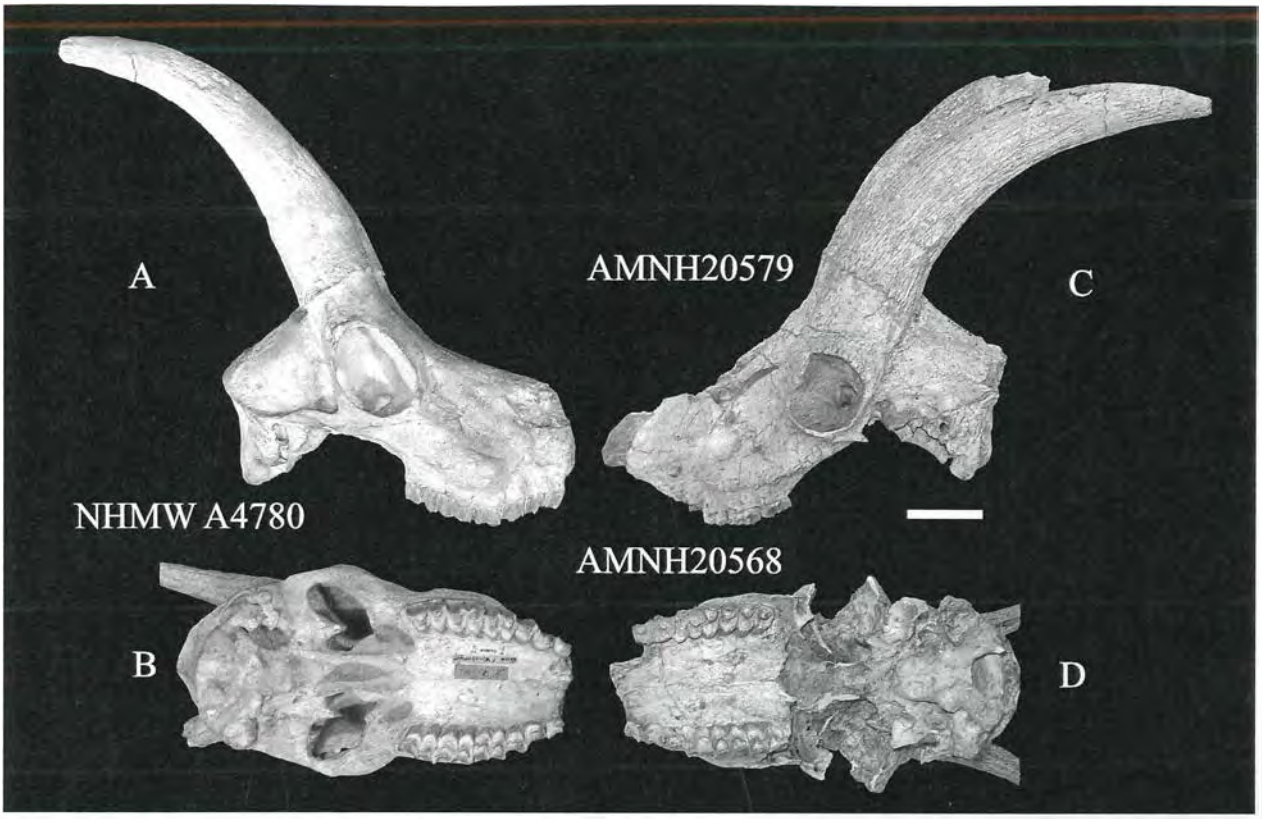

Figure 9: *Skoufotragus schlosseri* from Samos. Type cranium NHMW A4780 in lateral (A) and ventral (B) view and crania AMNH20579 (C) and AMNH20568 (D) in lateral and ventral view, respectively. Scale bar equals 5 cm.

Lectotype: the partially preserved skull illustrated by SCHLOSSER (1904:51, Pl. X, fig. 7)

Diagnosis: a small *Protoryx* with long, anteriorly keeled, closely settled and increasingly divergent horn-cores, curved openly and flattened laterally; basal cross-section rather sub-triangular; dorsal orbital margin relatively wide; supraorbital foramens well-spaced on the frontals; face bent gently on the cranial roof; frontals weakly raised.

Type Locality: Samos - unknown level, Greece

Remarks: The presence of *Protoryx* on Samos is highly problematic, mainly because of the taxonomic confusion among protoryxoid bovids and especially *Protoryx* MAJOR, 1891a, *Pachytragus* SCHLOSSER, 1904, and *Pseudotragus* SCHLOSSER, 1904 (e.g., GENTRY, 1971, 2000; SOLOUNIAS, 1981; KÖHLER, 1987; BOSSCHA-ERDBRINK, 1988).

The lectotype of *Pachytragus crassicornis* SCHLOSSER, 1904 (:56, Pl. XI, fig. 11) is notably different from the rest of the Samos specimens later assigned to this genus, but it does look morphometrically similar to the partial cranium of *Pseudotragus capricornis* SCHLOSSER, 1904 (: 51, Pl. X, fig. 7), as well as to the holotype cranium of *Pseudotragus longicornis* ANDRÉE, 1926 (:147, Pl. X, figs. 2-3). In distinction from other Samos specimens, these three crania appear smaller and relatively wide at the orbits and show closely settled and increasingly divergent, long, openly curved, laterally flattened and anteriorly keeled horn-cores of a rather sub-triangular basal cross-section, well-spaced supraorbital foramens, not very raised frontals and weakly bent face on the cranial roof. The basal cross-section of the lectotype of *Pseudotragus capricornis* (SCHLOSSER, 1904: Pl. X, fig.7) is certainly not as elongated as fig. 7a of SCHLOSSER (1904:Pl. X) lets one suppose, but rather sub-triangular with a blunt anterior keel; BOHLIN (1936) already noticed that Schlosser had taken this cross-section at 50mm above the base of the horn-core. The synonymy between *Pachytragus crassicornis*, *Pseudotragus capricornis* and *Pseudotragus longicornis* simultaneously raises the question of their generic attribution. Mainly judging from the best preserved specimen NHMW v37, I believe that most features characterizing the Samos species match *Protoryx*, even though it is significantly smaller and presumably more primitive than *Protoryx carolinae* from Pikermi. I propose, therefore, to assign it to *Protoryx capricornis* (SCHLOSSER, 1904). The merging of the types of both *Pachytragus* and *Pseudotragus* into *Protoryx* make both generic names unavailable for further use, leaving a set of allied species outside any known genus; I consequently suggest a new generic name for them.

Skoufotragus nomen novum

Synonyms:

1891a *Protoryx* (in part) MAJOR:609
1904 *Protoryx* MAJOR. SCHLOSSER:45 non *Pachytragus* SCHLOSSER, 1904:56
1926 *Pachytragus* SCHLOSSER. ANDRÉE:148
1926 *Protoryx* MAJOR. ANDRÉE:151, 156
1926 *Hippotragus* SUNDEVALL. ANDRÉE:158
1926 *Palaeoryx* (in part) GAUDRY. ANDRÉE: 162
1928 *Protoryx* (in part) MAJOR. PILGRIM & HOPWOOD:27
1971 *Pachytragus* (in part) SCHLOSSER. GENTRY:244

Table 12: Cranial measurements of *Skoufotragus laticeps* from MTLA, MTLB, PMMS, Samos.

	MTLB164	MTLA4	MTLA273b	MTLB56	MTLB346	PMMS95	PMMS99
Lbasion-P2						223.0	
Lsupraorbitals-frontoparietal	79.8	78.7	74.5	72.0		81.0	87.0
Lsupraorbital-occipital	148.0	149.2				151.6	150.6
Lfrontonasal-frontoparietal	100.3	104.0				103.4	
Lfrontonasal-occipital	161.0	165.0				166.0	
L parietals (dorsally)	52.2	55.8				49.9	51.5
W skull behind hc	89.4	81.3	67.9			86.5	
W skull at the lateral edges of hc	113.5	105.8	84.0	119.6		108.2	109.5
W bi-orbital	122.0	112.6				125.0	
W supraorbitals	43.0	38.3	45.0	52.0		44.4	40.0
W braincase	85.3	73.0				78.3	76.1
W bimastoids	91.0	92.0				95.7	90.0
W bicondyles	63.4	60.4					60.0
W ptbc	45.0	33.2				36.5	43.3
W atbc	23.4	27.0				29.5	27.8
H occiput	42.9	41.0				43.5	45.4
L hc (along anterior face)	300.0	355.0	300.0		300.0	330.0	
H hc (posterior chord)	265.0	285.0	250.0		245.0	270.0	
TD hc base	44.8	44.7	37.0	45.5	41.5	47.5	47.0
APD hc base	63.0	63.5	47.3	68.3	66.5	67.8	71.4
TD hc at 10cm above base	29.8	29.6	22.0	33.0	30.6	30.3	32.0
APD hc at 10 cm above base	48.5	51.0	40.0	56.5	52.4	52.0	51.5
Angle cranial roof-frontals	118.0	120.0				110.0	
Angle occipital-cranial roof	114.0	118.0				105.0	120.0

1981 *Protoryx* (in part) MAJOR. SOLOUNIAS:199
1987 *Protoryx* (in part) MAJOR. KÖHLER:168
1988 *Protoryx* (in part) MAJOR. BOSSCHA-ERDBRINK:150
2005 *Pachytragus* SCHLOSSER. KOSTOPOULOS:772
2006a*Pachytragus* SCHLOSSER. KOSTOPOULOS:175

Type species: *Skoufotragus schlosseri* (ANDRÉE, 1926)
Derivatio nominis: dedicated to the pioneer mammal paleontologist Theodor Skoufos, professor of the Athens University, who excavated on Samos at the beginning of 20th century.
Generic Diagnosis (modified from GENTRY, 1971:244): Slightly smaller than *Palaeoryx*; skulls fairly narrower than *Protoryx* with shorter braincase, having a less convex dorsal surface and parallel or wider anterior sides; opisthocranium morphometrically bimodal, with a long- and a short-brained variety; face shorter and deeper than in *Protoryx*; horn-cores are moderately long to long, medio-laterally compressed, more uprightly inserted even than in *Protoryx*, and appearing to rise more directly above the orbits than in *Palaeoryx*, set closer together, with an increased divergence towards the tips, the widest part of their transverse section lying mid-way along their anteroposterior axis, hollowed close to their bases; frontals are higher between the horn bases than in *Palaeoryx* or *Protoryx* and prolong anteriorly between the lachrymals and the nasals; mid-frontals suture rather raised; mid-frontals and frontoparietal sutures quite complicated; supraorbital pits less small and less widely spaced than in *Protoryx*; nasals long, domed, with a narrowly drawn-out back suture; ethmoidal fissure long and narrow, restricted mostly between the frontals and the lachrymals; zygomatic arch not deepened anteriorly; occipital surface in two planes, with each half facing partly laterally as well as backwards; basioccipital is narrow, longer than in *Protoryx*, with less localized anterior tuberosities and without marked central longitudinal groove; foramina ovalia are small to moderate and face mainly ventrally; auditory bullae are moderate to large; the ventral edge of the bulla passes downwards posteriorly on the front edge of the paroccipital process instead of rising to make the join; palatine foramina placed at the level of the back lobe of M2; teeth more hypsodont than in *Palaeoryx* and *Protoryx*; i1 is wider than i2; basal pillars are very small on upper molars and small on lower molars; upper molars with no late joining of the medial lobes, weak anterior and posterior indentations on the central fossetes, and a strong mesostyle with a tendency for the lateral wall behind to acquire a concave section; the paracone rib is strong on P3 and the styles are fairly strong on the upper premolars; medial walls of lower molars are little outbowed between the stylids; premolar row is short; hypoconid of p4 is quite pointed ; metaconid of p4 is rather bulbous in mid-wear; paraconid of p4 is less developed than in *Palaeoryx* and *Protoryx*.
Other species: *Skoufotragus laticeps* (ANDRÉE, 1926); *Skoufotragus zemalisorum* n.sp.

Specimen	LPM	LP	LM	Specimen	Lpm	Lp	Lm
MTLA491 dex	96.5	40.0	57.0	MTLB208b dex	101.1	39.0	62.0
MTLA491 sin	98.4	41.5	57.9	MTLB205 sin	97.4	38.0	58.0
MTLA181 dex	97.5		58.6	MTLB364 dex	95.0	35.0	61.6
MTLA181 sin	99.1	38.8		MTLB241 dex	101.4	39.3	62.5
MTLA182 dex	95.4	38.8	58.6	MTLB241 sin	103.4	39.8	64.0
MTLA182 sin	97.8	39.8	58.0	MTLB189 dex			65.3
MTLB3 dex	98.5	41.0	59.7	MTLB234 young			70.7
MTLB3 sin	98.9	40.9	60.3	MTLB232 sin	97.0	38.0	57.5
MTLA494 sin			59.5	MLB229 sin	96.5		62.0
MTLA21 sin	105.0	41.0	64.0	MTLB231 sin			
MTLA49 dex young	97.0		60.0	MTLB181 dex		37.5	60.8
MTLA544 dex	93.7	38.7	57.5	MTLB236 sin		38.0	
MTLA339 dex			60.0	MTLB366 dex		38.8	
MTLB15 sin	96.3	40.6	58.8	MTLB180 dex		36.5	
MTLB240 dex	96.5	38.5	58.0	MTLB176 dex			61.0
MTLB238 sin	98.0	38.7	61.2	MLA230 dex	95.0		
MTLB237 sin	99.3	37.7	62.6	MTLA231 sin	99.0	41.0	57.5
MTLB200 dex	97.3	39.2	58.7	MTLA542 sin	102.6	40.5	63.0
MTLB239 dex	96.0	38.7	58.6	MTLA149 sin		38.0	
PMMS 95 dex	104.8	40	66.2	MTLA317 dex	102.0		62.2
	Lpm	Lp	Lm	MTLA148 dex	103.0	39.5	65.0
MTLC24 sin	108	38.0	67.6	MTLA50 dex			63.5
MTLC26 dex	104.8	38.0		MTLA220 dex		41.5	
MTLB129 dex			65.0	MTLA409 dex			60.7
MTLB206 sin	105.0	41.7	63.8	MTLA28 dex			62.4

Table 13: Upper and lower tooth row measurements of *Skoufotragus laticeps* from MTLA, MTLB, MTLC and PMMS, Samos.

Skoufotragus schlosseri (Andrée, 1926)

Synonyms:

Pachytragus schlosseri Andrée, 1926:148; Pl. XIII: fig. 3; Pl. XIV, fig. 4

Palaeoryx cf. *stuetzeli* Schlosser. Andrée, 1926:162; Pl. XIV, figs 1-3

Pachytragus schlosseri Andrée. Pilgrim & Hopwood, 1928: 44

Pachytragus crassicornis (in part) Schlosser. Gentry, 1971: 253

Protoryx crassicornis (in part) Schlosser. Solounias, 1981: 201

Protoryx carolinae (in part) Major. Bosscha-Erdbrink, 1988: 150

Pachytragus crassicornis Schlosser. Kostopoulos, 2005:772

Holotype: the skull described and figured by Andrée (1926:148; Pl. XIII: fig. 3; Pl. XIV, fig. 4), NHMW A4780, Fig. 9A, B

Emended Diagnosis (modified from Pilgrim & Hopwood, 1928 and Gentry, 1971): slightly smaller than *Skoufotragus laticeps* with shorter and less curved horn-cores, often more medio-laterally compressed, more divergent and with anterior keel; horn insertions less upright than in *Sk. laticeps*; orbital rims rather wide; parietal region shortened; cranio-facial angle stronger; braincase top set at a steeper angle to the occipital surface; basioccipital with fairly localized anterior tuberosities, set apart posterior ones, and little development of a central longitudinal groove; teeth no smaller than in *Sk. laticeps*, but with more reduced premolar row.

Type Locality: Samos - unknown level, Greece

Occurences: O5-Samos; Akkaşdağı

Time Range: late MN 12 - early MN 13

Remarks: The species concept follows Gentry (1971) in uniting *Pachytragus schlosseri* Andrée, 1926, *Palaeoryx* cf. *stuetzeli* of Andrée (1926) and the entire AMNH sample from Q5 site of Samos (Fig. 9C, D). *Skoufotragus schlosseri* occurs in the uppermost fossil levels of Samos (the lightly red fossilization hue of both the Vienna specimens is in favor of this stratigraphic assignment) and it obviously represents an advanced evolutionary stage of its precursor *Sk. laticeps*. The transition from *Sk. laticeps* to *Sk. schlosseri* reveals a size reversal, associated by a shortening of the braincase and the horn-cores, a relative reduction of the premolars and an increase of the face slope on the cranial roof, changes that used to show adaptation to harsher environmental conditions.

Skoufotragus laticeps (Andrée, 1926)

(Plate 4)

Synonyms:

as in Gentry (1971:244-245) and

Pachytragus laticeps (in part) Andrée. Gentry, 1971:244

Protoryx laticeps Andrée. Solounias, 1981:199

Protoryx carolinae (in part) Major. Bosscha-Erdbrink, 1988:150

Holotype: The partially preserved skull in Münster figured by Andrée (1926:Pl. XII, figs. 5, 9), PIM8

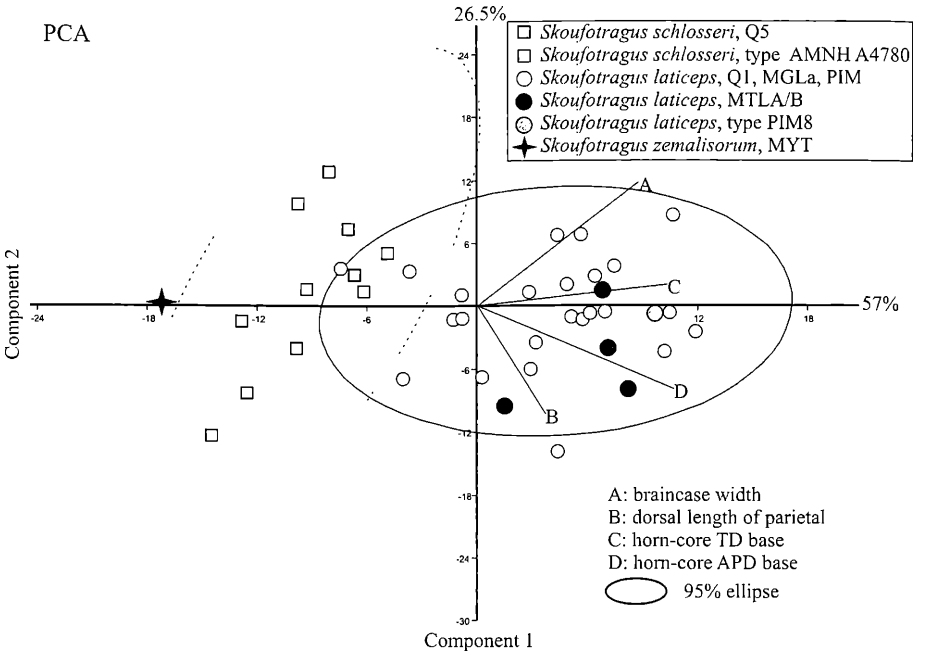

Figure 10: PCA analysis of *Skoufotragus* from Samos, based on four horn-cores and cranial variables (A-D).

Diagnosis: as in GENTRY (1971:245).
Type Locality: Samos - unknown level, Greece
Occurences: Q4, Q1, MTLA, MTLB, all from Samos; Kemiklitepe A; Maragheh
Time Range: Early - Middle Turolian, MN 12
Remarks: The species concept is the same as that proposed by GENTRY (1971) with modifications introduced by KOSTOPOULOS (2005:776-777).

Localities: Mytilinii 1A (MTLA), Mytilinii 1B (MTLB), Samos Island, Greece
Material: cranium, PMMS95; part of cranium with horn-cores, MTLA4, MTLB164, PMMS99; frontlet, MTLA273b, MTLB56; part of horn-core, MTLA351 (38.5 x 60.5 mm), MTLB346, MTLC11 (28.8 x 43.3); palate, MTLA181, MTLA182, MTLA491, MTLB3; P2-M3 dex, MTLA49, MTLA544, MTLB200, MTLB239, MTLB240; P2-M3 sin, MTLA21, MTLB15, MTLB237, MTLB238; M1-M3 sin, MTLA494; M1-M3 dex, MTLA339; M2-M3 sin, MTLB365, MTLB197; M1-M2 sin, MTLB66, MTLB368; P4-M3 dex, MTLB367; P4-M1 dex, MTLB168; M3 dex, MTLB369; mandible, MTLB241; p2-m3 dex, MTLA148, MTLA230, MTLA317, MTLB181, MTLB208b, MTLB364, MTLC26; p2-m3 sin, MTLA231, MTLA542, MTLB205, MTLB206, MTLB229, MTLB231, MTLB232, MTLC24; p2-p4 dex, MTLA220, MTLB180, MTLB366; p2-m2 sin, MTLA149; p2-p4 sin, MTLB236; m1-m3 dex, MTLA50, MTLA409, MTLB129, MTLB176, MTLB189, MTLB234; m1-m3 sin, MTLA28; m1-m2 dex, MTLA188; m2-m3 sin, MTLA411; p3-m1 sin, MTLB402; m2-m3 sin, MTLB178.
Description & Comparison:
MTLB164 (Pl. 4, fig. 2) differs from MTLA4 and PMMS99 (Pl. 4, figs. 1, 3) in the wider braincase, the stronger external occipital protuberance and the more marked relief of the occiput, the more distant parietal lines (44.5 mm at their junction with the intraparietal, instead of 26.0-27.5 mm for MTLA4 and PMMS99), the wider intraparietal, the more triangular-shaped and shorter basioccipital, the weaker anterior tuberosities and the presence of a sharp crest in front of them. Furthermore, MTLB164 has shorter horn-cores, settled more widely apart on the frontals, with an incipient anterior keel at the middle of their length and a clearer torsion. Cranial measurements are given in Table 12.
The palatal width ranges between 45.5-54.5 mm (n = 4) at the posterior lobe of M3 and between 32.0 and 36.2 mm in front of P2. The upper premolars represent 60-71% of the molars (Table 13). The length of P2 decreases with wear and the occlusal surface becomes quadrangular; it is always bilobed lingually. The paracone is very strong and located at the anterolabial corner; the parastyle is weak and places anteriorly (Pl. 4, figs. 5, 6). The P3 is usually bilobed and always with a more developed posterior part (trapezoidal-shaped). The sharp parastyle and the strong paracone converge towards the crown base and the paracone is oblique in labial view. Most P3 specimens show a clear, moderately developed metastyle. The lingual face of P4 is angular and points antero-lingually (10 out of 13 specimens; Pl. 4, figs. 5, 6). The paracone is centrally placed and weakly developed, while the metastyle and particularly the parastyle are strong, protruding buccally. The upper

	Skoufotragus laticeps		*Skoufotragus schlosseri*
	Q1-Q4	MTLA-B	Q5
P/M	59.8-67.1	60.2-71.6	61.1-65.2
	64.2 (n = 8)	66.9 (n = 14)	63 (n = 7)
p/m	58.0-63.4	56.2-66.0	52.9-59.9
	60.9 (n = 11)	62.2 (n = 11)	56.0 (n = 4)

Table 14: Premolar/molar ratio in *Skoufotragus laticeps* and *Skoufotragus schlosseri* from Samos.

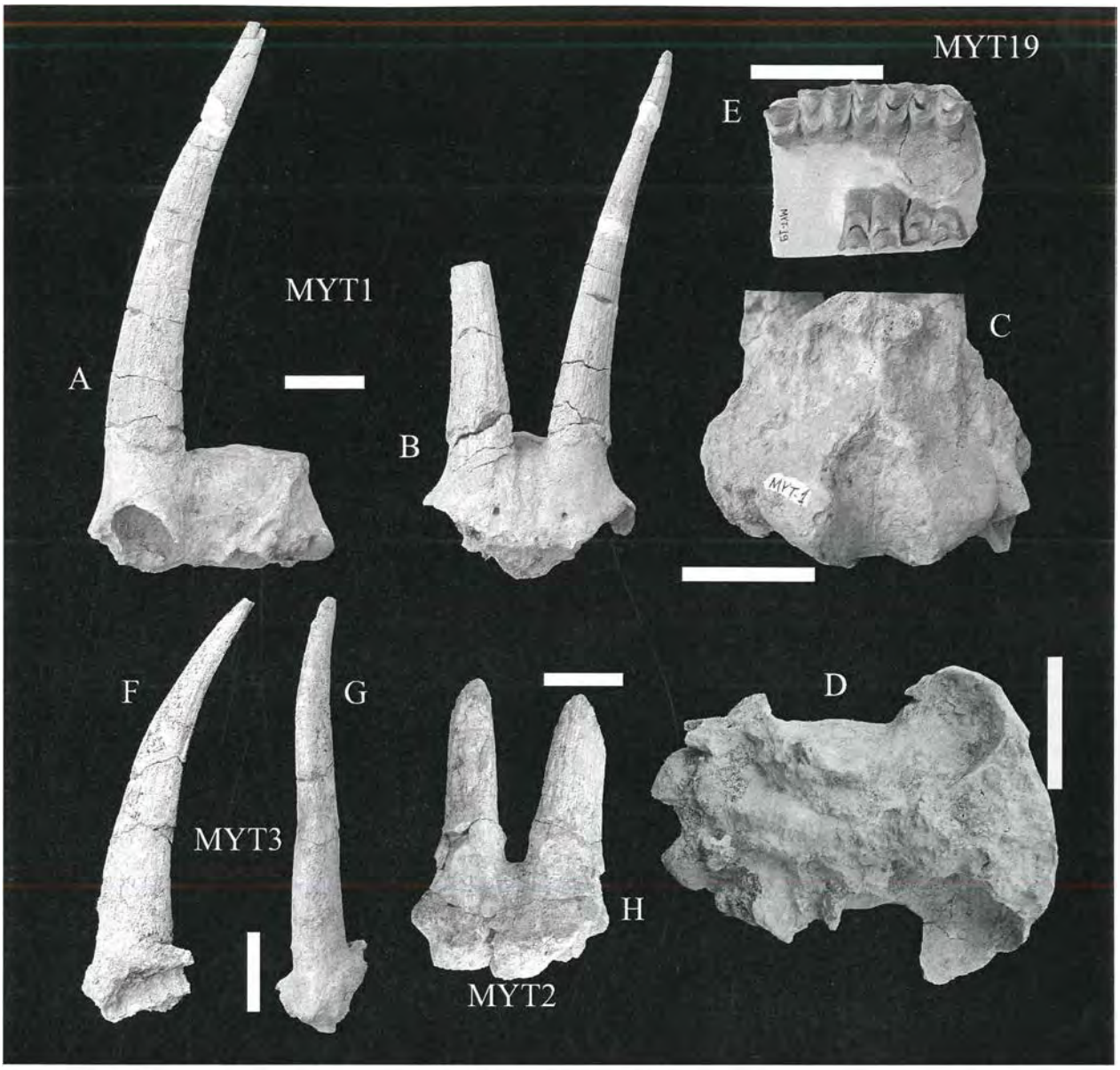

Figure 11: *Skoufotragus zemalisorum* n.sp. from MYT, Samos. Cranium MYT1 in lateral (A), frontal (B), occipital (C) and basi-occipital (D) view; palate MYT19 in occlusal view (E), right horn-core MYT3 in medial (F) and anterior (G) view; frontlet MYT2 in anterior (H) view. Scale bar equals 5 cm.

molars frequently bear a tiny basal tubercle that in a few cases becomes a pillar (Pl. 4, fig. 5). A central islet can be present on M1, and, but less so, on M2-M3. Incipient anterior and posterior indentations are also common on the central fossetes. The M1 has a narrow protocone that protrudes lingually; this characteristic is much less frequent on M2-M3. The parastyle and mesostyle are always strong; the mesostyle is thinner and vertical to the tooth axis. The metastyle is developed on M3, marked by a postero-labial groove but it does not flare distally (Pl. 4, figs. 5, 6). The paracone rib is strong, while the metacone rib is weak to absent. The hypsodonty index (H/W) is high, ranging from 102.5-127.6 on M2 (n = 4) and from 110.0-144.0 on M3 (n = 7). The lower premolars represent 56-71% of the molars (Table 13). The i1 is wider than i2 (9.0 vs 7.5 mm), which in its turn is slightly larger than i3 (6.1 mm); the width of c (6.3 mm) exceeds that of i3 (Pl. 4, fig. 4). A similar incisor-canine relation (i1 > i2 ≥ i3 ≤ c) has been reported for *Skoufotragus schlosseri* from Akkaşdağı, Turkey (Kostopoulos, 2005). The development of the entoconid on p2 varies significantly, but 7 out of 10 specimens have a clearly visible entoconid (Pl. 4, fig. 4). On p3, there is almost always a basal bridge between the paraconid and the metaconid, forming a closed valley at the near bottom of the crown. On half of the specimens (n = 7) the metaconid shows a weak basal anterior expansion and it fuses with the entoconid (Pl. 4, fig. 4). The hypoconid is always visible, but moderately developed. The paraconid of the p4 is variably developed: in unworn teeth it is strong and curves posteriorly, while in mid- and extensively worn specimens it is weak. On unworn p4s, the lingual wall of the metaconid is strongly convex, but later it becomes flat lingually and sub-squarish in occlusal view. The metaconid is always developed anteroposteriorly, but the anterior

Table 15: Cranial measurements of *Skoufotragus zemalisorum* n. sp. from MYT, Samos.

	MYT1		MYT2		MYT3
L front hc-occipital	119.7				
W braincase	70.5		77.7		
W skull behind hc	85.6		99.5		
W supraorbitals	37.3		40.6		
W bi-orbital	(117)				
W bimastoids	92.0				
W bicondyles	55.0				
TD orbit	39.3				
W ptbc	35.9				
W atbc	18.6				
L hc along anterior face)	270.0				250.0
H hc (posterior chord)	242.0				220.0
TD hc base	30.7	32.9	39.0	34.4	31.3
APD hc base	53.2	47.6	55.0	(53)	50.4
TD hc at 10 cm		19.7			22.5
APD hc at 10 cm		33.3			33.0

valley remains open (Pl. 4, fig. 4). The hypoconid may be narrow or wide, separated from the usually angular protoconid by a well-developed furrow.

A basal pillar is present on 7 out of 15 m1 and 4 out of 14 m3; 10 out of 15 m2 also have a basal pillar, sometimes double or wide, but always low, restricted below the middle of the crown's height. The entostylid is stronger than the parastylid on m1-m2, and it is also clear on m3. The metastylid is present on little-worn m3. The paraconid and the entoconid are weakly developed and gently convex. The third lobe of m3 increases toward the base.

Skoufotragus laticeps and its individual variability has already been exposed in detail by GENTRY (1971, 2000), who also discussed the entire old Samos collection, for which additional information can be found in SOLOUNIAS (1981) and KOSTOPOULOS (2005). PMMS99 and MTLA4 represent the so-called "long-brained" variety, whereas the specimen MTLA273b could belong to a young-adult individual of the same morphotype. MTLB164 follows the characteristics seen in the "short-brained" variety (GENTRY, 1971); the specimen MTLB56 is very robust, suggesting a large individual of the same short variety. PMMS95 is metrically placed in between these to groups. I have already suggested (KOSTOPOULOS, 2005) that cranial bimodality in *Skoufotragus laticeps* and *Sk. schlosseri* from Samos might be strongly related to the mechanical response of the skull to the degree of lengthening and backward curvature of the horns, whereas the presence of an antero-distal keel, preferably on the short-horned individuals of both species, may substitute the behavioural function of a long, sabre-look horn. PCA analysis of some cranial and horn core values (Fig. 10) indicates a good discrimination between *Sk. laticeps* and *Sk. schlosseri*. Although GENTRY (1971) suggested a distinction of the premolar shortness in the Samos sample, this is impossible, elaboration of the available data (Table 14) shows that even though greatly overlapping, the premolar/molar ratios of *Sk. laticeps* are at average larger than those of *Sk. schlosseri*, indicating a relative reduction of the premolars through time.

***Skoufotragus zemalisorum* n.sp.**

Synonym:

Pseudotragus capricornis SCHLOSSER. ANDRÉE, 1926:146, Pl. XIII, fig. 7

Holotype: partially preserved skull, MYT1, Aegean Museum of Natural History, Samos.

Type Locality: Mytilinii-3 (MYT), Samos.

Age: early middle Turolian (MN 12)

Derivatio nominis: Dedicated to Konstantinos and Maria Zemalis, founders of the Aegean Museum of Natural History, Samos.

Diagnosis: Smaller than *S. laticeps* and *S. schlosseri* and larger than *Protoryx enanus*. Horn-cores of same pattern as *Sk. laticeps*, but smaller, without anterior keel, less upright insertions and weaker posterior curvature. Supraorbital foramina very small and not sunken into pits. Anterior tuberosities of the basioccipital more localized than in *Sk. laticeps* and less posteriorly extended. Tooth row large compared to the skull size.

Material: Braincase with horn-cores, MYT1; frontlet, MYT-2; right horn-core, MYT3; part of juvenile horn-core, MYT66; palate with P2-M3 sin and M2-M3 dex, MYT19; P3-M3 sin, MYT46; P2-M1 sin, MYT84; D3-M1 sin and dex, MYT24; left mandible with p2-m3, MYT87; right mandible with p4-m3, MYT57; left mandible with p3-m3, MYT129; juvenile right mandible with d2-m1, MYT47; distal humerus, MYT43; metacarpal, MYT20 (L = 242.3; TDproximal = 35.2; TDdiaphysis = 19.7; TDdistal = 31.1), MYT21; proximal metacarpal, MYT26b; distal metatarsal, MYT16.

Description & Comparison:

The upper and lower milk dentitions belong to a single individual. The opisthocranium (MYT1) is moderately long and rather narrow (Table 15; Figs. 11A-D). The parietals are gently swelling and the parietal lines are thin, stronger in their anterior part and converge to the

	MYT19	MYT46	MYT84		MYT87	MYT129
PM		(89.5)		pm	101.5	
P			36.8	p	36.9	
M	56.0			m	64.1	
LP2			11.1	Lp2	10.2	
WP2			9.0	Wp2	6.0	
LP3		12.5	12.2	Lp3	12.3	12.7
WP3		10.7	10.5	Wp3	7.0	6.7
LP4	12.7	11.5	12.4	Lp4	14.5	14.6
WP4	13.1	13.0	12.8	Wp4	8.0	7.7
LM1	17.9	18.0	16.6	Lm1	16.5	
WM1	16.8	16.8	17.0	Wm1	12.2	
LM2	20.5	21.0		Lm2	21.0	
WM2	18.0	18.5		Wm2	12.5	
LM3	20.3	19.6		Lm3	27.8	25.6
WM3	15.7	15.5		Wm3	11.6	11.0

Table 16: Upper and lower dental measurements of *Skoufotragus zemalisorum* n.sp. from MYT, Samos.

rear. The frontals are moderately inflated between the horn bases and weakly depressed behind the pedicles. The fronto-parietal suture is highly complicated and the interfrontal suture is constricted. The anterior part of the frontal forms an angle of 115° with the cranial roof. The supraorbital foramens are small, not sunken into pits but extended anteriorly through narrow grooves; they are placed close to each other and far forwards from the horn-bases (Fig. 11B). The orbits are rather rounded and their postero-dorsal margins extend laterally. There is no postcornual fossa. The occipital face is sub-triangular, defined by a rather strong nuchal crest (Fig. 11C); it forms an angle of 110° with the cranial roof. The external occipital protuberance is well-developed, marked by strong ligament scars on either side. The mastoids are large and face mostly laterally. The condyles point postero-ventrally, as do the paroccipital processes. The posterior tuberosities of the basioccipital are strong, crest-like and vertical to the sagittal plane (Fig. 11D). The anterior tuberosities are long and parallel to the sagittal plane, but less extended posteriorly than in *Sk. laticeps*. A wide groove runs along the basioccipital. The foramen ovale is small and faces laterally. The pedicles are anteriorly higher than posteriorly. The horn-cores are inserted behind the orbits and point backwards. They show a weak divergence in anterior view and they are faintly curved laterally and recurved inwards near their tips (Figs. 11A, B, F, G). They appear to be strongly medio-laterally compressed along their length. Their basal greater anteroposterior diameter forms a 30-40° angle with the sagittal plane. The thickest part of the horn-core base lies medially. The frontlet MYT2 (Table 15; Fig. 11H) is very similar to MYT1, but slightly larger and with more closely settled horn-cores at the base. MYT66 is a thin strongly medio-laterally compressed horn-core that probably represents an immature ontogenetic stage.

The anterior lobe of D3 is almost square-shaped and fuses quickly with the posterior lobe. The paracone rib and the mesostyle are strong. The D4 is fully molariform, with the two lobes converging lingually. The d2-d4 length is 41.7 mm (MYT47). On the d2 the parastylid and the paraconid are undistinguished, the metaconid is centrally placed and the entoconid forms a closed valley with the incipient entostylid. The morphology of d3 is simple, with a posteriorly oriented paraconid and an anteriorly oriented metaconid without, however, closing the anterior valley. The entoconid and the hypoconid are weakly developed. The anterior lobe of d4 is rhomboidal-shaped. The upper premolar row is 38 mm long (MYT84; Table 16). P2 and P3 are asymmetrical, with strong paracone rib in anterior position. The parastyle of P2 is hardly distinguishable and anteriorly placed, whereas it is strong on P3 and merges with the paracone at the crown's base. Both available P3 and one out of three P4 show an incipient lingual bilobation. The parastyle of P4 is strong and thickens towards the base. The paracone rib is more centrally placed and the metastyle is well-developed (Fig. 11E). The molars are rather hypsodont (hypsodonty index: 125.7 for one M1; 110 for one M2 and 137 for two M3), with a strong and thick parastyle, a strong but thin mesostyle and a weak metastyle except for M3, on which the metastyle is equally strong as the parastyle, marked posteriorly by a concave wall. The paracone is strong, whereas the metacone becomes flat from M1 to M3 (Fig. 11E). There are no basal pillars. The protocone is narrow and protrudes lingually more than the hypocone. A central islet is present on medium-worn M1.

From three available mandibles, only one bears the entire tooth row (Table 16), which indicates short premolars compared to the molars (p/m ratio = 57.5; MYT87). The p2 and p3 are simple, with a weakly developed hypoconid, a feeble and posteriorly placed metaconid and an open anterior valley. The entoconid and the entostylid form a closed posterior valley from the first stages of wear. On p2, there is no paraconid. The p4 is quite similar with the p3, but its metaconid is stronger and extends somewhat anteriorly, whereas the narrow hypoconid is well individualized. A basal pillar exists only on m1. The parastylid is strong in all molars. The entostylid extends posteriorly on m1 and m2, and it is strong on m3. There is no goat fold. A metastylid is present on little-worn m2 and m3. The entoconid is more developed than the paraconid. The third lobe of m3 is single-cuspid and has a concave lingual wall.

The preserved metacarpals are elongated with narrow epiphyses; the robusticity index is 8.1 (MYT20). They belong to the type B of Köhler (1993), indicating adaptation to open, flat and dry habitats.

The overall size of MYT1 indicates a species slightly larger than '*Protoryx*' *enanus* Köhler, 1987, but with much sturdier horn-cores and close to '*Protoryx*' *solignaci* (Robinson, 1972) from which it differs in the absence

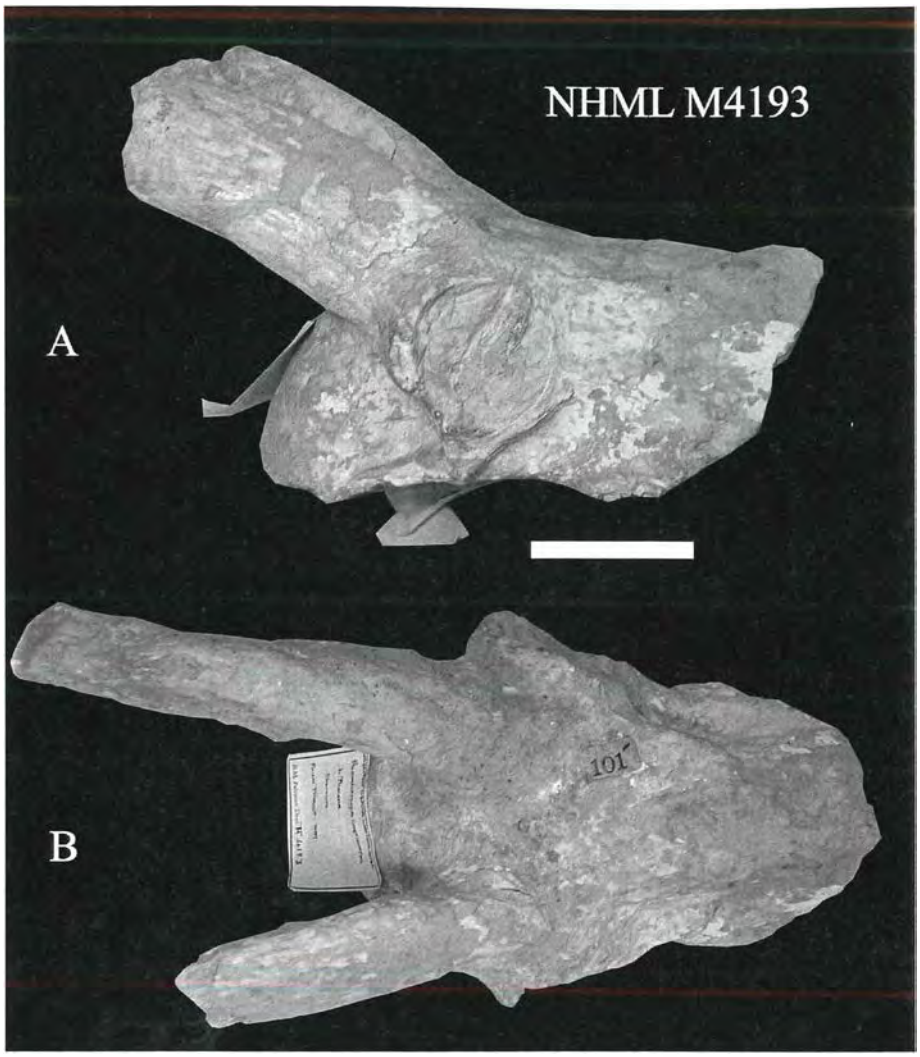

Figure 12: *Tragoreas oryxoides* from Samos, cranium NHML M4193 in lateral (A) and dorsal (B) view. Scale bar equals 5 cm.

of a sharp anterior keel on the horn-cores, the longer tooth row (but with equally shorter premolars) and the more advanced lower premolar pattern. Some cranial measurements of MYT1 approach those of *Skoufotragus schlosseri* from Q5 of Samos (Fig. 10), but the craniofacial flexion and the basioccipital structure are quite different. The opistocranium morphology of MYT1 perfectly fits that of the so-called "long-brained" variety of *Skoufotragus laticeps* (Andrée, 1926) from Q4, Q1 and MTLA of Samos, even though being about 20% smaller (Fig. 10). Though the MYT species is similar in cranial proportions to the smaller individuals of *Skoufotragus laticeps* (i.e., MGL S22), its horn-cores are significantly smaller in basal dimensions (~30%). Furthermore, its dentition is similar in size and morphology to that of later *Skoufotragus* species, suggesting a proportionally larger tooth row compared to the skull size. Cranial and dental morphometrical features of MYT1 perfectly match those of the Samos skull specimens PIM 2, and PIM XIII7, the latter assigned to *Pseudotragus capricornis* (Andrée, 1926:Pl. XIII, fig. 7). The main morphological difference between MYT and PIM XIII7 is the weaker posterior curvature of the horn-cores but PIM2 shows that this characteristic may vary within the species, as it does in *Skoufotragus laticeps*.

Discussion:

Protoryxoid bovids are by far the most abundant Bovidae in the Samos fauna, represented by several dozens of crania and frontlets. The number of occurring genera and species has been briefly cited and discussed by Pilgrim & Hopwood (1928) and in more detail by Gentry (1971), who drastically revised their taxonomy; further discussion also exists in Solounias (1981), Köhler (1987) and Bosscha-Erdbrink (1988). All these systematic efforts are strictly based on morphological criteria, lacking any stratigraphic information. As a result, there was no conception 'of what was happening to the species in time' (Gentry, 1971:256), nor of the temporal relations between different genera. The updated chrono-stratigraphic concept of the Samos fossil sites (Kostopoulos et al. 2003, this volume; Kostopoulos, this volume) together with the new and stratigraphically controlled bovid material, allowed a different approach to the problem – exposed in the previous paragraphs – that allowed recognizing the following species: *Protoryx capricornis* (Schlosser, 1904), *Skoufotragus laticeps* (Andrée, 1926), *Skoufotragus schlosseri* (Andrée, 1926) and *Skoufotragus zemalisorum* n.sp. Evidently, *Sk. zemalisorum*, *Sk. laticeps* and *Sk. schlosseri* are phylogenetically close, building a distinct lineage. Despite a caprine-like appearance, the relations of *Skoufotragus* with the

Caprini are debatable (see Gentry, 1971, 2000; Köhler, 1987; Bosscha-Erdbrink, 1988; Kostopoulos, 2005). Schlosser (1904:34, Pl. VI, figs. 1, 9) also described another Samos skull as *Tragoreas oryxoides*, later discussed by Gentry (1971:284) and Solounias (1981:188). Recently, Gentry (2000) suggested synonymizing *Tragoreas oryxoides* with *Pseudotragus capricornis* Schlosser, 1904 but the lectotypes of the two species differ in the position and curvature of the horn-cores, the cranio-facial angle and the size. On the contrary, a partial cranium in London (NHML M4193; Fig. 12) assigned to *Pseudotragus capricornis* by Pilgrim & Hopwood (1928:39) and another cranium in New York (AMNH20577) ascribed to *Ps. capricornis* by Solounias (1981:fig. 66c, d), show great morphometrical similarity to the lectotype of *Tragoreas oryxoides*. All these specimens represent a rather small-sized bovid with weakly divergent, moderately tilted backwards and long, rather straight, keelless horn-cores of elliptical cross-section (compression index 56-65); the lachrymal fossa is deep posteriorly and long; the face slopes weakly on the cranial roof; the opisthocranium curves gently down to the rear; the frontals are not raised between the horn-cores; the parietals are laterally inflated; the premolar row is moderately long compared to the molars (70-73%). I see them as conspecific.

Leptotragus pseudotragoides Bohlin, 1936 might also belong to the same species, but its horn-cores show an anterior keel (Bohlin, 1936: fig. 3; but see also Schlosser, 1904: Pl. VI, fig. 8, where the keel is missing). In my viewpoint, *Tragoreas oryxoides* is worth species distinction, representing a species with primitive features. The holotype of *Dorcadoryx triquetricornis* Teilhard & Trassaert, 1938 (:32, fig. 33; cast AMNH131901) shows great similarities with *Tragoreas oryxoides,* and especially with the specimen NHML M4193, suggesting close phylogenetic relationships. The *D. triqueticornis* specimen No. 10.062 (Teilhard & Trassaert, 1938: fig. 35) is probably conspecific with ?*Tragoreas largelii* Bohlin (1935b), and they could belong to a distinct taxon.

Genus *Urmiatherium* Rodler, 1888

Synonym:
Parurmiatherium Sickenberg, 1932

Urmiatherium rugosifrons (Sickenberg, 1932)

Lectotype: the partially preserved skull NHMW A4758, illustrated by Sickenberg (1933:Pl. V)
Synonyms:
Parurmiatherium rugosifrons Sickenberg, 1932

Emended Diagnosis: small-sized *Urmiatherium* with short, robust, homonymously twisted and closely settled horn-cores placed above the back of the orbits and prolonged anteriorly along the thick, hollowed frontals; reduced parietal very openly angled on the occipital plane; occipital extremely thick and semicircular shaped; basioccipital with fused, strong and ventrally developed posterior tuberosities, forming an additional articular facet for atlas; occipital condyles large and rounded; short premolar row; p4 with open anterior valley and anteroposteriorly expanded metaconid; lower molars without goat folds or basal pillars; oval shaped talonid on m3
Occurences: Samos, Injana
Time Range: Middle Turolian
Locality: Mytilinii 1A (MTLA)
Material: Opisthocranium, MTLA273a; mandible with i2-i3 dex and p2-m3 sin, MTLA146 (Lpm = 98.3; Lp = 36.0; Lm = 61.5 mm); p2-m3 dex, MTLA54 (Lpm = 97.5; Lp = 34.6; Lm = 61.7 mm)

Description & Comparison:
MTLA273a is a badly preserved opisthocranium with horn-cores crushed at their base (Table 17). In lateral view, the frontoparietal region is placed on the same level with the occipital face (Figs. 13C, D). The contribution of the parietal on the cranial roof is restricted. The fronto-parietal suture is closed and a moderate hump is developed in this part of the cranial roof. The occipital is extremely thick and its face is semi-circular-shaped (Fig. 13D). The external occipital protuberance is small and localized, surrounded by two shallow ligament scars. The mastoids are large and face laterally. The occipital condyles are large, rounded and they point backwards. The basioccipital is thick, short and narrow. Its posterior tuberosities are placed close together and they are raised, forming a semi-oval articular facet on their posterior face. The paroccipital processes are not completely preserved, but they seem to incline posteroventrally; there are articular facets for the atlas on the medial face of their base. The foramen ovale is small and faces laterally.

The lower premolar row is remarkably short, compared to the molars (56-58%). The paraconid and parastylid of p3 and p4 are quickly fused, forming a quadrangular anterior cuspid. The metaconid of p3 points backwards, whereas that of p4 is anteroposteriorly oriented, but without closing the anterior valley. The p4 is small, compared to the molars, which have rounded labial crescents and a weakly undulated lingual wall. The hypoconid of the molars protrudes more labially than the protoconid. The third lobe of m3 is large and points labially. There is no goat fold, nor a basal pillar on the molars.

Most of the morphological features detected on MTLA273a are typical for ovibovines (e.g., Bosscha-Erdbrink, 1978; Bouvrain & Bonis, 1985; Bouvrain et al., 1995), even though the monophyly of this tribe has been abolished. During late Miocene several Eurasian bovid genera developed similar opisthocranial morphology: *Tsaidamotherium* Bohlin, 1935b, *Urmiatherium* Rodler, 1888, *Plesiaddax* Schlosser, 1903, *Criotherium* Major, 1891a and *Parurmiatherium* Sickenberg, 1932; the last two are originally known from Samos. *Tsaidamotherium hedini* Bohlin, 1935b is known by a single opisthocranium that differs from MTLA273a in the quadrangular-shaped occipital face, the strong parietal lines, the obtuse angle between the parietal and the occipital, and the more elongated and primitive basioccipital. *Criotherium argalio-*

Table 17: Cranial measurements of *Urmiatherium rugosifrons* (MTLA273a; NHMW A4757, 4678) from Samos and *Plesiaddax depereti* (NHML M15811) from China.

	MTLA273a	NHMW A4758	NHMW A4757	NHML M15811
W braincase	83.5	79.1	79.9	96.2
W skull behind horn-cores	95.0	96.0	—	—
W bimastoids	79.0	77.6	82.0	(110)
W bicondyles	62.0	50.0	60.1	50.5
L back hc- upper margin of foramen magnum	(105)	94.6	112.7	85.0
W ptbc	24.0	30.0	—	37.3

ides Major, 1891a from Samos is larger than MTLA273a, from which it also differs in the more primitive parieto-occipital structure (the occipital forms an obtuse angle with the parietal; the basioccipital is less thickened with distinct anterior and posterior tuberosities and a median groove) and the heteronymous horn-core pattern.

The last genera to be compared with MTLA273a, *Urmiatherium*, *Plesiaddax* and *Parurmiatherium*, are not decisively discriminated. Solounias (1981) suggested synonymizing *Plesiaddax* and *Parurmiatherium*, but Bouvrain et al. (1995) had second thoughts about this, and proposed retaining *Parurmiatherium* for the Samos species. *Plesiaddax depereti* Schlosser, 1903 from China (NHML M15811) is slightly larger than MTLA273a (Table 17), but differs in acquiring a large, squarish occiput, a comparatively shorter opisthocranium, smaller and more closely settled occipital condyles and an oblique trapezoidal-shaped articular facet, formed by the posterior tuberosities of the basioccipital. The p2-m3 length of Samos is smaller than in *Plesiaddax* from Garkin and slightly smaller than in *Criotherium* from Samos, but the premolar/molar ratio is comparable to that of *Criotherium* (56-64), being larger than in *Plesiaddax* (52, n = 1) (Bouvrain, 1994b).

Gentry et al. (1999) suggested including *Parurmiatherium* into *Urmiatherium*, and I agree with them, as differences between *P. rugosifrons* and the type species of *Urmiatherium*, *U. polaki* Rodler, 1888, do not merit generic distinction. MTLA273a perfectly matches with the two cranial specimens of *U. rugosifrons* from Samos, stored in Vienna (NHMW A4757, A4758) and described by Sickenberg (1932) (Table 17, Fig. 13). The dentition of the Samos form was not known, but the lower dental morphology and proportions of MTLA54, MTLA146

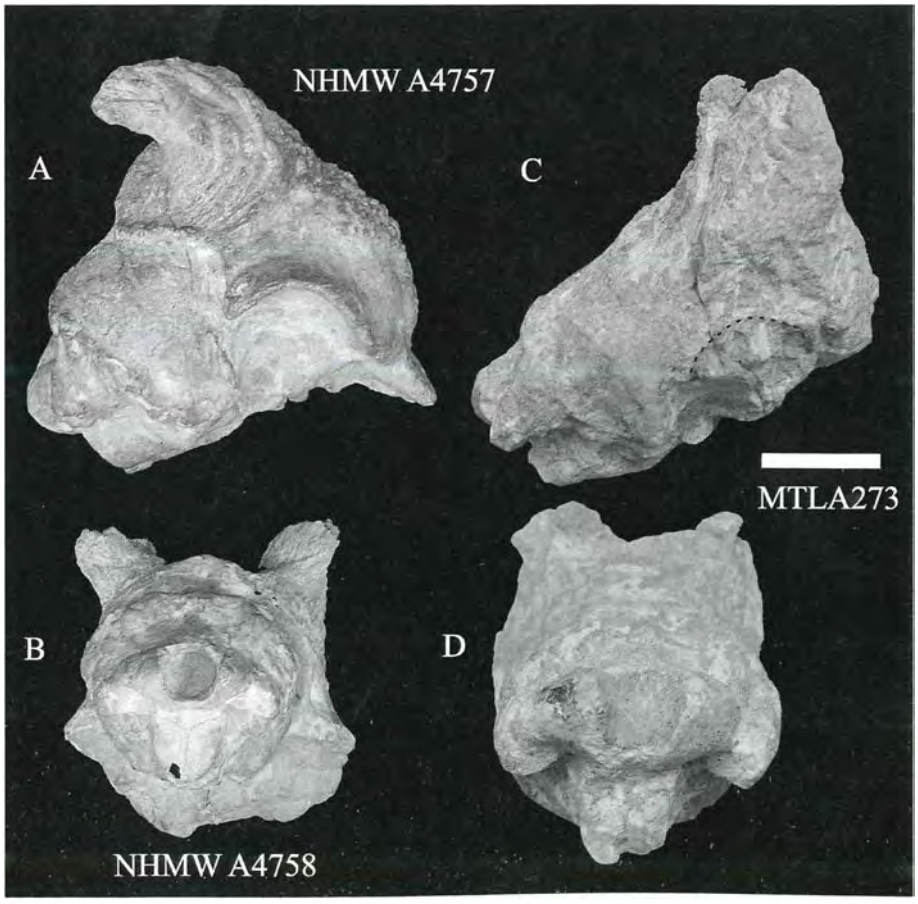

Figure 13: *Urmiatherium rugosifrons* from Samos. Crania NHMW A4757 (A) in lateral view, NHMW A4758 (B) in occipital view and MTLA273a in lateral (C) and occipital (D) view. Scale bar equals 5 cm.

fit pretty well with those of *U. rugosifrons* from Iraq (Bouvrain et al., 1995). *Urmiatherium polaki* from Maragheh and *U. intermedium* Bohlin, 1935a from China are larger than MTLA273, with a shorter premolar row (p/m ratio = 47.7% in *U. polaki* and 47.6-49.2% in *U. intermedium*), a semi-circular-shaped talonid on m3, a shorter opisthocranium and a more reduced parietal sector on the cranial roof. *U. polaki* also differs in the much more thickened occipital region and the untwisted horn-cores that largely cover the cranial roof. All evidences imply *U. rugosifrons* as more primitive than both the Maragheh and Chinese species.

3. Biochronology

The extraordinary puzzle of the Samos bovids has kept the interest of specialists alive for more than one century, as core issues (such as how many bovid species and how many bovid assemblages through time) remain poorly resolved. The consequences of this vagueness seem to affect not only the local (SE European) biochronology, but also - to some extent - the entire edifice of bovid evolution, since several Quaternary and living lineages have their origin or 'pass through' the Samos bovid assemblage. As Solounias (1981) stated in the final sentence of his classic essay "more systematic work needs to be done before the Samos bovids can be known better" and the new bovid material offers such an option.

The current study allows recognizing the following species per fossil site:

- **Mytilinii-4 (MLN)**: *Tragoportax* sp., *Miotragocerus* sp., *Gazella pilgrimi* and ?*Palaeoryx* sp.
- **Mytilinii-3 (MYT)**: *Gazella pilgrimi*, ?*Majoreas* sp., *Sporadotragus parvidens*, *Skoufotragus zemalisorum* n.sp. and ?*Palaeoryx* sp.
- **Mytilinii-1A (MTLA)**: *Miotragocerus valenciennesi*, *Gazella pilgrimi*, *Gazella* cf. *capricornis*, *Gazella mytilinii*, *Sporadotragus parvidens*, *Skoufotragus laticeps* ('long-brained' variety), *Palaeoryx pallasi* and *Urmiatherium rugosifrons*.
- **Mytilinii-1B (MTLB)**: *Miotragocerus valenciennesi*, *Tragoportax rugosifrons*, *Gazella pilgrimi*, *Gazella* cf. *capricornis*, *Gazella mytilinii*, *Skoufotragus laticeps* ('short-brained' variety), *Palaeoryx majori* and *Palaeoryx pallasi*.
- **Mytilinii-1C (MTLC)**: *Miotragocerus valenciennesi*, *Gazella* cf. *capricornis* and *Palaeoryx majori*.

The Mytilinii-4 (MLN) site has provided a poor bovid assemblage with four taxa, the taxonomy of which hardly attains species level. The site is directly correlated to B. Brown's Q2 (Kostopoulos, this volume: Giraffidae), and dated at 7.4-7.6 My; *G. pilgrimi* is rather in favor of an Early Turolian age. The bovid assemblage from Mytilinii-3 (MYT) is quite small, but characteristic, including five taxa; *G. pilgrimi*, *Sporadotragus parvidens* and ?*Palaeoryx* sp. imply chronological relations with MTLA/B level, but *Skoufotragus zemalisorum* indicates a more primitive bovid assemblage in accordance with the chronostratigraphic data that places the site at ~7.3 My (Kostopoulos et al., 2003). The Mytilinii-1 site from Adrianos ravine is certainly the richest in bovid taxa and number of specimens. The bovid assemblage from MTLA-B-C, dated at 7.1-7.0 My (Kostopoulos et al., 2003) includes ten species plus two undetermined ones that have been excluded from this work. Even though the bovid composition of these horizons does not show important changes or renewals over time, partly because of the inadequate data from the lower levels, it does shed light on stagnant taxonomical and chronological problems, especially in combination with data extracted from the old collections.

The systematic study of the new bovid collection and its correlation with the old material allows a review of the entire Samos bovid assemblage, summarized in Table 18. Starting from a total of 47 reported species, only 26 are considered to be valid, plus the new species *Skoufotragus zemalisorum*. Fig. 14 illustrates the time distribution of several Samos bovids, for which chronological indication is available.

Miotragocerus valenciennesi is present in the NHML collection that most probably comes from the lowermost level (Vryssoula-Qx), in Q2, Q6, Q1 and Q5 of AMNH- B. Brown's collection, in MGL - Forsyth-Major's collection labeled 'Adriano', in MTLA-B and possibly in MLN. This indicates a continuous presence throughout the Samos faunal succession (Fig. 14).

The concurrent presence of *T. rugosifrons* and *T. punjabicus* at Samos unfortunately cannot be proved, though it is possible. *T. rugosifrons* is present in the samples unearthed from the lower fossil levels (specimens NHML M4195, SMNS13269, AMNHnn-Q6), but is still present in the upper fossil sites MTLB and Q1 (MTLB159; AMNH86631, 86626, 86587, 20704) (Fig. 14). On the other hand, *T. punjabicus* is certainly known from Q5 (AMNH20566) but it also exists in the Münster (PIM) and Vienna (NHMW) collections (PIM68, 69, 70; NHMW A4790), which were partly coming from lower levels (Fig. 14). The persistence of *Tragoportax rugosifrons* in the upper MN12 levels from Samos seems to contradict its time-range in Continental Greece, where it is considered to be a typical Early Turolian element, with its last known occurrence at Perivolaki (early MN12; Kostopoulos, 2006a). *T. rugosifrons* is replaced in younger faunas of Continental Greece and Bulgaria by *T. amalthea*, originally known from Pikermi and the same may be true for Samos, though the origin of the few *T. amalthea* specimens from Samos is questionable.

Samos specimens attributed to *Samokeros minotaurus* lack any stratigraphic indication. A skull in AMNH (23036) is labeled as coming from Rongia, which is at the junction of the Andrianos stream with Potamies. The specimen has the typical fossilization status seen in specimens from Adrianos ravine, suggesting a late MN12 age. Nevertheless, Bernor et al. (1996) record *Samokeros* in the Middle Maragheh levels of presumably early Turolian age.

Gazella pilgrimi seems to characterize the entire Samos faunal succession, being present in Qx, MLN, MYT, MTLA-B and Q5. This time distribution (Fig. 14) is slightly

Taxon	Schlosser, 1904	Andrée, 1926	Solounias, 1981	Bernor et al., 1996	present work	Remarks
Miotragocerus valenciennesi			+	+	+	Both species are recorded by Solounias (1981) but re-examination of the entire material does not confirm the presence of *M. monacensis* (see text).
Miotragocerus monacensis			+	+		
Tragoportax amalthea	+	+	+	+	?	Material of *Tr. rugosifrons* and/or *T. punjabicus* used to confuse with this species, which, however, might be present in later Samos levels.
Tragoportax rugosifrons*	•				+	Discussed by Solounias (1981), Bouvrain & Bonis (1984), Bouvrain (1994a) and Spassov & Geraads (2004).
*Tragoportax recticornis**		•				
Tragoportax punjabicus						Discussed by Solounias (1981) and Spassov & Geraads (2004). *T. curvicornis* is considered to be synonymous of *T. punjabicus* together with *T. browni* (see text).
*Tragoportax curvicornis**		•	+	+		
Samokeros minotaurus*				+		Discussed by Solounias (1981); the species is little known and its phylogenetic relations need confirmation (see text).
Tragelaphus?		+				
Prostrepsiceros fraasii*				+		Gentry (1971) regard this species as synonymous of *Pr. rotundicornis* but Bouvrain & Thomas (1992) and Kostopoulos (2006a) consider it valid.
Prostrepsicros zitteli*						Used to confuse with other *Prostrepsiceros* species (Gentry, 1971; Solounias, 1981; Bibi, 2008). Discussed by Bouvrain (1982), Geraads & Gülek (1999), Kostopoulos (2004).
Majoreas woodwardi*						Kostopoulos (2004) regarded part of this material as belonging to *Pr. zitteli* and part to *Majoreas woodwardi* (Pilgrim & Hopwood, 1928).
Prostrepsiceros houtumschindleri			+	+		
Palaeoreas lindermayeri			+	+		
Protragelaphus skuzesi		+	+	+	○	Known by a single frontlet described and figured by Andrée (1926)
Gazella pilgrimi* (= *G. gaudryi*)	•		+	+	+	Revised by Bohlin (1935) and discussed by Gentry (1970) and Bouvrain (1996). It includes also *G. dorcadoides* of Solounias (1981) (see text).
G. longicornis		•				
Gazella mytilinii*						Revised by Pilgrim & Hopwood (1928) and discussed by Solounias (1981). For further review see text.
G. schlosseri Andrée			+		+	
Gazella sp.	+	+				
Gazella capricornis			+		cf.	Recorded by Solounias (1981) but on a wrong basis (see text).
Gazella n. sp.		•				
Gazella ancyrensis					cf.	Used to confuse with other *Gazella* species (see text).
Oioceros wegneri*		•	+	+	○	Known by a few specimens of unknown stratigraphic level. Discussed by Solounias (1981).
Samotragus crassicrornis*						Known by a single cranium described by Sickenberg (1936). Reviewed and discussed by Bouvrain & Bonis (1985) and Masini & Thomas (1989)

Table 18: Systematic revision of Samos Bovidae. Bovid species recorded (+) at Samos faunal assemblage(s) by several authors; closed circles represent original references; open circles represent species recognized in the present work but not included in the new material. Each left box gives the valid species name (in bold) and its synonyms (plain letters) after present-work's revision. Species marked with an asterisk have Samos as the type locality. Remarks include main references and basic systematic comments.

Taxon	Schlosser, 1904	Andrée, 1926	Solounias, 1981	Bernor et al., 1996	present work	Remarks
Samotragus sp.*						Reported by Solounias (1981) as *Prosinotragus* n. sp. It is quite possible that it represents a species or variety of *Samotragus*.
Samodorcas kuhlmani*		•	+	+	○	Revised by Bouvrain & Bonis (1985).
Criotherium argalioides*	+			+		Discussed by Pilgrim & Hopwood (1928), Solounias (1981), Bouvrain (1994) and Geraads & Spassov (2008).
Urmiatherium rugosifrons*				+	+	Created by Sickenberg (1932) and commented by Bouvrain et al. (1995) and Gentry et al. (1999) (see text).
Palaeoryx pallasi		+		+	+	Discussed by Gentry (1971), Solounias (1981) and Kostopoulos (2005)
Palaeoryx majori*					+	Discussed by Pilgrim & Hopwood (1928), Gentry (1971), Solounias (1981) and restored by Kostopoulos (2005). For further review see text.
*Palaeoryx laticeps**		•				
Sporadotragus parvidens		+				Discussed by Gentry (1971, 2000), Solounias (1981), Köhler (1987), Bosscha-Erdbrink (1988), Roussiakis (1996) and Geraads et al. (2006) (see text).
*Sporadotragus schafferi**						
*Palaeoryx stuetzeli**	•					
*Pseudotragus capricornis**	•		+	+	+	Discussed by Gentry (1971, 2000), Solounias (1981), Köhler (1987). These three species are considered to represent a single species: ***Protoryx capricornis*** (Schlosser, 1904); for review see text.
*Pseudotragus longicornis**						
*Pachytragus crassicornis**	•	+	+	+		
Tragoreas oryxoides*			+			Discussed by Gentry (1971, 2000) and Solounias (1981). It is considered to be valid and probably congeneric with *Dorcadoryx* Teilhard & Trassaert, 1936. For further comments see text.
Skoufotragus schlosseri*		•				Discussed by Gentry (1971), Solounias (1981), Bosscha-Erdbrink (1988) and Kostopoulos (2005). It is considered to be the genotype of the new genus *Skoufotragus*. For complete revision see text.
Palaeoryx cf. *stuetzeli*						
Protoryx/Pachytragus crassicornis			part			
Skoufotragus laticeps*		•				Re-defined by Gentry (1971) and discussed by Solounias (1981), Köhler (1987), Bosscha-Erdbrink (1988). For further review see text.
Protoryx carolinae	+		+		+	
*Hippotragus kopassi**						
*Protoryx hentscheli**	•					
Skoufotragus zemalisorum*					•	new species; see text.
*Palaeoryx ingens**	•					Nomen dubium; see comments on Gentry (1971) and Solounias (1981).
*Prodamaliscus gracilidens**	•					See comments on Solounias (1981).
*Oioceros? proaries**	•					Highly disputable and most probably synonymous of another taxon.

Table 18: Systematic revision of the Samos Bovidae. Bovid species recorded (+) in Samos faunal assemblage(s) by several authors; closed circles represent original references; open circles represent species recognized in the present work but not included in the new material. Each left box gives the valid species name (in bold) and its synonyms (plain letters) after present work's revision. Species marked with an asterisk have Samos as the type locality. Remarks include main references and basic systematic comments.

longer than that occurring in Continental Greece, where the species disappears after the beginning of MN12 (Kostopoulos, 2006a). Nevertheless, *G. pilgrimi* also exists at Akkaşdağı, Turkey (Kostopoulos, 2005), indicating that it probably lasted longer in the East. Both in Samos upper levels and at Akkaşdağı, *G. pilgrimi* is much less important than other *Gazella* species, probably indicating that it also fades out here. In accordance with continental Greece, *G.* cf. *capricornis* is lacking from early Samos levels, but it is present in Q1, MTLA-B and Q5, suggesting a later invasion than *G. pilgrimi* and characterizing the upper MN12-early MN13 Samos mammal assemblages (Fig. 14). In Turkey, a very similar form occurs in Kemiklitepe A/B, Kinik, Akkaşdağı and Mahmutgazi (Bouvrain, 1994b; Köhler, 1987; Kostopoulos, 2005), indicating a similar time range. The strong similarities between the Samos and the Akkaşdağı predominant gazelles and their distinction from the typical Pikermi sample might be due to either temporal or most probably spatial separation. *G. mytilinii* certainly appears at Samos in Q1-MTLA/B level (Fig. 14), but judging from NHML M5420 and AMNH20571 from Q5 it may be also present in earlier and/or later levels. The probably conspecific *Gazella* sp. form II from Garkin, Turkey (Köhler, 1987), dated to early MN12 certifies an earlier appearence. According to the original labels and fossilization status, all specimens ascribed to *G.* cf. *ancyrensis* should originate from the lower fossil levels of Samos (Vryssoula, Qx, 'Stefano'), whereas the species is also present in the neighbouring Kemiklitepe D site (Turkey), dated at 7.7 My (Sen et al., 1994), in Middle Maragheh of early Turolian age and possibly in Kayadibi, dated at ~8.2 My and in Garkin (*Gazella* sp. form III of Köhler, 1987).

Majoreas woodwardi (Pilgrim & Hopwood, 1928) and *Prostrepsiceros zitteli* are the only spiral antelopes for which chronological data can be extracted. The former is present in the NHML collection from Vryssoula-Qx level, as well as in the AMNH-Q6 sample (a frontlet without catalogue number) and in the MGL collection labeled 'Stefano', all representing the lower fossil levels of Samos (Fig. 14). The species is also present in Çorak Yerler, Kemiklitepe D and Garkin, Turkey, indicating a late MN11 - early MN12 time distribution (Kostopoulos, 2004; Geraads & Gülek, 1999). According to Schlosser (1904) the lectotype of *Pr. zitteli* originates from the 'gelblichbraunen Tonen" of Samos, whereas one frontlet and an isolated horn-core of this species in the AMNH collection (AMNH20575 and AMNH20576) come from B. Brown's Q5. Both evidences suggest a late MN12 – early MN13 time distribution (Fig. 14), but the species recently has been identified in Kavakdere, Turkey (Geraads & Gülek, 1999), dated at 8.1 My, indicating a much longer time distribution reaching back to the late MN11. The stratigraphic location of *Protragelaphus skuzesi*, *Samotragus crassicornis*, *Samodorcas kuhlmani* and *Oioceros wegneri* from Samos is unknown. *Oioceros wegneri* is recorded in Garkin and Mahmutgazi, Turkey (Köhler, 1987) suggesting a late MN12 age. On the other hand, the fossilization status of the only known specimen (SMNS13278) of *Prostrepsiceros fraasi* (Andrée, 1926) from Samos, rather indicates an origin from the lower fossil horizons.

The lower fossil levels of Samos provided copious material of *C. argalioides*, an otherwise rare large bovid; Schlosser (1904) indicates that the rich but lost - Munich collection originates exclusively from the 'braunen Tuffen' (AMNH10743 belongs to this sample), whereas the species is also well-documented in the NHML collection (M4199-M4202). More definite evidence comes from Q2 (AMNH22802), Q6 (AMNH20774, AMNH20771), Q4 (AMNH20761) and Potamies (MGL S71). Thus the chronological distribution of *Criotherium* covers MN11 and the very first part of MN 12 (Fig. 14). Two additional specimens, the cranium PIM151 and the opisthocranium MGL S58 also belong to this species; the former lacks stratigraphic indication, but the latter is labeled as being from Forsyth-Major's 'Adriano', a possibility that seems not very credible, even more so because its preservation status is identical with that of MGL S71 from 'Potamies'.

The stratigraphic origin of the two *Urmiatherium rugosifrons* crania in NHMW, described by Sickenberg (1936), is unknown. The new data showed, however, that the species certainly occurs in MTLA, suggesting that this specialized bovid was present in the upper part of MN12. A mandible from Q5 (AMNH 86522) might also belong to this species, extending its time distribution until the beginning of MN13 (Fig. 14). If indeed *C. argalioides* and *U. rugosifrons* share an ecological niche, as their skull and dental anatomy suggests, it is quite possible that *U. rugosifrons* supersedes *C. argalioides* in the Samos faunal succession.

The stratigraphic evidence of *Sporadotragus parvidens* suggests a continuous presence throughout the entire Samos faunal succession. The species is present in Qx (AMNH20777), Q1 (AMNH23035, 20689) and Q5 (AMNH22941, 84452) of Barnum Brown, as well as in MYT and MTLA (Fig. 14).

Palaeoryx is represented on Samos by two distinct species: *Palaeoryx pallasi* (Wagner, 1857) and *Palaeoryx majori* Schlosser, 1904 that coexist in the middle Turolian levels (MTLB). *P. pallasi* is known from Forsyth-Major's 'Adriano', as well as from Q6, Q4 and Q1 of B. Brown (AMNH) and MTLA, suggesting a vast occurrence on Samos during MN12; its presence in MLN is also probable (Fig. 14). *P. majori* certainly occurs in the upper part of MN12, but its chronological extension before and after the MTLA/B level is uncertain; the species is also present in Akkaşdağı (Turkey), dated at 7.0 My.

The time distribution of *Protoryx capricornis* is unknown, since none of the specimens brings any indication of origin. Nevertheless, Schlosser (1904) mentioned that material of '*Pseudotragus capricornis*' is coming 'ausschliesslich aus den weisslichen kalkigen Ablagerungen', suggesting a provenance from the MLN level, whereas '*Pachytragus crassicornis*' and '*Pseudotragus longicornis*' are most probably coming from underlying and overlying fossil levels, respectively (Fig. 14).

Tragoreas oryxoides is most probably coming from the lower fossil levels of Samos: NHML M4193 is certainly

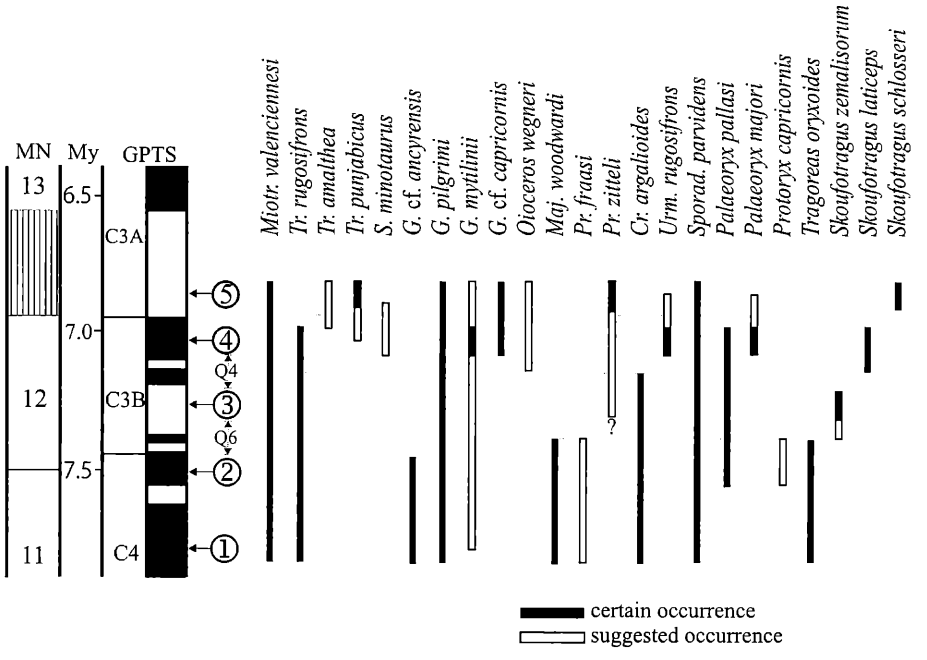

Figure 14: Chronological distribution of the Samos Bovidae.

MN: European land mammal Neogene assemblages; striped area marks the undefined MN12-MN13 boundary; GPTS: Geo-Polarity Time Scale; Fossil levels (1): Qx, Vryssoula; (2): Q2, MLN, 'Stefano'; (3): Q3, MYT; (4): Q1, MTLA-B-C, 'Adriano'; (5): Q5 (data from KOSTOPOULOS et al., 2003, this volume; KOSTOPOULOS, this volume). Black bars represent certain distribution; white bars represent suggested distribution.

from Vryssoula-Qx level, whereas AMNH20577 is from B. Brown's Q6. SCHLOSSER (1904:35) mentioned that the *T. oryxoides* material originates from the 'braunen Tuffen' and 'grauen Tonen', both terms also suggesting lower fossil levels of Samos (Fig. 14). The species might also be present in Kavakdere, Turkey, dated at 8.1 My (GENTRY, 2003).

Skoufotragus zemalisorum is known from MYT and it predates *Skoufotragus laticeps,* which seems to appear for the first time in Q4 level (Fig. 14). *Skoufotragus* samples from the middle Sinap localities 26 and 33 (= Kavakdere) of late MN11 age (GENTRY, 2003), might also belong to *Sk. zemalisorum*. *Skoufotragus laticeps* occurs on Samos in Q4, Q1, MTLA and MTLB. All specimens in the Lausanne collection (MGL S20, 22, 26, 27, 28, 30, 31, 57, 201, 298 and 1124) labeled as from 'Adriano', belong to this species. The Münster crania PIM3, 4, 5, 6, 9, 11 and 15 are also assigned to *Sk. laticeps* and, although they lack any stratigraphic indication, they were most probably unearthed from Adrianos ravine. Thus the species characterizes the middle - late MN12 Samos faunal assemblages, but the Maragheh record is probably older (Fig. 14). *Skoufotragus schlosseri* occurs at Q5, suggesting a latest MN12 to early MN13 distribution (Fig. 14). The species also occurs in the Turkish sites Akkaşdağı, Kinik and possibly Çoban Pinar (GENTRY, 2003; KOSTOPOULOS, 2005), indicating a similar time distribution.

Judging from the time distribution of the bovid species (Fig. 14), four successive bovid assemblages can be distinguished on Samos:

• **Primary bovid assemblage** [sites Qx, Q2, Q6, MLN, 'Stefano', NHML, Munich; age ~7.8-7.4 My]:
Miotragocerus vallenciennesi, *Tragoportax rugosifrons*, *Sporadotragus parvidens*, *Gazella pilgrimi*, *Gazella* cf. *ancyrensis*, *Majoreas woodwardi*, *Criotherium argalioides*, *Tragoreas oryxoides*, *Prostrepsiceros fraasi*, ± *?G. mytilinii*, *Protoryx capricornis* and *Palaeoryx* sp.

• **Intermediary bovid assemblage** [site MYT; age ~7.4-7.2]:
Miotragocerus vallenciennesi, *Tragoportax rugosifrons*, *Sporadotragus parvidens*, *Gazella pilgrimi*, *Palaeoryx pallasi*, *Criotherium argalioides*, *Skoufotragus zemalisorum* ± *Gazella mytilinii*, *Prostrepsiceros zitteli*, *Prostrepsiceros fraasi*.

• **Dominant bovid assemblage** [sites Q4, Q1, MTLA, MTLB, 'Adriano'; age ~7.2-7.0 My]:
Miotragocerus vallenciennesi, *Tragoportax rugosifrons*, *Sporadotragus parvidens*, *Gazella pilgrimi*, *Gazella* cf. *capricornis*, *Gazella mytilinii*, *Palaeoryx pallasi*, *Palaeoryx majori*, *Urmiatherium rugosifrons*, *Skoufotragus laticeps* ± *Prostrepsiceros zitteli*, *Oioceros wegneri*, *Tragoportax punjabicus*, *Samokeros minotaurus*.

• **Final bovid assemblage** [site Q5; age ~7.0-6.8 My]:
Miotragocerus vallenciennesi, *Tragoportax punjabicus*, *Sporadotragus parvidens*, *Gazella pilgrimi*, *Gazella* cf. *capricornis*, *Prostrepsiceros zitteli*, *Skoufotragus schlosseri* ± *Samokeros minotaurus*, *Gazella mytilinii*, *Oioceros wegneri*, *Palaeoryx majori*, *Tragoportax amalthea*, *Urmiatherium rugosifrons*.

It is worth mentioning that this interpretation strongly recalls HEISSIG (1975) in recognizing four stages of evolution in the Samos fauna. Similarities with the late Miocene Turkish mammal sites are also obvious. A bovid assemblage of the Samos primary type occurs in the neighboring Kemiklitepe D (BOUVRAIN, 1994b), dated at ~7.7 My (SEN et al., 1994). The bovid association from Kemiklitepe A/B, dated at 7.2 My (SEN et al., 1994), corresponds with the Samos intermediary-to-dominant bovid assemblage, whereas that from Akkaşdağı (7.0 ± 0.1 My; KARADENIZLI et al., 2005) fits the final Samos type, although it might be slightly older. On the contrary, comparison with the contemporaneous faunas from the Greek mainland indicates significant differences, especially concerning the signal of caprine- and ovibovine-like bovids. *Criotherium* has been recently identified in the late MN11 Bulgarian record (GERAADS & SPASSOV, 2008), but its contribution

to the mainland bovid assemblage is certainly less important than in Samos. The dominant bovid assemblage of Samos certainly shares common elements with Pikermi (*Gazella capricornis*, *Miotragocerus valenciennesi*, *Palaeoryx pallasi*, *Sporadotragus parvidens*), but the general aspect of the Samos bovid community is extremely different, as it is characterized by the predominance of *Skoufotragus* + multiple *Gazella* species, while in the West, boselaphines and various small antilopines form the greatest part of the bovid assemblage. The final bovid stage of Samos still shares important elements with the previous one, but the boselaphines strengthen their presence and *Skoufotragus* evolves to more specialized forms.

4. Conclusions

The study of the new bovid material collected from Mytilinii basin, Samos, Greece, allows recognizing 13 species from five fossil sites, MLN, MYT, MTLA, MTLB and MTLC. Comparison with Samos bovid material in several museums across the world leads to an extensive systematic revision of the entire Samos bovid assemblage, validating 27 species. Among them, *Tragoportax curvicornis* Andrée, 1926) is considered to be synonymous with *Tragoportax punjabicus* (Pilgrim, 1910); *Pachytragus crassicornis* Schlosser, 1904, *Pseudotragus capricornis* Schlosser, 1904 and *Pseudotragus longicornis* Andrée, 1926 are placed into *Protoryx capricornis* (Schlosser, 1904); *Tragoreas oryxoides* Schlosser, 1904 is regarded as valid and close to the Chinese *Dorcadoryx* Teilhard & Trassaert, 1938; the systematic status of the Samos *Gazella* species has been restored and re-defined; the taxonomic distinction of the two *Palaeoryx* species from Samos has been improved; the new replacement for the generic name *Pachytragus* is *Skoufotragus*, including *Pachytragus laticeps* Andrée, 1926 and part of *Pachytragus crassicornis* Andrée, 1926 is settled and the new species *Skoufotragus zemalisorum* has been described. Discussion of the time distribution of bovid species allows recognizing four chronological bovid assemblages on Samos, representing four successive stages of evolution, ranging from late Early to early Late Turolian.

5. Acknowledgements

The excavations on Samos have been supported by the Prefecture of Samos and the "Konstantinos and Maria Zimalis" Foundation. The Municipality of Mytilinii provided generous help too. The Natural History Museum of the Aegean offered us the premises for the preparation and storage of the fossils. Thanks are due to Prof. A. Baud (University of Lausanne), Dr. A. Currant and Dr. A. Gentry (Natural History Museum, London), Dr. G. Daxner-Höck (Naturhistorisches Museum Wien), Dr. E. Delson and S. Bell (American Museum of Natural History), Dr. S. Sen, Dr. P. Tassy and Dr. C. Sagne (Muséum national d'Histoire naturelle de Paris), Dr. M. Bertling (Paläontologisches Institut Münster) and Dr. S. Roussiakis (University of Athens). Dr. D. Geraads is also thanked for providing me with photos of several Samos specimens. Mr. Nikos Chatzispyridou and all colleagues and students who worked in the field and laboratory are deeply thanked for their assistance. Alan and Anthea Gentry have highly improved the paper with their insightful comments and suggestions.

6. References

Andrée, J., 1926. Neue Cavicornier aus dem Pliocän von Samos. — Palaeontographica, 67(6):135–175, Stuttgart.

Arambourg, C. & Piveteau, J., 1929. Les vertébrés du Pontien de Salonique. — Annales de Paléontologie, 18:1–82.

Bernor, R.L., Solounias, N., Swisher III, C.C. & van Couvering, J.A., 1996. The correlation of three classical "Pikermian" mammal faunas – Maragheh, Samos, Pikermi – with the European MN Unit System. — [in:] Bernor, R.L., Fahlbusch, V., Mittman, H.-W. (eds). The evolution of Western Eurasian Neogene Mammal Faunas. – 137–154, New York – Columbia University Press.

Bibi, F., 2008. Bovidae (Mammalia: Artiodactyla) from the late Miocene of Sivas, Turkey. — Journal of Vertebrate Paleontology, 28:501–519.

Blainville, H.M.D., 1816. Prodrome d'une nouvelle distribution systématique du règne animal. — Bulletin des Sciences Société Philomathique de Paris, s. 3:105–124, Paris.

Bohlin, B., 1935a. Cavicornier der Hipparion-Fauna Nord-Chinas. — Palaeontologia Sinica, C, 9(4):1–166, Peking.

Bohlin, B., 1935b. *Tsaidamotherium hedini* n. g., n. sp. — Hyllningsskrift Sven Hedin, 66–74, Stockholm.

Bohlin, B., 1936. Bemerkungen über einige pontische Antilopen-Gattungen. — Arkiv för Zoologi, 28A, 18:1–22, Stockholm.

Bohlin, B., 1941. *Gazella* (*Protetraceros*) *gaudryi* (Schlosser) and *Gazella dorcadoides* Schlosser. — Bulletin of the Geological Institution Upsala, 28:79–122.

Bosscha-Erdbrink, D.P., 1978. Fossil Ovibovines from Garkin near Afyon, Turkey (I) & (II). — Proceedings of the Koninklijke Nederlandse Akademie van Wetenschappen, B, 81(2):145–185, Amsterdam.

Bosscha-Erdbrink, D.P., 1988. *Protoryx* from three localities East of Maragha, NW Iran. — Proceedings of the Koninklijke Nederlandse Akademie van Wetenschappen, B, 91(2):101–159, Amsterdam.

Bouvrain, G., 1988. Les *Tragoportax* (Bovidae, Mammalia) des gisements du Miocène supérieur de Dityko (Macédoine, Grèce). — Annales de Paléontologie, 74(1):43–63.

Bouvrain, G., 1994a. Un bovide du Turolien inferieur d'Europe orientale *Tragoportax rugosifrons*. — Annales de Paléontologie, 80:61–87.

Bouvrain, G., 1994b. Les gisements de mammifères

du Miocène supérieur de Kemiklitepe, Turquie: 9. Bovidae. — Bulletin du Muséum National d'Histoire Naturelle, (4), sect. C., **16**(1):175–209, Paris.

BOUVRAIN, G., 1996. Les gazelles du Miocène supérieur de Macédoine, Grèce. — Neues Jahrbuch für Geologie und Paläontologie, Abhandlungen, **199**:111–132.

BOUVRAIN, G., 2001. Les Bovidés (Mammalia, Artiodactyla) des gisements du Miocène supérieur de Vathylakkos (Grèce du Nord). — Neues Jahrbuch für Geologie und Paläontologie, Abhandlungen, **220**: 225–244.

BOUVRAIN, G. & BONIS, L. de, 1984. Étude d'une Miotragocère du Miocène supérieur de Macédoine (Grèce). — [in:] BUFFETAUT, E., MAZIN, J.M. & SALMON, E. (eds). Actes du Symposium paléontologique G. Cuvier, Montbéliard. p. 35–51.

BOUVRAIN, G. & BONIS, L. de, 1985. Le genre *Samotragus* (Artiodactyla, Bovidae) une antilope du Miocène Supérieur de Grèce. — Annales du Paléontologie, **71**(4):257–299.

BOUVRAIN, G. & THOMAS, H., 1992. Une antilope à chevilles spiralées: *Prostrepsiceros zitteli* (Bovidae), Miocène supérieur du Jebel Hamrin en Irak. — Geobios, **25**:525–533.

BOUVRAIN, G., SEN, S. & THOMAS, H., 1995. *Parurmiatherium rugosifrons* SICKENBERG, 1932, un ovibovinae (Bovidae) du Miocène supérieur d'Injana (Djebel Hamrin, Irak). — Geobios, **28**(6):719–726.

DAMES, W.B., 1883. Hirsche und Mäuse von Pikermi in Attica. — Zeitschrift der Deutschen Geologischen Gesellschaft, **35**:92–101.

GAILLARD, C., 1902. Le bélier de Mèndes ou le mouton domestique de l'ancienne Egypte. — Bulletin Société d'Anthropologie Biologique de Lyon, **20**:70–103.

GAUDRY, A., 1861. Notes sur les antilopes trouvées à Pikermi (Grèce). — Bulletin de la Societé Géologique de France, **18**:388–400.

GAUDRY, A., 1873. Animaux fossils du Mont Luberon (Vaucluse). — Étude sur les vertébrés. Savi F. (ed) Paris, – 1–112.

GENTRY, A.W., 1970. The Bovidae (Mammalia) of the Fort Ternan fossil fauna. — [in:] LEAKEY, L.S.B. & SAVAGE, R.J.G. (eds.). Fossil vertebrates of Africa. – 2:243–323, Academic Press, London.

GENTRY, A.W., 1971. The earliest goats and other antelopes from Samos *Hipparion* Fauna. — Bulletin of the British Museum (Natural History), Geology, **20**:229–296.

GENTRY, A.W., 1999. Fossil Pecorans from the Baynunah Formation, Emirate of Abu Dhabi, United Arab Emirates. — [in:] WHYBROW, P. & HILL, A. (eds). Fossil Vertebrates of Arabia. – 290–316, Yale University Press, New Haven.

GENTRY, A.W., 2000. Caprinae and Hippotragini (Bovidae, Mammalia) in the upper Miocene. — [in:] VBRA, E.S. & SCHALLER, G.B. (eds). Antelopes, deer and relatives: fossil record, behavioral ecology, systematics and conservation. – 65–83, Yale University Press, New Haven.

GENTRY, A.W., 2001. An ovibovine (Mammalia, Bovidae) from the Neogene of Stratzing, Austria. — Annalen des Naturhistorischen Museums Wien, **102A**:189–199, Wien.

GENTRY, A.W., 2003. Ruminantia (Artiodactyla). — [in:] FORTELIUS, M., KAPPELMAN, J., SEN, S., BERNOR, R. (eds.). Geology and Paleontology of the Miocene Sinap Formation, Turkey. – 332– 379, Columbia University Press, New York.

GENTRY, A.W., RÖSSNER, G.E. & HEIZMANN, P.J., 1999. Suborder Ruminantia. — [in:] RÖSSNER, G. & HEISSIG, K. (eds.). The Miocene land mammals of Europe. –225-258, Munich (Verlag Dr. F. Pfeil).

GERAADS, D. & GÜLEK, E., 1999. On some spiral-horned antelopes (Mammalia: Artiodactyla: Bovidae) from the late Miocene of Turkey, with remarks on their distribution. — Paläontologische Zeitschrift, **73**(3/4):403–409.

GERAADS, D. & SPASSOV, N., 2008. A new species of *Criotherium* (Bovidae, Mammalia) from the late Miocene of Bulgaria. — Hellenic Journal of Geosciences, in press.

GERAADS, D., SPASSOV, N. & KOVACHEV, D., 2006. A new *Sporadotragus* (Bovidae, Mammalia) from the late Miocene of Bulgaria. — Rivista Italiana de Paleontologia e Stratigrafia, **112**(3):473–479.

GRAY, J.E., 1821. On the natural arrangement of vertebrose animals. — London Medical Repository, **15**:296–310.

GROMOLARD, C., 1980. Une nouvelle interprétation des grands Bovidae (Artiodactyla, Mammalia) du Pliocène d'Europe occidentale classés jusqu'à présent dans le genre *Parabos*: *Parabos cordieri* (DE CHRISTOL) emend., ?*Parabos boodon* (GERVAIS) et *Alephis lyrix* n. gen. n. sp. — Geobios, **13**:767–775.

GUÉRIN, C., 1965. *Gallogoral* (nov. gen.) *meneghinii* (RÜTIMEYER, 1878) un rupicapriné du Villafranchien d'Europe occidentale. — Documents des Laboratoires de Géologie de la Faculté des Sciences de Lyon, **11**: 1–353.

HEINTZ, E., 1971. *Gazella deperdita* (GERVAIS) 1847 (Bovidae, Artiodactyla, Mammalia) du Pontien du Mont Luberon, Vaucluse, France. — Annales de Paléontologie, **57**(2):209–229.

HEISSIG, K., 1975. Rhinocerotidae aus dem Jungtertiär Anatoliens. — Geologisches Jahrbuch, B, **15**: 145–151.

KARADENIZLI, L., SEYITOĞLU, G., SEN, S., ARNAUD, N., KAZANCI, N., SARAÇ, G. & ALÇIÇEK, C., 2005. Mammal bearing late Miocene tuffs of the Akkaşdağı region; distribution, age, petrographical and geochemical characteristics. — Geodiversitas, **27**(4):553–566.

KNOTTNERUS-MEYER, T., 1907. Über das Tränenbein der Huftiere. — Archiv für Naturgeschichte, **73**(1):1–151.

KÖHLER, M., 1987. Boviden des türkischen Miozäns (Känozoikum und Braunkohlen der Türkei). — Paleontologia i Evolucio, **21**:133–246.

KÖHLER, M., 1993. Skeleton and habitat of recent and

fossil ruminants. — Münchner Geowissenschaftliche Abhandlungen, A, 25:1–88.

Korotkevitch, E.L., 1976. The late Neogene gazelles. — Naukova Doumka, 1–251, Kiev.

Korotkevitch, E.L., 1988. Genesis of the Hipparion fauna of eastern Europe. — Naukova Doumka, 1–160, Kiev.

Kostopoulos, D.S., 2004. Revision of some late Miocene spiral horned antelopes (Bovidae, Mammalia). — Neues Jahrbuch für Geologie und Paläontologie, 231:167–190.

Kostopoulos, D.S., 2005. The Bovidae (Artiodactyla, Mammalia) from the Late Miocene mammal locality of Akkaşdağı (Central Anatolia, Turkey). — Geodiversitas, 27(4):747–791.

Kostopoulos, D.S., 2006a. The late Miocene vertebrate locality of Perivolaki, Thessaly, Greece. 9. Cervidae and Bovidae. — Palaeontographica, Abt. A, 276(1-6):151–183, Stuttgart.

Kostopoulos, D.S., 2006b. Greek bovids through time. — Hellenic Journal of Geosciences, 41(1):141–152.

Kostopoulos, D.S., this volume. The Late Miocene Mammal Faunas of the Mytilinii Basin, Samos Island, Greece: New Collection. 13. Giraffidae. — Beiträge zur Paläontologie, 31:299–343. Wien.

Kostopoulos, D.S. & Koufos, G.D., 1996. Late Miocene bovids (Mammalia, Artiodactyla) from the locality "Nikiti-1" (NKT), Macedonia, Greece. — Annales de Paléontologie, 81:251–300.

Kostopoulos, D.S. & Koufos, G.D., 1999. The Bovidae (Mammalia, Artiodactyla) of the Nikiti-2 (NIK) faunal assemblage (Chalkidiki peninsula, N. Greece). — Annales de Paléontologie, 85:193–218.

Kostopoulos, D.S., Sen, S. & Koufos, G.D., 2003. Magnetostratigraphy and revised chronology of the late Miocene mammal localities of Samos, Greece. — International Journal of Earth Sciences, 92:779–794.

Kostopoulos, D.S., Koufos, G.D., Sylvestrou, I.A., Syrides, G. & Tsombachidou, E., this volume. The Late Miocene Mammal Faunas of the Mytilinii Basin, Samos Island, Greece: New Collection. 2. Lithostratigraphy and Fossiliferous Sites. — Beiträge zur Paläontologie, 31:13–26, Wien.

Koufos, G.D. & Melentis, J., 1982. The late Miocene (Turolian) mammalian fauna of Samos Island (Greece). — Scientific Annals, Faculty of Physics and Mathematics, University of Thessaloniki, 22:175–192.

Koufos, G.D., Syrides, G., Kostopoulos, D.S., Koliadimou, K., Sylvestrou, I., Seitanides, G. & Vlachou, Th., 1997. New excavations in the Neogene mammalian localities of Mytilinii, Samos island, Greece. — Geodiversitas, 19(4):877–885.

Kretzoi, M., 1941. Neue Antilopen-Form aus dem Soproner Sarmat. — Földtani Közlöny Mayer, 71:336–343.

Kretzoi, M., 1968. New generic names for homonyms. — Vertebrata Hungarica, 10(1-2):163–166.

Major, C.I.F., 1888. Sur un gisement d'ossements fossiles dans l'île de Samos, contemporains de l'age de Pikermi. — Comptes Rendus Hebdomadaires des Séances de l'Académie des Sciences Paris, 107:1178–1181.

Major, C.I.F., 1891a. Considerations nouvelles sur la faune des vertèbres du Miocène superieur dans l'île de Samos. — Comptes Rendus Hebdomadaires des Séances de l'Académie des Sciences de Paris, 113:608–610.

Major, C.I.F., 1891b. Sur l'age de la faune de Samos. — Comptes Rendus Hebdomadaires des Séances de l'Academie des Sciences Paris, 113:708–710.

Major, C.I.F., 1894. Le gisement ossifère de Mytilini et catalogue d'osséments fossiles. – 1–51, Lausanne.

Masini, F. & Thomas, H., 1989. *Samotragus occidentalis* n. sp. a new bovid from the late Messinian of Italy. — Bollettino della Società Paleontologica Italiana, 28(2-3):307–316.

Melentis, J., 1969. Paläontologische Ausgrabungen auf der Insel Samos (eine vorläufige Mitteilung). — Proceedings of the Academy of Athens, 43:344–349, Athens.

Moyà-Solà, S., 1983. Los Boselaphini (Bovidae, Mammalia) del Neogeno de la Peninsula Iberica. — Publicaciones de Geologia, 18:1–236.

Pavlow, M., 1913. Mammifères tertiaires de la Nouvelle Russie. — Nouvelles Mémoires de la Societé Impériale Moscou, 17:1–67, Moscow.

Pilgrim, G.E., 1910. Notices of new mammalian genera and species from the Tertiaries of India. — Records of the Geological Survey of India, 40:63–71.

Pilgrim, G.E., 1926. On the names and types of certain Pontian antelopes. — Annals and Magazine of Natural History, s. 9, 18:464.

Pilgrim, G.E., 1937. Siwalik antelopes and oxen in the American Museum of Natural History. — Bulletin of the American Museum of Natural History, 72:729–847.

Pilgrim, G. & Hopwood, A., 1928. Catalogue of the Pontian Bovidae of Europe. — British Museum (Natural History), – 1–106.

Robinson, P., 1972. *Pachytragus solignaci*, a new species of caprine bovid from the late Miocene Beglia Formation of Tunisia. — Notes du Service Géologique de Tunisie, 37:73–94.

Rodler, A., 1888. Notiz über ein im Besitze des Dr. J.E. Polak befindliches Schädelfragment eines Sivatheriden vom Knochenfelde von Maragha am Urmiasee in Nordpersien. — Anzeiger der Österreichischen Akademie der Wissenschaften, Mathematisch-Naturwissenschaftliche Klasse, 25:114–115, Wien.

Rodler, A. & Weithofer, K.A., 1890. Die Wiederkäuer der Fauna von Maragha. — Denkschriften der Kaiserlichen Akademie der Wissenschaften, Mathematisch-Naturwissenschaftliche Klasse, 57:753–771, Wien.

Roth, J. & Wagner, A., 1854. Die fossilen Knochenüberreste von Pikermi in Griechenland. — Abhandlungen der Bayerischen Akademie der Wissenschaften, 7:371–464, München.

Roussiakis, S., 1996. Contribution to the study of fossil mammals from the classical Pikermi site. — PhD

Thesis, University of Athens, – 1–259, (unpublished, in Greek).

SCHAUB, S., 1923. Neue und wenig bekannte Cavicornier von Senèze. — Eclogae Geologicae Helvetiae, **18**:281–295, Basel.

SCHLOSSER, M., 1903. Die fossilen Säugetiere Chinas nebst einer Odontographie der recenten Antilopen. — Abhandlungen der Bayerischen Akademie der Wissenschaften, Mathematisch-Naturwissenschaftliche Klasse, **22**:1–221, München.

SCHLOSSER, M., 1904. Die fossilen Cavicornier von Samos. — Beiträge zur Paläontologie und Geologie Österreich-Ungarns, **17**:21–118, Wien.

SEN, S., BONIS, L. de, DALFES, N., GERAADS, D. & KOUFOS, G., 1994. Les gisements de mammifères du Miocène supérieur de Kemiklitepe, Turquie: 1. Stratigraphie et magnetostratigraphie. — Bulletin du Muséum National d' Histoire Naturelle, (4), sect. C., **16**(1):5–17.

SICKENBERG, O., 1932. Eine neue Antilope, *Parurmiatherium rugosifrons* nov. gen., nov. sp. aus dem Unterpliozän von Samos. — Anzeiger der Österreichischen Akademie der Wissenschaften, Mathematisch-Naturwissenschaftliche Klasse, Wien, **1**:1–8, Wien.

SICKENBERG, O., 1933. *Parurmiatherium rugosifrons* ein neuer Bovide aus dem Unterpliozän von Samos. — Palaeobiologica, **5**:81–102, Wien.

SICKENBERG, O., 1936. Über *Samotragus crassicornis* nov. gen. et spec. aus dem Unterpliozän von Samos. — Palaeontologische Zeitschrift, **18**:90–94.

SOLOUNIAS, N., 1981. The Turolian fauna from the island of Samos, Greece. — Contribution on Vertebrate Evolution, **6**:1–232.

SOLOUNIAS, N., 1994. Cranial restoration and dietary determination of two extinct antelopes from the Miocene of Greece. — Annales Musei Goulandris, **9**:511–520.

SPASSOV, N. & GERAADS, D., 2004. *Tragoportax* PILGRIM, 1937 and *Miotragocerus* STROMER, 1928 (Mammalia, Bovidae) from the Turolian of Hadjidimovo, Bulgaria, and a revision of the late Miocene Mediterranean Boselaphini. — Geodiversitas, **26**(2):339–370.

STROMER, E., 1928. Wirbeltiere im obermiozänen Flinz Münchens. — Abhandlungen der Bayerischen Akademie der Wissenschaften, Mathematisch-Naturwissenschaftliche Klasse, **32**:1–71.

TEILHARD DE CHARDIN, P. & TRASSAERT, M., 1938. Cavicornia of south-eastern Shansi. — Palaeontologia Sinica, C, **6**:1–98.

TEKKAYA, I., 1973. Une nouvelle èspece de gazelle de Sinap moyen. — Bulletin of the Mineral Research and Exploration Institute, Turkey, **80**:118–143.

WAGNER, A., 1848. Urweltliche Säugethier-Überreste aus Griechenland. — Abhandlungen der Bayerischen Akademie der Wissenschaften, Mathematisch-Naturwissenschaftliche Klasse, **5**:333–378, München.

WAGNER, A., 1857. Neue Beiträge zur Kenntniss der fossilen Säugethier-Überreste von Pikermi. — Abhandlungen der Bayerischen Akademie der Wissenschaften, Mathematisch-Naturwissenschaftliche Klasse, **8**:111–158, München.

WEIDMANN, M., SOLOUNIAS, N., DRAKE, R. & CURTIS G., 1984. Neogene stratigraphy of the eastern basin, Samos Island, Greece. — Geobios, **17**(4):477–490.

WEITHOFER, K.A., 1888. Beiträge zur Kenntnis der Fauna von Pikermi bei Athen. — Beiträge zur Paläontologie und Geologie Österreich-Ungarns, **6**:225–292, Wien.

PLATE 1

Gazella from Samos

Fig. 1. *Gazella* cf. *capricornis*, frontlet MTLA298 in frontal (a) and lateral (b) view

Fig. 2. *Gazella mytilinii*, left horn-core MTLB58 in anterior (a) and lateral (b) view

Fig. 3. ?*Gazella mytilinii*, female skull PMMS63 in dorsal (a) and lateral (b) view

Fig. 4. *Gazella* cf. *capricornis*, cranium MTLB16 in lateral view

Fig. 5. *Gazella mytilinii*, frontlet MTLB136 in frontal view

Fig. 6. *Gazella mytilinii*, frontlet MTLA518 in frontal (a) and lateral (b) view

Fig. 7. *Gazella pilgrimi*, left mandible MTLA183 in lingual view

Fig. 8. *Gazella* cf. *capricornis*, right maxilla MTLB199 in occlusal view

Fig. 9. *Gazella mytilinii*, right mandible MTLB362 in lingual view

Fig. 10. *Gazella* cf. *capricornis*, right mandible MTLB5 in lingual view

Fig. 11. *Gazella pilgrimi*, right mandible MLN51 in lingual view

Scale bars equal 5 cm.

PLATE 1

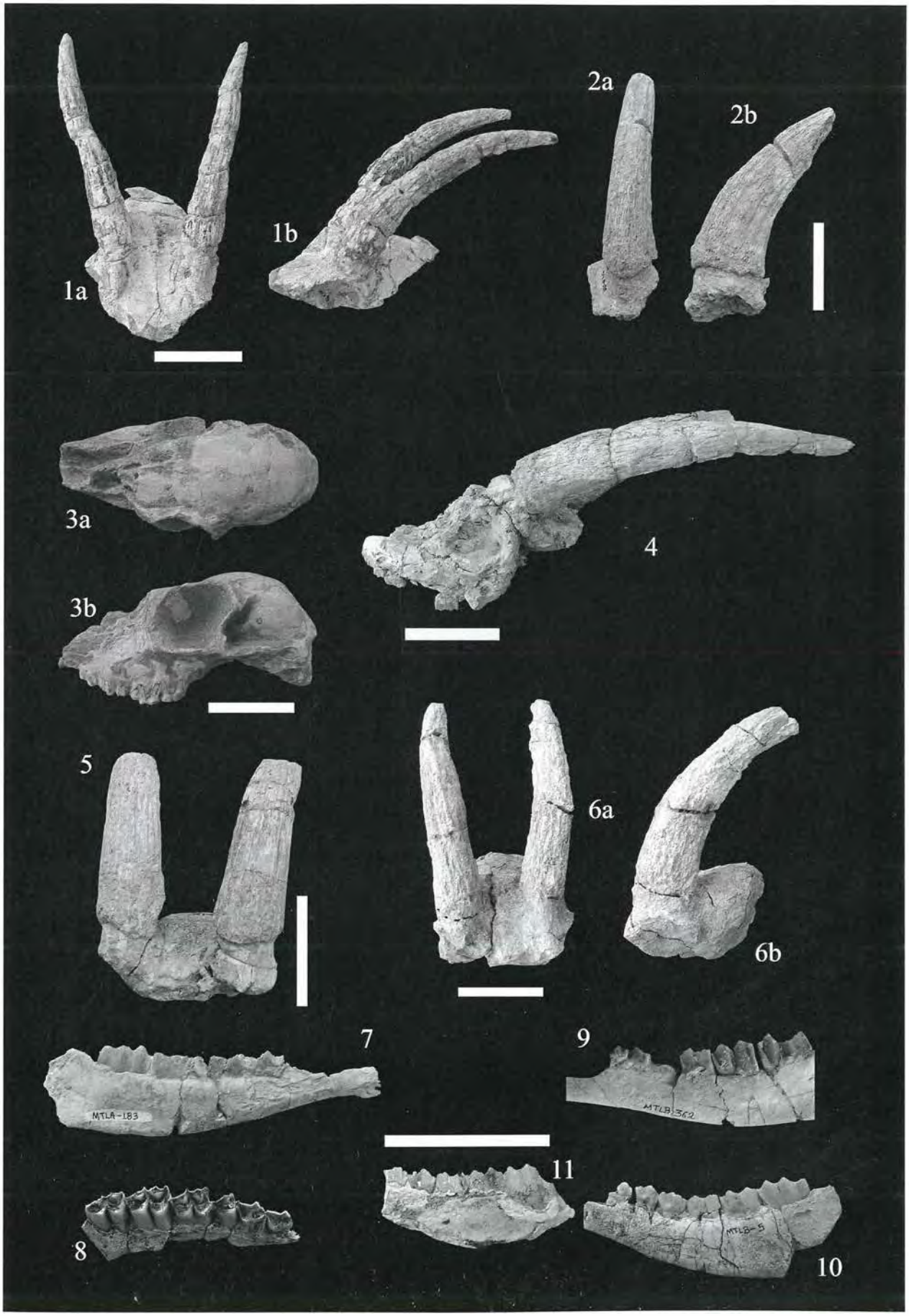

PLATE 2

Sporadotragus parvidens from Samos

Fig. 1. Cranium MTLA3 in lateral view

Fig. 2. Cranium MTLA13 in lateral (a) and basioccipital (b-reversed) view

Fig. 3. Cranium PMMS97 in lateral view

Fig. 4. Right P2-M3, MTLA22 in occlusal view

Fig. 5. Right mandible with p2-m3, MTLA301 in occlusal view

Fig. 6. Right incisor arcade i1-c, MTLA270 in lateral view

Fig. 7. Left mandible with p2-m3, MTLA270 in occlusal view

Scale bars equal 5 cm.

PLATE 2

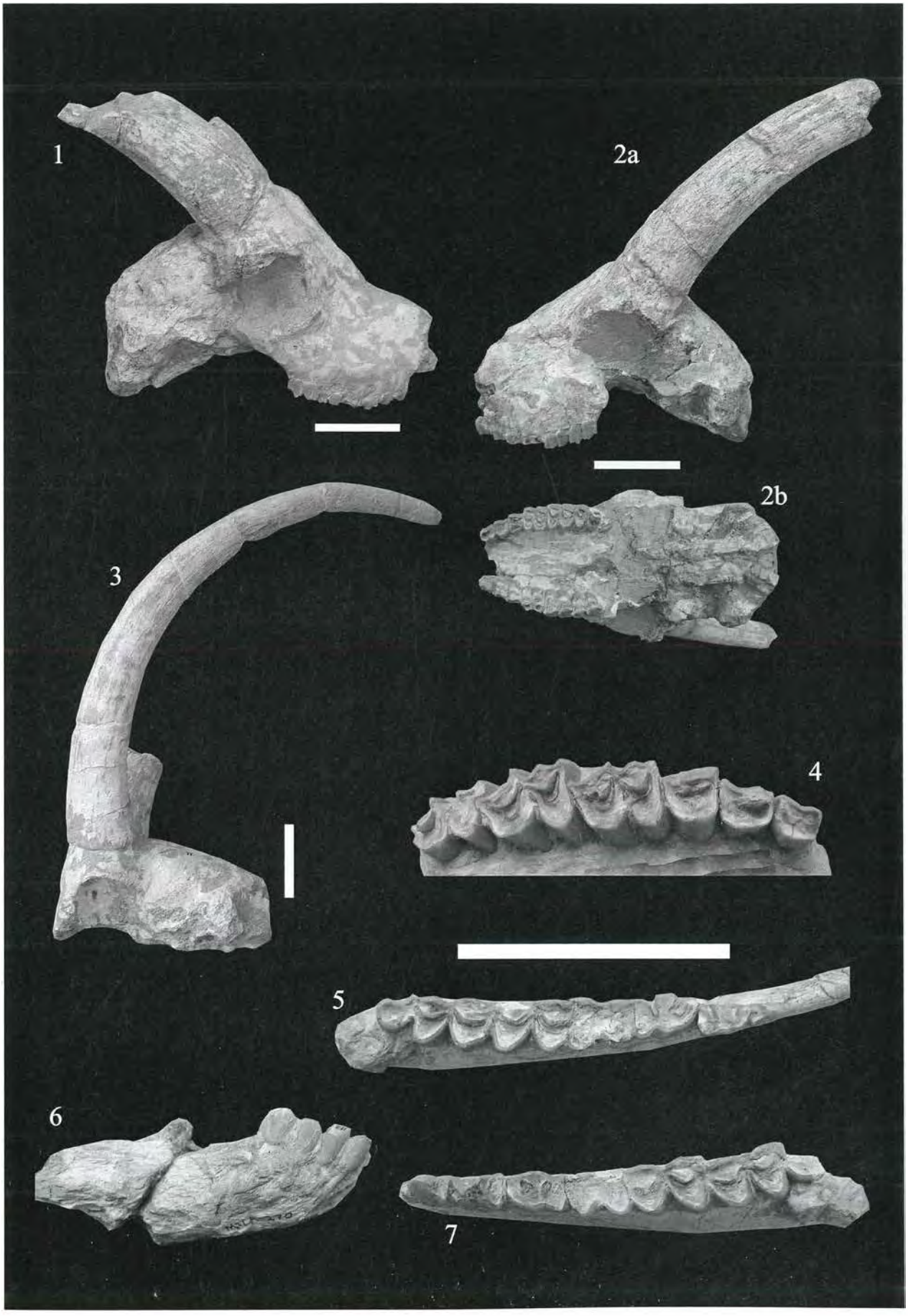

PLATE 3

Palaeoryx from Samos

Fig. 1. *Palaeoryx majori*, cranium MTLB160b in lateral (a), dorsal (b), occipital (c) and basioccipital (d) view

Fig. 2. *Palaeoryx pallasi*, cranium MTLA113 in lateral (a), basioccipital (b), palatal (c) and dorsal (d) view

Fig. 3. *Palaeoryx* sp., metacarpal III+IV, MLN6 in anterior view

Fig. 4. *Palaeoryx pallasi*, cranium MTLA114 in lateral view

Scale bars equal 5 cm.

PLATE 3

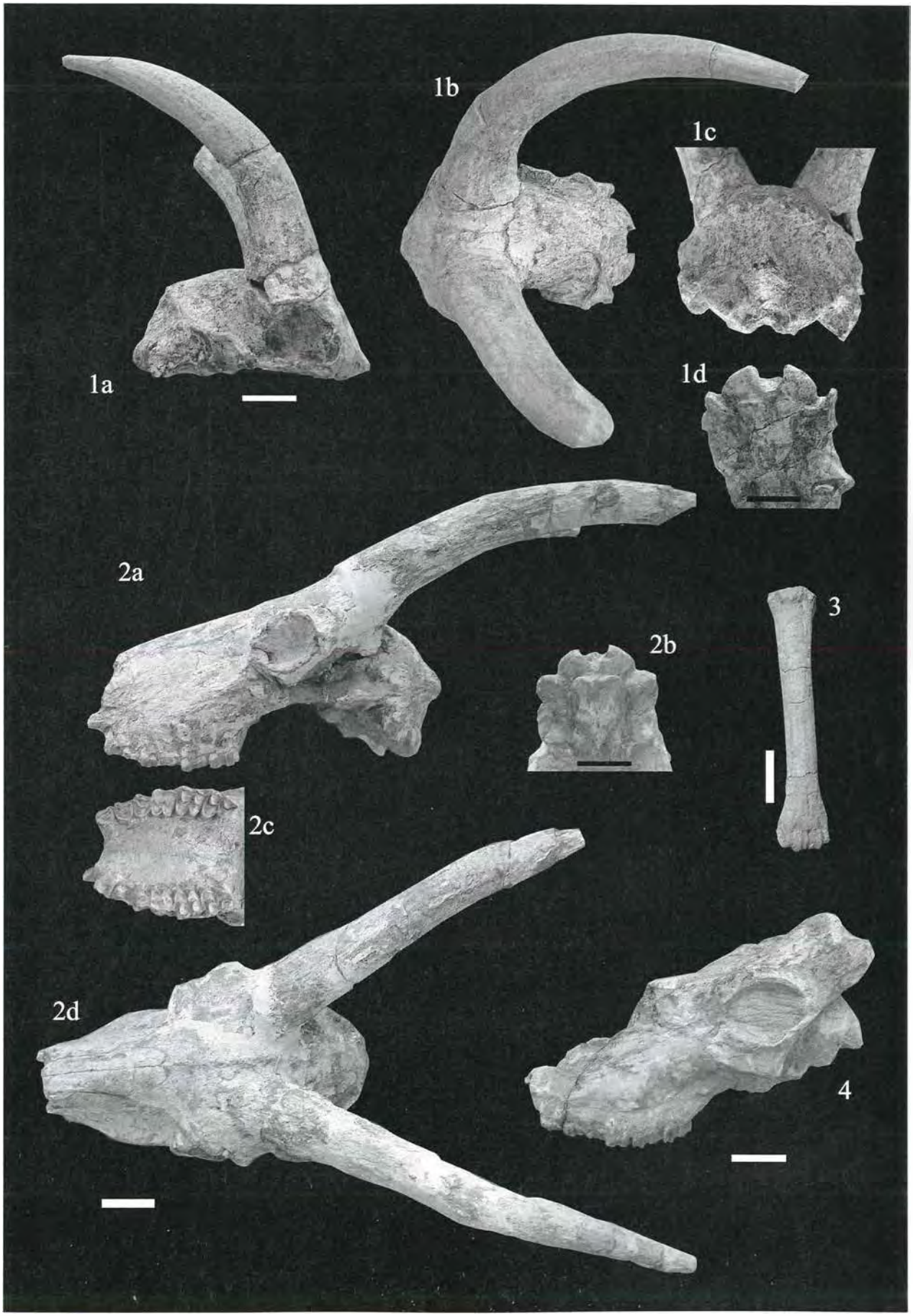

PLATE 4

Skoufotragus laticeps from Samos

Fig. 1. Cranium MTLA4 ('long-brained' variety) in lateral (a) and frontal (b) view

Fig. 2. Cranium MTLB164 ('short-brained' variety) in lateral (a), occipital (b) and basioccipital (c) view

Fig. 3. Cranium PMMS95 ('long-brained' variety) in lateral (a), dorsal (b) and basioccipital (c) view

Fig. 4. Left mandible MTLB24 in occlusal (a) and labial (b) view

Fig. 5. Left P2-M3 MTLA21 in occlusal view

Fig. 6. Right P2-M3 MTLB239 in occlusal view

Scale bars equal 5cm.

PLATE 4